Vehicle Platooning

Thesis report

Vishrut Jain

Longitudinal control for
heterogeneous Vehicle Platooning
with uncertain dynamics

TU Delft

Vehicle Platooning

Thesis report

by

Vishrut Jain

to obtain the degree of Master of Science in Vehicle Engineering
at the Delft University of Technology,
to be defended publicly on Tuesday July 9, 2019 at 1:35 PM.

Student number:	4736214	
Panel :	Prof. R. Happee	Chair
	Prof. S. Baldi	Supervisor
	Prof. M. Alirezaei	Co-supervisor

TU Delft

Acknowledgement

Firstly, I would like to thank my supervisor, Dr. Simone Baldi for guiding me through with the thesis and helping me in every possible way, whenever I got stuck during the whole phase of my thesis. Thank you for your quick replies over the mail and being there whenever any help was needed. I would also like to thank my co-supervisor, Dr. Mohsen Alirezaei for adding the pragmatic perspective to the thesis. I am thankful to Dr. Riender Happee to take out his valuable time for chairing my defense.

I would also like to thank my friend Anoosh for listening me out and discussing the problems I got stuck in. I would also like to acknowledge Vishant, Arsel, Daniel, Gabriele, Abigail, Jochem, Orçun, Nishant, Rupak, Michael, Kevin, Lucas, Nico, Karan, Arvind and Achin for having consistent faith in me and being the much needed stress busters during the course of the thesis.

Lastly, I would like to thank my parents, Alpana and Ajay and my sister, Shinzani for supporting me and encouraging me throughout the course of my study. It wouldn't have been possible to be at this stage without your support.

Vishrut Jain

Delft, July 2019

Abstract

The work presented in this report focuses on longitudinal control of heterogeneous platoon. Firstly, merging maneuver is looked upon, considering heterogeneity in the vehicles i.e. considering different dynamics for the vehicles involved. Then heterogeneity in platoon, arising from the difference in potential limits of the vehicles is taken into account, which the current literature fails to address.

The uncertain/heterogeneous dynamics are addressed through the difference in the engine driveline constant, which differs for different vehicles and keeps on changing during operation. These heterogeneities are tackled by using adaptive control, which adapts to the changing dynamics and estimates the uncertainty to act accordingly.

Adaptive strategies for formation keeping in platoons of automated vehicles have been recently proposed; while these strategies are able to cope with uncertain vehicle parameters, they have the drawback of handling only acyclic graphs (e.g. look-ahead topology). This prevents from enhancing formation keeping protocols with more complex platooning maneuvers such as synchronized merging/splitting. This work proposes an adaptive strategy for performing synchronized merging maneuvers in the presence of uncertain vehicle parameters: during these maneuvers, a cyclic communication graph is instantiated, which must be handled in a suitable way. The strategy is framed as a synchronization protocol with a set of adaptive control laws, designed via Lyapunov stability theory. A benchmark scenario in which two platoons formed in different lanes are required to merge, (e.g. due to a lane closure because of roadworks) is presented to show the effectiveness of the proposed strategy. The approach is proven to be scalable to platoons with arbitrary number of vehicles.

In later part of the work, a method is proposed which takes the limits of the vehicles into consideration, to make the platooning realistic. An adaptive platooning strategy is used, so as the vehicles can adaptively synchronize to desired reference dynamics. In order to handle engine limits, a mechanism is proposed based on making the reference dynamics 'not too demanding', by properly saturating their control action. Such saturation action will allow all vehicles in the platoon to remain in their engine potential limits throughout.

Another problem that affects the stability of the platoon is that, any perturbations or disturbance in the platoon leaves the vehicle scattered if the vehicles are already running at their potential limits. This work proposes an adaptive platooning method with bi-directional interaction and a mechanism coping with engine constraints. The bi-directional interaction allows the vehicle to not only look at the error in spacing from the preceding vehicle (vehicle in front) but also the succeeding vehicle, this makes the vehicle's control action (desired acceleration) depend on both front and back errors. The vehicle can thus slow down for the following vehicle if it lags behind. The bi-directional

strategy developed is then proved string stable, which the literature struggles to establish with the already developed bi-directional strategies.

Simulations are then conducted to validate the theoretical analysis and show the effectiveness of the method in retaining cohesiveness of the platoon. The simulations include a merging maneuver to check the effectiveness of merging with synchronized cyclic communication. For the engine potential limits, firstly the state of the art algorithm's simulation is run which is then compared to the performance of the proposed algorithm. Finally, to check the effectiveness of bi-directional CACC strategy simulations for a specific case is run for both uni-directional and bi-directional strategies proposed in the thesis and are then compared, showing the advantage of using bi-directional CACC strategy over uni-directional strategy.

Contents

List of Figures

List of Tables

1 Introduction

Smart traffic is an active area of research which strives to enhance road safety, manage traffic congestion and reduce vehicles' emission. For the same various methods have been developed, for example by using traffic light control [4], freeway ramp metering [5], adaptive speed limits and dynamic and individual route guidance. On the other hand, automation in the vehicles can also be used to promote smart traffic, like using automated highway systems for automated vehicles [6]. This kind of system requires special infrastructure and dedicated lanes though; and for the vehicles to reach full automation would require some time before it becoming legal and replacing manually driven vehicles.

Advanced Driving Assistance Systems (ADAS) like Adaptive Cruise Control (ACC) and Cooperative Adaptive Cruise Control (CACC) have proven to be helpful in efficient traffic flow. ACC and CACC systems reduce the distance between the vehicle and in this manner more vehicles can be placed in a same span of the road.

Although, the main feature of CACC and ACC is to reduce the gap between the vehicles, these systems have various other advantages. As a result of lower spacing between the vehicles, the aerodynamic drag for the vehicles decrease and due to this reason the vehicular emissions are lower [7]. This is one of the main reasons for the growing interest of research in this area. Also, the response time for ACC system is of the order of 0.1–0.2s, which is negligible when compared with the human reaction time of about 1s [8].

Vehicle platoons employ ACC or CACC or a combination of both (CACC in some vehicles and ACC in the others) for their longitudinal control. Thus, in a platoon only the front vehicle needs to be manually driven and rest of the vehicles in platoon follow the leader/front vehicle.

It may seem that the sole purpose of platooning is to mimic the behaviour of the vehicle ahead, but there are many intricacies involved while controlling a platoon, merging is one of such problems. There can be vehicles which want to join or leave the platoon, the control of the platoon should also consider such cases.

1.1. Current Research Scenario

It may seem like ACC and CACC systems have been well established, but there are a lot of areas where more research is required. Different control strategies have been developed for the same and are still being developed for better performance.

The current control algorithms for merging maneuvers provide a slower outcome than manual merging. This is because of the fact that the current works use quite restrictive protocols for the implementation of merging. One of the main reasons for any automation system is for performance improvement, and hence it requires more work to be done.

Most of the research that has been done is on homogeneous platoon i.e. platoon consisting of same vehicles, and not a lot of literature is present for heterogeneous platooning. When a heterogeneous platoon is considered the dynamics of the vehicles in the platoon change, and so does the potential or bounds/limits of the vehicles.

Problem Statements

This thesis consists of two major problem statements

- Developing a merging strategy which resembles to human driver behavior during merging.
- Developing a control structure for heterogeneous vehicle platoon such that the vehicles do not exceed their potential limits.

1.2. Overview

In this report the problems stated above are addressed. The second chapter briefly covers the preliminary knowledge required to understand the basics of platooning, the third chapter then introduces the plan that would be followed in order to tackle the problems established in the introduction. For the merging maneuver, the model and the control algorithm is then developed in the fourth chapter; which are defined to obtain a human driver like behaviour during merging. Simulations are then carried out, whose results are presented later in the same chapter. The fifth chapter deals with model definition of the vehicles for vehicle following, for which a strategy is developed in the same chapter, to tackle heterogeneity in the vehicle potentials. The strategy is then tested, and the results for the same are presented later in the same chapter. The sixth chapter concludes the report.
Appendices can then be found for supporting some of the work given in the report.

2

Preliminary Knowledge

This chapter aims at providing the basic understanding of vehicle platooning and to make the reader acquainted with the concepts and definitions which are used in the report in later chapters.

2.1. Vehicle Platooning

Automated vehicles are a hot topic of research at this point of time. Vehicle platooning can be thought of as the starting step in automation of vehicles, it allows vehicles to follow the leading vehicle without any input from the driver.

Basic Definition
Vehicle Platooning can be defined as grouping of multiple vehicles together one after the other in such a manner, that all the vehicles follow the leading vehicle with some defined spacing between them. The front vehicle is driven manually while all the other vehicles are given the input in such a manner that they follow the leading vehicle.

An ideal vehicle platoon is one where all the vehicles can keep the desired distances between the vehicles at all times. For the implementation, the error is defined by the deviation of position of a vehicle from it's desired position; this error is then used to push the current position of the vehicle to its desired position.

According to the vehicles involved in the platoon the platoon can be broadly classified into *homogeneous platoon* and *heterogeneous platoon*

2.1.1. Homogeneous Platoon

If there is no discrepancy in the vehicles grouped in the platoon, i.e. if all the vehicles in the platoon are the same (platoon of multiple Prius), also, the controllers being used for the vehicles in the platoon should be the same.

2.1.2. Heterogeneous Platoon

Heterogeneity in platoon can arise due to several reasons. One of the possible reasons for heterogeneity can be difference in the vehicles i.e. presence of different vehicles rather

than multiple similar vehicles. If the vehicles change the dynamics of the model changes and hence the control action needs to be different for every vehicle for a stable platoon. Another type of heterogeneity would be different types of controllers for the vehicles [9].

As it is unrealistic to have a platoon consisting of only one type of vehicle in the platoon the heterogeneity of the platoon can not be ignored. Hence, while developing a controller for the vehicle, heterogeneity has to be taken in consideration.

2.2. String Stability

String stability is a property specific to vehicle platooning. The notion of "String Stability" was introduced in platoon control, where it was observed that one does not want the transient error in the separation distance between vehicles to grow as one proceeds down a line of vehicles in the platoon: systems which have this property were said to be "string stable" [10].

During platooning many perturbations/disturbances could enter the string of vehicles. The ability to attenuate these perturbations, introduced by an arbitrary vehicle in the platoon along the string in upstream direction, is a desired requirement. This requirement describes the notion of string stability. Shockingly, there is no uniform definition of string stability. The most formal approach is based on Lyapunov stability, of which [11] provides an early description, which is comprehensively formalized in [10]. String stability is also interpreted as asymptotic stability of interconnected systems [12].

All the approaches defined above, to describe sting stability, considers theory-oriented approach. In [13] a performance-oriented approach is adopted, to investigate a warning system for preventing head-tail collisions in mixed traffic. In this approach, string stability is characterized by the amplification in the upstream direction of either distance error, velocity, or acceleration, the specific choice defined by the design requirements at hand.

The performance-oriented approach to describe the property seems to be a better choice, as string stability is a concept introduced for vehicle platooning and thus, should be tailored specifically for that application. Hence, in this work,the definition provided above (performance-oriented approach) is considered as the definition for string stability.

It is also important to be able to judge whether a platoon is string stable or not. For this purpose, as the definition suggested, amplification in the upstream direction of the distance error, velocity, or acceleration should be checked.

If there is an amplification in velocity or acceleration up the stream in a platoon the last vehicles would not be able to catch up to the platoon as the vehicles can not achieve any velocity/acceleration, there is an upper limit to these for any vehicle. Thus, it makes sense to check the amplification of velocity and acceleration up the stream, to ensure that all vehicles can follow the platoon.

To check the amplification of these errors due to the disturbance induced, transfer func-

tion between the error of one vehicle to the error of the one following it can be found. If there is no amplification in the magnitude of the transfer function, the platoon is said to be string stable.

2.3. Adaptive Cruise Control

Adaptive cruise control or ACC, as name suggests, performs cruise control on the vehicle it is equipped in, additionally it maintains a desired (pre-defined) distance from the vehicle in front of it, i.e. adapting the vehicle's states to the vehicle in front of it. When adaptive cruise control is active, driver does not need to give any acceleration input to the vehicle, the vehicle automatically adjusts its speed to keep a safe distance from the vehicle ahead. Not only does it allow following of the front vehicle, but also it is safer, as it has a lower reaction delay when compared with human beings [8, 14, 15].

Figure 2.1: Vehicle following through adaptive cruise control

In figure 2.1, it can be seen that the silver vehicle is following the orange vehicle. The silver vehicle is equipped with a sensor to measure the distance between it and the rear bumper of the car in front. The distance is then compared to desired distance, the discrepancy between the two is the error and is pushed to zero though control action. Hence, the only information required for the ACC system is distance. This distance is defined by headway.

2.3.1. Headway

One of the important properties to look upon in platooning is headway. Headway can be defined as a measurement of distance or time in between the vehicles. So, if a vehicle requires 2 seconds to reach the rear of the other vehicle, the time headway is 2s. When headway is measured in distance, it is called distance headway; when measured in time, it is called time headway. So, the distance that a vehicle has to maintain with the vehicle it is following is defined using headway. When a vehicle is at high velocity, it is sensible to have a greater distance between it and the vehicle in front for safety. Hence, having a constant time headway makes sense for this application, also in [16], it has been pointed out that constant time headway can aid in reducing oscillations in the motion of the vehicle.

A constant time headway means to have a constant time difference in between the vehicles i.e. to reach the other vehicle a particular amount of time is required. The distance for time headway thus depends on the velocity of the vehicle.

$$d = CTH \times v \tag{2.1}$$

where,
d is the desired spacing distance, CTH is constant time headway and v is velocity.

In addition to the headway, an additional safety distance is generally added to the headway which is standstill distance. Standstill distance is the distance that the vehicle should maintain if the vehicles are at rest. The spacing distance is thus given by

$$d = CTH \times v + d_{ss} \tag{2.2}$$

where,
d_{ss} is the standstill distance

Although, ACC might look like a perfect option for platooning, as it can follow the vehicle in front with a desired distance between them; but string stability, a crucial requirement for vehicle platooning kicks in here. ACC systems allow the vehicle to follow another vehicle, however, if multiple vehicles are stacked together in a platoon the error grows up the stream of vehicle, hence creating a traffic shock wave. Hence ACC can lead to string instablility [17].

2.4. Cooperative Adaptive Cruise Control

Cooperative Adaptive Cruise Control or CACC is adaptive cruise control with added communication. In CACC the vehicles can communicate necessary information to one another. The information that is communicated is generally the position, velocity, acceleration of the vehicle ahead [18]. Some literature studies also consider the input of the vehicle ahead as an additional information to be communicated [1, 19–21], which is then used as a feedforward term. Because of presence of communication, there is redundancy in the system. Information of the distance can be compared with the measured values through the sensors, and hence, the possibility of error is lesser.

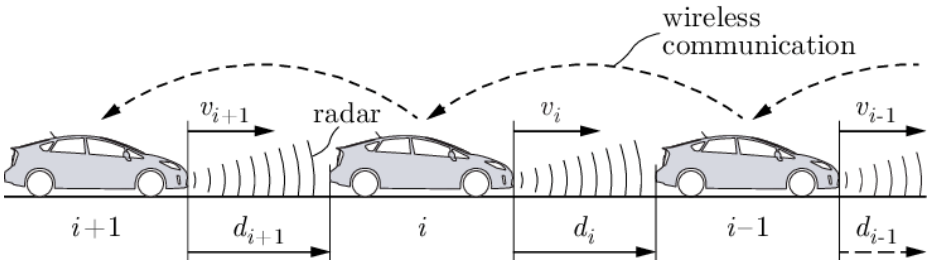

Figure 2.2: Homogeneous Vehicle platoon equipped with CACC [1]

In figure 2.2, it can be seen that the vehicles can communicate with each other. Through the communicated information, the difference between the positions of the vehicles can be found. This spacing between the vehicles is then compared with the desired spacing, and then, the error is pushed to zero using control.

Does communication make a big difference?
Is CACC really better than ACC?

Research on string stability by Naus et al. [22] report on minimal time headways of 2.8s for ACC systems and 0.8s for CACC systems. In [3] it has been shown that, the time headway for CACC can be as low as 0.7s, also, theoretical analysis showed that it can be lowered to 0.3s. Hence there is a huge difference between ACC and CACC. Also, the measurements are generally full of noise (noisy measurements) and if there the position is communicated from one vehicle to another the noise is lower (considering the vehicle need to measure its position).

Just like ACC systems, CACC uses time headway for specifying the spacing between the two vehicles, and hence, the spacing policy for CACC system is as given in equation 2.2.

3

Plan

This thesis can be divided into two parts, in the first part of the thesis we would look at merging maneuvers with heterogeneous platoon. The second part would look upon vehicle following, and cover heterogeneity in platoon and dealing with the different potential limits of the vehicles in the platoon.

3.1. Merging Maneuver

Recent surveys on the practical challenges of CACC were conducted by [23, 24]. Among the challenges, a relevant one is how to include merging maneuvers in the platooning formation keeping protocol: currently, ad-hoc and quite restrictive protocols are used to implement the merging maneuver. Such protocols, usually based on state machines, take care of opening the gap between two vehicle; however, the communication between the vehicle that opens the gap and the vehicle that wants to merge-in is not bi-directional at all times. A clear example is provided in [25]; a vehicle makes a gap; once the gap is open, the state machine will go into the `Wait For Merge` state; the vehicle that opened the gap sends the `Safe To Merge` flag; when the merging vehicle indicates that it has finished merging the state will change back to `Pace Making`. Clearly, because the phases occur one after the other, this is not a synchronization protocol (cf. [26–28] and references therein for examples of synchronization protocols).

In a synchronization protocol, a vehicle creates a gap while the other starts merging, in a seamless way similar to human driving. Consequently, the merging maneuver needs constant bidirectional (and thus cyclic) communication. Recently, it was shown that handling cycles in platooning protocols is difficult, because the input of a vehicle turns out to depend on the input of the neighbors [29]; this creates algebraic loops that can make the input not well posed and that are usually solved by assigning priorities to remove the cycles [30]. When the merging is supervised by the aforementioned non bi-directional state machine, the problem of well-posedness of the input can be overlooked; however, when implementing a synchronized maneuver, such aspect becomes crucial. Note that safety in state machine with bi-directional communication is not trivial, as pointed out in [31] for example.

3.1.1. Plan

This thesis focuses on a lane reduction benchmark scenario, in which two platoons formed in different lanes are required to merge (e.g. due to a lane closure because of roadworks). This type of scenario has become popular mainly thanks to the activities of the Grand Cooperative Driving Challenge (GCDC 2011 and 2016), a competition aiming at testing in real-life implementation and interoperability of communication-based automated driving [2, 32].

All teams of the most recent GCDC 2016 adopted ad-hoc merging protocols that do not address synchronization and uncertainty issues [25, 33, 34]. Even when relying on the standard CACC controller as in [35] (synchronization is achieved while the standstill distance is slowly increased), no parametric uncertainty is taken into account, and no well-posedness of the input is studied during the merging. It is worth mentioning that, this thesis focuses on the longitudinal dynamics only (gap creation and gap closing). The main reason is that synchronization for lateral dynamics is to a great extent still an unsolved problem; it is to be noted that the team Halmstad, winner of GCDC 2016, had no support for lateral control of the vehicle [33].

Other works considering ad-hoc protocols for merging maneuvers include [36, 37] (vehicle entry and leaving via finite state machines); [38] (creating merging gaps for on-ramp vehicles); [39] (platoon merge and split); [40–42] (lane changing, merging and overtaking). Heterogeneity and uncertainty are often overlooked in the aforementioned works, and the merging maneuver is not embedded in any synchronization protocol. This thesis, would tackle these issues by showing that synchronization can be extended to the merging maneuvers. In addition, we show how to guarantee well posedness of the actual inputs at every time instant.

3.2. Vehicle following

Cooperative Adaptive Cruise Control (CACC), also referred to as platooning, is a way of grouping vehicles into platoons with a defined inter-vehicle spacing policy, by using vehicle-to-vehicle wireless communication in addition to on-board sensors [43, 44]. After initial studies on homogeneous platoons [3, 45], it was soon recognized that several heterogeneities might influence the platooning effectiveness: networked-induced delays and packet losses have been well studied in literature as they generate some level of heterogeneity in wireless CACC communication [19, 46, 47]. Methods used to achieve platooning over unreliable communication include observers [48, 49] or switched CACC strategies [50, 51].

However, a more substantial level of heterogeneity arises from the vehicle dynamics [52]: notably, cohesiveness of a platoon of nonidentical (heterogeneous) vehicles can be severely limited by saturating engine performance (one can think about a family car struggling to maintain cohesiveness in a platoon with sport cars). As opposed to standard unidirectional look-ahead interaction (adjusting the spacing with the front vehicle independently on the rear vehicle), the use of bidirectional interaction (with both the front and the rear vehicle) was proposed to improve cohesiveness [53].

Unfortunately, bidirectionality creates the open challenge of defining bidirectional string stability [54, 55] (string stability refers to the attenuation of disturbances as they propagate through the platoon [56]). To the best of the authors' knowledge, this challenge makes bidirectionality not well studied in CACC, especially in the presence of saturation. In fact, all the forthcoming cited works refer to unidirectional platooning.

A pioneering work considering the fundamental limitations in the control of platoons was [57, 58] also studied the limitations of platoons subject to saturation. Both works come to similar conclusions: loss of cohesiveness can be systematically eliminated only at the price of losing performance so as to prevent engine saturation. In line with these works are the recent works [59] (homogeneous single integrators with actuator faults), [60] (consensus for homogeneous platoons with velocity constraints), [61] (low-gain control to accommodate input saturation), and [62] (antiwindup strategy).

Unfortunately, these works on saturation focus on initial formation errors rather then on heterogeneity in platoon engine dynamics: uncertainty in such dynamics is an important source of heterogeneity. Recently, CACC strategies were proposed to address vehicle heterogeneity by adapting the control gains [21, 63, 64]. Such strategies basically define some homogeneous reference dynamics that the heterogenous platoon should adaptively match. Distributed matching conditions define the control gains that match the reference dynamics [29] and, when the vehicle dynamics are uncertain, such matching gains can be learned via appropriate adaptive laws [65].

Despite the progress in the field, the research in this work stems from the following open questions: is it possible to improve platoon cohesiveness adaptively when the engine dynamics of the vehicles are uncertain and subject to saturation? Can the adaptation law benefit from the presence of bidirectional communication? The main contribution of this work is enhancing the adaptive platooning methodology by giving a positive answer to these questions.

3.2.1. Plan

First, a bidirectional homogeneous platoon would be designed (i.e. reference dynamics to which the heterogeneous platoon should homogenize), whose string stability properties are shown via appropriate criteria. Then, in order to handle engine constraints, we propose a mechanism based on making the reference dynamics 'not too demanding', by applying a properly designed saturation action. Such saturation action will allow all vehicles to not hit their engine bounds.

This is in line with the studies [57, 58], i.e. saturation can be eliminated only at the price of losing performance. As even the most recent literature on platooning focuses on longitudinal dynamics (lateral string stability and nonholonomic constraints arising from lateral dynamics are unsolved challenges up to now [33, 34, 66, 67]), in this work as well only longitudinal dynamics are considered.

4

Merging maneuvers under heterogeneity

In this section, the problem related to heterogeneity in platoon during merging maneuver will be looked upon. First, modelling of the vehicle is done, for which control algorithms are then derived in order to successfully perform the merging maneuver. The result of implementation of the proposed algorithm is then portrayed later on in the chapter.

4.1. CACC System Structure

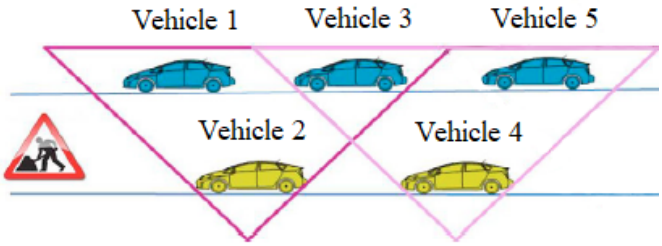

Figure 4.1: Merging maneuver under consideration: the two yellow vehicles must merge with the blue vehicles due to traffic roadworks (figure edited from [2]).

For the sake of concreteness, consider a heterogeneous platoon with 5 vehicles as shown in Fig. 4.1 (the scenario can be easily extended to considering an arbitrary number N of vehicles): the figure represents a benchmark scenario in which two platoons formed in different lanes are required to merge, e.g. due to a lane closure because of roadworks.

Define v_i and d_i to be the velocity (m/s) of vehicle i, and the distance (m) between vehicle i and its preceding vehicle $i-1$, respectively. Let us define two sets of indexes, one for each platoon, i.e. the "odd" vehicles $S_N^o = \{i \in \mathbb{N} |\ i = 1, 3, 5, ...\}$ and the "even" vehicles $S_N^e = \{i \in \mathbb{N} |\ i = 2, 4, ...\}$. Also, let us define $S_N = S_N^o \cup S_N^e = \{i \in \mathbb{N} |\ i = 1, 2, 3, ...\}$.

In addition, we reserve the index $i = 0$ to a virtual vehicle, representing the platoon's desired behavior (virtual leading vehicle, not shown in Fig. 5.1). In line with most CACC literature, we will focus on the longitudinal dynamics only, while for the lateral

dynamics a separate steering controller is assumed to be in place (this setting has been also considered in most GCDC architectures [25, 33–35]). The following longitudinal model, derived by [3], is used

$$\begin{pmatrix} \dot{d}_i \\ \dot{v}_i \\ \dot{a}_i \end{pmatrix} = \underbrace{\begin{pmatrix} 0 & 1 & 0 \\ 0 & 0 & 1 \\ 0 & 0 & -\frac{1}{\tau_i} \end{pmatrix}}_{A_i} \underbrace{\begin{pmatrix} d_i \\ v_i \\ a_i \end{pmatrix}}_{x_i} + \underbrace{\begin{pmatrix} 0 \\ 0 \\ \frac{1}{\tau_i} \end{pmatrix}}_{b_i} u_i, \;\; i \in S_N \tag{4.1}$$

where a_i and u_i are respectively the acceleration (m/s^2) and external input (m/s^2) (desired acceleration) of the i^{th} vehicle, and τ_i (s) represents each vehicle's driveline time constant. We will focus on an uncertain scenario in which the driveline time constants of all vehicles are unknown: this scenario has been shown to be challenging for standard CACC algorithms [3], and an adaptive solution to this problem has been proposed only recently [50].

Such an adaptive solution is based on defining some target dynamics for the virtual leading vehicle

$$\begin{aligned} \begin{pmatrix} \dot{d}_0 \\ \dot{v}_0 \\ \dot{a}_0 \end{pmatrix} &= \underbrace{\begin{pmatrix} 0 & 1 & 0 \\ 0 & 0 & 1 \\ 0 & 0 & -\frac{1}{\tau_0} \end{pmatrix}}_{A_0} \begin{pmatrix} d_0 \\ v_0 \\ a_0 \end{pmatrix} + \underbrace{\begin{pmatrix} 0 \\ 0 \\ \frac{1}{\tau_0} \end{pmatrix}}_{b_0} u_0 \\ \begin{pmatrix} \dot{d}_0 \\ \dot{v}_0 \\ \dot{a}_0 \end{pmatrix} &= \underbrace{\begin{pmatrix} 0 & 1 & 0 \\ 0 & 0 & 1 \\ a_{01} & a_{02} & a_{03} \end{pmatrix}}_{A_m} \underbrace{\begin{pmatrix} d_0 \\ v_0 \\ a_0 \end{pmatrix}}_{x_m} + \underbrace{\begin{pmatrix} 0 \\ 0 \\ b_{00} \end{pmatrix}}_{b_m} r \end{aligned} \tag{4.2}$$

where (A_0, b_0) represent some nominal homogeneous dynamics (being τ_0 the homogeneous driveline time constant), and the second equation has been obtained assuming that, the lead vehicle is controlled by a state-feedback controller $u_0 = k_0^{*\prime} x_m + l_0^* r$ that makes its dynamic stable: therefore a_{01}, a_{02}, a_{03} are design parameters selected such that the matrix A_m is Hurwitz. Note that, under the assumption of a homogeneous platoon, we have $\tau_i = \tau_0$, $\forall i \in S_N$. In this work, we remove the homogeneous assumption by considering that $\forall i \in S_N$, τ_i is an unknown parameter. The motivation is that, in practice, τ_i sensibly changes according to vehicle and road conditions.

The main goal of every vehicle, except the leading vehicle, is to maintain a desired distance between itself and its preceding vehicle. For this purpose, a constant time headway (CTH) spacing policy defines the desired distance as:

$$r_{j,i}(t) = \bar{r}_{j,i}(t) + h v_i(t) \;\; , \;\; i,j \in S_N \tag{4.3}$$

where $r_{j,i}(t)$ is the distance between vehicles i and j (which might be located in the same platoon or in two different platoons), $\bar{r}_{j,i}$ is the standstill distance (m) between the same vehicles and h is the time headway (s). Note that $r_{j,i}$ depends on time because it

can change during the merging maneuver: this can be due to a change in the velocity v_i, but also to a change in $\bar{r}_{j,i}$ as a consequence of increasing/decreasing the gap during merging. It is important to note that the stability analysis proposed in this paper is valid for constants $r_{j,i}$, even though in practice stability is achieved also for slowly-time varying $r_{j,i}(t)$ typically arising during merging. The CTH in (4.3) indicates that the vehicle's desired velocity must be proportional to the inter-vehicle spacing: this is done to imitate the driving intuition of slowing down, as the inter-vehicle spacing decrease. It has been shown that such spacing policy improves string stability and safety [3]: constant spacing policies are also possible, but typically they require larger gaps in order to achieve string stability [68]. Let us now define the state error (spacing distance, the relative velocity, and relative acceleration) between the j^{th} and the i^{th} vehicle as:

$$e_{j,i}(t) = \begin{pmatrix} d_j(t) \\ v_j(t) \\ a_j(t) \end{pmatrix} - \begin{pmatrix} d_i(t) \\ v_i(t) \\ a_i(t) \end{pmatrix} + \begin{pmatrix} r_{j,i}(t) \\ 0 \\ 0 \end{pmatrix}. \tag{4.4}$$

Because we consider formations of automated vehicles, (4.4) is defined for any two adjacent vehicles between which a communication link is instantiated. The control objective is to regulate $e_{j,i}$ to zero for all such adjacent vehicles.

Problem 4.1.1: With reference to the benchmark of Fig. 5.1, given the leading dynamics (4.2) and the vehicle dynamics (4.1) with unknown driveline constants, find an adaptive strategy for u_i, and a CTH strategy for (4.3) such that merging can be achieved. This is equivalent to proving that $e_{j,i}$ in (4.4) can be regulated to zero for all links instantiated during all phases of the merging.

In the next section, we present how $r_{j,i}$ in (4.3) and the communication links change during the merging maneuver.

4.2. The synchronization protocol

To describe the merging maneuver, let us consider the communication graphs in Fig. 4.2. An arrow indicates a communication link from the vehicle where the arrow starts to the vehicle where the arrow ends. States and inputs can be communicated among such vehicles.

At this point, it is convenient to introduce the following compact notation for the vehicle uncertain dynamics

$$\dot{x}_i = A_i x_i + b_i u_i, \quad i \in S_N \tag{4.5}$$

where, A_i and b_i are *unknown* matrices in the form of (4.1).
Also, consider the virtual leader,

$$\dot{x}_m = A_0 x_m + b_0 u_0 = A_m x_m + b_m r \tag{4.6}$$

where, A_m and b_m are *known* matrices in the form of (4.2). Fig. 4.2 shows that, before attempting to merge, vehicle 2 aligns to vehicle 3 and vehicle 4 aligns to vehicle 5 (graph 1). When the merging starts (graph 2), cyclic communications appear (bidirectional link between vehicles 2 - 3 and vehicles 4 - 5) and vehicle 3 and vehicle 5 increase their

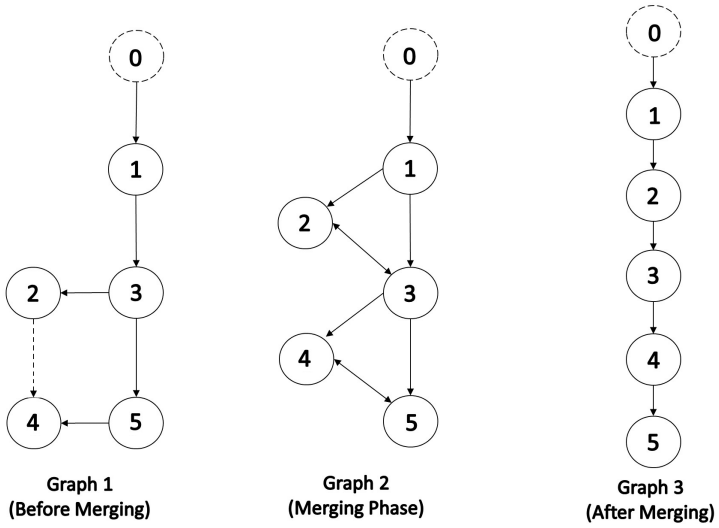

Figure 4.2: Communication graph before/during/after merging. The dashed arrow between vehicles 2 and 4 in graph 1 represents the second platoon just before the merging maneuver is initiated.

distance from vehicle 1 and vehicle 3 respectively, while the vehicles 2 tries to maintain its distances with vehicle 1 and vehicle 4 tries to maintain its distance from vehicle 3. Finally, in graph 3, the merging is completed and a new acyclic directed network is established between the five vehicles in the platoon.

Because of the spatial configuration of the vehicles, the communication links are instantiated accordingly. In particular, in graph 2 the bidirectional links between vehicles 2 - 3 and vehicles 4 - 5 are used for safety reasons by vehicle 2 and vehicle 4, to watch the behavior of vehicle 3 and vehicle 5 and vice versa during merging. This emulates the human behavior in which a vehicle that wants to merge will look at the vehicle to be overtaken, and vice versa.

With reference to the CTH in (4.3), the following spacing policies are considered:

- *Graph 1:* $r_{2i,2i+1} = 0$, $r_{2i+1,2i-1} = hv_{2i+1} + r$, $i = 1, 2, ...$, where r is standstill distance and h is the time headway;
- *Graph 2:* $r_{2i,2i+1}$ decreases gradually from 0 to $-(hv_{2i+1} + r)$
  $r_{2i+1,2i-1}$ increases gradually from $hv_{2i+1} + r$ to $hv_{2i+1} + hv_{2i} + 2r$, $i = 1, 2, ...$;
- *Graph 3:* $r_{i+1,i} = hv_{i+1} + r$, $i = 1, 2, 3, ...$

The term "gradually" refers to any (slowly time-varying) interpolation policy between the two extreme values of $r_{j,i}$, where the interpolation can be linear or of higher order. A detail of the spacing policy during and after merging can be seen in Fig. 4.3.

Being the system matrices in (4.5) unknown, the synchronization task has to be achieved in an adaptive fashion. The term "adaptive" refers to the fact that the problem is solved by some appropriate vectors or constants that are unknown, and that must therefore be estimated. The following result, derived from [29], justifies that the adaptive problem is

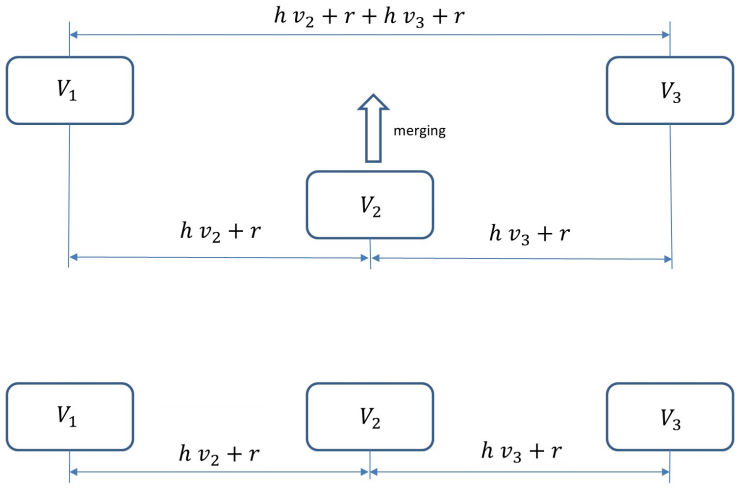

Figure 4.3: Spacing policy during and after merging (only the first 3 vehicles are indicated). Note that the distances are calculated with respect to the vehicle center of mass for simplicity.

well posed in the sense of [69, 70], i.e. the unknown vectors and constants solving the problem exist.

Proposition 4.2.1. For dynamics in the form (4.1) and (4.2), there exist vectors k_i^* and scalars l_i^* such that

$$A_m = A_i + b_i k_i^{*\prime}, \quad b_m = b_i l_i^*, \quad i \in S_N \tag{4.7}$$

In addition, the signs of l_i^*s are positive, and there exist vectors $k_{2i+1,2i-1}^* = k_{2i+1}^* - k_{2i-1}^* l_{2i+1}^*/l_{2i-1}^*$, $k_{2i,2i-1}^* = k_{2i}^* - k_{2i-1}^* l_{2i}^*/l_{2i-1}^*$, $k_{2i,2i+1}^* = k_{2i}^* - k_{2i+1}^* l_{2i}^*/l_{2i+1}^*$, $k_{2i+1,2i}^* = k_{2i}^* - k_{2i}^* l_{2i+1}^*/l_{2i}^*$ and scalars $l_{2i+1,2i-1}^* = l_{2i+1}^*/l_{2i-1}^*$, $l_{2i,2i-1}^* = l_{2i}^*/l_{2i-1}^*$, $l_{2i,2i+1}^* = l_{2i}^*/l_{2i+1}^*$, $l_{2i+1,2i}^* = l_{2i+1}^*/l_{2i}^*$ such that

$$\begin{aligned} A_{2i-1} &= A_{2i+1} + b_{2i+1} k_{2i+1,2i-1}^{*\prime} & b_{2i-1} &= b_{2i+1} l_{2i+1,2i-1}^*, \\ A_{2i-1} &= A_{2i} + b_{2i} k_{2i,2i-1}^{*\prime} & b_{2i-1} &= b_{2i} l_{2i,2i-1}^*, \\ A_{2i+1} &= A_{2i} + b_{2i} k_{2i,2i+1}^{*\prime} & b_{2i+1} &= b_{2i} l_{2i,2i+1}^*, \\ A_{2i} &= A_{2i+1} + b_{2i+1} k_{2i+1,2i}^{*\prime} & b_{2i} &= b_{2i+1} l_{2i+1,2i}^* \end{aligned} \tag{4.8}$$

where $i = 1, 2, \ldots$.
For the proof, the interested reader is referred to [29].
Note that (4.8) also implies

$$A_0 = A_i + b_i k_{i,0}^{*\prime}, \quad b_0 = b_i l_{i,0}^* \tag{4.9}$$

for some ideal gains $k_{i,0}^* = k_i^* - k_0^* l_i^*/l_0^*$ and $l_{i,0}^* = l_i^*/l_0^*$, where k_0^* and l_0^* are the gains of the controller defined after (4.2).

In the following, we will show how the result in Proposition 4.2.1 can be used to develop the adaptive controllers solving Problem 4.1.1.

4.2.1. The adaptive controller: acyclic graphs

Because graphs 1 and 3 are acyclic, the corresponding control laws can be derived from the approach in [29]. Therefore, in the following the adaptive laws are given without proof.

Graph 1

For vehicle 1, consider the controller

$$u_1(t) = k'_{1,0}(t)x_m(t) + k'_1(t)e_{1,0}(t) + l_{1,0}(t)u_0(t) \tag{4.10}$$

where $k_{1,0}(t)$, $k_1(t)$ and $l_{1,0}(t)$ are the estimates of $k^*_{1,0}$, k^*_1 and $l^*_{1,0}$ adapted by

$$\begin{aligned} \dot{k}'_{1,0}(t) &= -\gamma_k b'_m P e_{1,0}(t) x'_m(t) \\ \dot{k}'_1(t) &= -\gamma_k b'_m P e_{1,0}(t) e'_{1,0}(t) \\ \dot{l}_{1,0}(t) &= -\gamma_l b'_m P e_{1,0}(t) u_0(t) \end{aligned} \tag{4.11}$$

For vehicle $2, 4, ...$, consider the controller

$$u_{2i}(t) = k'_{2i,2i+1}(t)x_{2i+1}(t) + k'_{2i}(t)e_{2i,2i+1}(t) + l_{2i,2i+1}(t)u_{2i+1}(t) \tag{4.12}$$

where $i = 1, 2, ...$, and $k_{2i,2i+1}(t)$, $k_{2i}(t)$ and $l_{2i,2i+1}(t)$ are the estimates of $k^*_{2i,2i+1}$, k^*_{2i} and $l^*_{2i,2i+1}$ adapted by

$$\begin{aligned} \dot{k}'_{2i,2i+1}(t) &= -\gamma_k b'_m P e_{2i,2i+1}(t) x'_{2i+1}(t) \\ \dot{k}'_{2i+1}(t) &= -\gamma_k b'_m P e_{2i,2i+1}(t) e'_{2i,2i+1}(t) \\ \dot{l}_{2i,2i+1}(t) &= -\gamma_l b'_m P e_{2i,2i+1}(t) u_{2i+1}(t) \end{aligned} \tag{4.13}$$

For vehicle $3, 5, ...$, consider the controller

$$\begin{aligned} u_{2i+1}(t) = {} & k'_{2i+1,2i-1}(t)x_{2i-1}(t) + k'_{2i-1}(t)e_{2i+1,2i-1}(t) \\ & + l_{2i+1,2i-1}(t)u_{2i-1}(t) \end{aligned} \tag{4.14}$$

where $i = 1, 2, ...$, and $k_{2i+1,2i-1}(t)$, $k_{2i-1}(t)$ and $l_{2i+1,2i-1}(t)$ are the estimates of $k^*_{2i+1,2i-1}$, k^*_{2i-1} and $l^*_{2i+1,2i-1}$ adapted by

$$\begin{aligned} \dot{k}'_{2i+1,2i-1}(t) &= -\gamma_k b'_m P e_{2i+1,2i-1}(t) x'_{2i-1}(t) \\ \dot{k}'_{2i-1}(t) &= -\gamma_k b'_m P e_{2i+1,2i-1}(t) e'_{2i+1,2i-1}(t) \\ \dot{l}_{2i+1,2i-1}(t) &= -\gamma_l b'_m P e_{2i+1,2i-1}(t) u_{2i-1}(t) \end{aligned} \tag{4.15}$$

In all adaptive laws the scalars $\gamma_k, \gamma_l > 0$ are adaptive gains, and P is a positive definite matrix satisfying the Lyapunov equation

$$PA_m + A'_m P = -Q, \qquad Q > 0. \tag{4.16}$$

It has to be noted that the vehicle that has to merge considers the vehicle to its side as its preceding vehicle.

Graph 3

For both graph 1 and graph 3 the structure of the control law remains the same but the index of the preceding vehicle changes. For vehicle 1, consider the controller (4.10) and the adaptive laws (4.11). For all other vehicles $2, 3, 4, ...$, consider the controller

$$u_{i+1}(t) = k'_{i+1,i}(t)x_i(t) + k'_{i+1}(t)e_{i+1,i}(t) + l_{i+1,i}(t)u_i(t) \tag{4.17}$$

where $i = 1, 2, ...$, and the gains are adapted in a similar fashion as in (4.11), (4.13), (4.15) (modulo the different preceding vehicles requiring different indexes).

Remark 4.1. *By inspecting the structure of A_i and b_i in (4.1), it is possible to see that k^*_{ji} in (4.8) is a vector with three components, whose first two components are zero. This implies two things: even though, for simplicity of notation, we will keep writing a vector adaptation law, it is enough to estimate only the last component of k_{ji} via a scalar adaptation law; no absolute position measurements are necessary in any control law, since the first two components of any state post-multiplying k_{ji} would be ineffective in the control law. Therefore, the proposed control law can be applied via measurements of relative position, velocity and acceleration, as well as measurements of own acceleration, which is in line with most CACC strategies [3].*

4.2.2. The adaptive controller: cyclic graph

The adaptive control for merging with cyclic graph has been proposed already, which will be iterated with a refined spacing policy and an additional mixing architecture to smoothen the control action during the switching of the controllers. Due to the need of handling the cyclic communication, its design will be explained with more details and proved analytically. The following result holds.

Theorem 4.1. *For vehicle 1, consider the controller* (4.10) *and the adaptive laws* (4.11)*. For vehicle* $3, 5, ...$*, consider the controller*

$$\begin{aligned} u_{2i+1}(t) = {} & k'_{2i+1,2i}(t)\frac{x_{2i}(t)}{2} + k'_{2i+1,2i-1}(t)\frac{x_{2i-1}(t)}{2} + k'_{2i+1}(t)\frac{e_{2i+1,2i}(t) + e_{2i+1,2i-1}(t)}{2} \\ & + l_{2i+1,2i}(t)\frac{u_{2i}(t)}{2} + l_{2i+1,2i-1}(t)\frac{u_{2i-1}(t)}{2} \end{aligned} \tag{4.18}$$

($i = 1, 2, ...$) and the adaptive laws

$$\begin{aligned} \dot{k}'_{2i+1,2i}(t) &= -\gamma_k b'_m P(e_{2i+1,2i}(t) + e_{2i+1,2i-1}(t))x'_{2i}(t) \\ \dot{k}'_{2i+1,2i-1}(t) &= -\gamma_k b'_m P(e_{2i+1,2i}(t) + e_{2i+1,2i-1}(t))x'_{2i-1}(t) \\ \dot{k}'_{2i+1}(t) &= -\gamma_k b'_m P(e_{2i+1,2i}(t) + e_{2i+1,2i-1}(t))(e_{2i+1,2i}(t) + e_{2i+1,2i-1}(t))' \\ \dot{l}_{2i+1,2i}(t) &= -\gamma_l b'_m P(e_{2i+1,2i}(t) + e_{2i+1,2i-1}(t))u_{2i}(t) \\ \dot{l}_{2i+1,2i-1}(t) &= -\gamma_l b'_m P(e_{2i+1,2i}(t) + e_{2i+1,2i-1}(t))u_{2i-1}(t) \end{aligned} \tag{4.19}$$

For vehicle $2, 4, ...$*, consider the controller*

$$\begin{aligned} u_{2i}(t) = {} & k'_{2i,2i-1}(t)\frac{x_{2i-1}(t)}{2} + k'_{2i,2i+1}(t)\frac{x_{2i+1}(t)}{2} + k'_{2i}(t)\frac{e_{2i,2i-1}(t) + e_{2i,2i+1}(t)}{2} \\ & + l_{2i,2i-1}(t)\frac{u_{2i-1}(t)}{2} + l_{2i,2i+1}(t)\frac{u_{2i+1}(t)}{2} \end{aligned} \tag{4.20}$$

($i = 1, 2, ...$) and the adaptive laws

$$\begin{aligned}
\dot{k}'_{2i,2i-1}(t) &= -\gamma_k b'_m P(e_{2i,2i-1}(t) + e_{2i,2i+1}(t))x'_{2i-1}(t) \\
\dot{k}'_{2i,2i+1}(t) &= -\gamma_k b'_m P(e_{2i,2i-1}(t) + e_{2i,2i+1}(t))x'_{2i+1}(t) \\
\dot{k}'_{2i}(t) &= -\gamma_k b'_m P(e_{2i,2i-1}(t) + e_{2i,2i+1}(t))(e_{2i,2i-1}(t) + e_{2i,2i+1}(t))' \\
\dot{l}_{2i,2i-1}(t) &= -\gamma_l b'_m P(e_{2i,2i-1}(t) + e_{2i,2i+1}(t))u_{2i-1}(t) \\
\dot{l}_{2i,2i+1}(t) &= -\gamma_l b'_m P(e_{2i,2i-1}(t) + e_{2i,2i+1}(t))u_{2i+1}(t)
\end{aligned} \tag{4.21}$$

where all variables and parameters have a similar meaning with those in Section 4.2.1. Then, provided that the inputs are well defined at very time instant, merging is achieved in graph 2.

For the proof of synchronization of the above derived control actions and the well posedness of the input, Appendix-A and Appendix-B can be referred respectively.

4.3. Simulation and results

4.3.1. Scenario

For simulating merging maneuver 5 vehicles are considered which are initially in two separate platoons in two different lanes. These two platoons are required to merge into one.In fig 4.1 it can be seen that because of the roadworks the two platoons need to merge into one.

4.3.2. Parameters

The parameters of the reference model are taken as: $a_{01} = -5$, $a_{02} = -12$, $a_{03} = -1.5$, and $b_{00} = 1$, while the exact dynamics of the vehicles in (4.1) are unknown for simulation purposes.

Table 4.1: Vehicles parameters and initial conditions

Vehicle i	τ_i	$x_i(0)$
Vehicle 1	0.5	[-2,1,0]
Vehicle 2	0.2	[-20,2,1]
Vehicle 3	0.33	[-15,2,1]
Vehicle 4	0.14	[-30,2,1]
Vehicle 5	0.17	[-25,2,1]

Table 4.1 shows the parameter used to simulate each vehicle i, together with the initial conditions for the states.

The reference signal r is taken to be a ramp (this corresponds to a leader driving at constant velocity while the merging is performed). The simulations are carried out for a steady state speed of approximately 15m/s. The design parameter are taken as: $Q = diag(1, 1, 5)$, with adaptive gains $\gamma_k = 1.5 \cdot 10^{-3}, \gamma_l = 2.5 \cdot 10^{-4}$. All initial estimates of the control gains are initialized based on a (wrong) priori knowledge that

all vehicles are homogeneous with driveline time constant $\tau_0 = 0.28$: this amounts to taking $k_{ij}(0) = 0$, $l_{ij}(0) = 1$ and $k_i(0) = \tau_0[a_{01}\ a_{02}\ (a_{03} + 1/\tau_0)]'$. Please note that $\tau_0 = 0.28$ corresponds to a 100% uncertainty around the nominal value of $[0.14, 0.56]$, which covers the uncertainty in Table 4.1. The time headway h is 0.7sec. The maneuver is organized as:

- 0-50 s: vehicle 2 aligns with vehicle 3 and vehicle 4 aligns with vehicle 5, while vehicles 1, 3 and 5 achieve the initial formation.
- 50-70s: vehicle 3 creates an increasing gap for vehicle 2 and vehicle 5 creates an increasing gap for vehicle 4, while vehicle 2 and vehicle 4 start the merging.
- 70-90s: the final formation for the platoon is achieved.

It can be noted that different merging times have been selected for different vehicles in order to highlight the heterogeneity in the maneuver (the first three vehicles start the maneuver before the other vehicles).

4.3.3. Mixing architecture

Theorems 4.1 and B.1 (in Appendix B) do not fully consider the effect of switching topologies (cf. Fig. 4.2): in order words, stability is proven for the stand-alone topologies, but not for their combined switching. On the other hand, it is well known from switched systems theory that if the switching is slow enough, stability will not be destroyed [71]. It is important to note that during the different phases of the merging, each vehicle might end up having a different number of neighboring vehicles: specifically, vehicles 2, 3, 4 and 5 have: one neighboring vehicle in graph 1 (vehicle 3, vehicle 1, vehicle 5 and vehicle 3, respectively); two neighboring vehicles in graph 2 (vehicles 1 and 3; vehicles 1 and 2; vehicle 3 and 5, vehicle 3 and 4, respectively); one neighboring vehicle in graph 3 (vehicle 1, vehicle 2, vehicle 3 and vehicle 4, respectively).

Because vehicles 2, 3, 4 and 5 end up having a different number of neighboring vehicles, it is required to implement a different controller for each different topology. Even though a switching control scheme might seem the most appropriate one to implement, this might lead to discontinuities in the control action that might result in undesirable peaks. For this reason, inspired by the results in [72, 73], in these simulations we explore a mixing action that smoothly goes from one communication topology to another one. This idea is represented in Fig. 4.4.

The figure shows that three different adaptive controllers might be possible for vehicle 2, vehicle 3, vehicle 4 and vehicle 5: instead of activating only one of them, we will smoothly switch on and off them depending on the active communication graph during the merging phase. The simulation in the next section are performed to show the effectiveness of such mixed architecture.

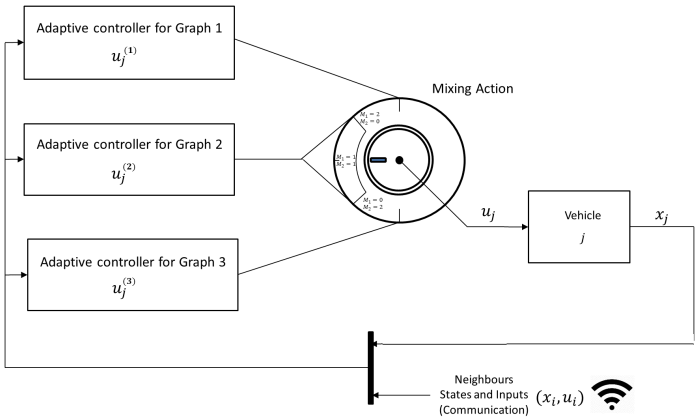

Figure 4.4: The switching adaptive control for vehicle k

To formalize the mixing idea, let us consider the following control action for vehicle $2, 4, \ldots$

$$\begin{aligned} u_{2i}(t) = \; & \mathcal{M}_1(t)(k'_{2i,2i-1}(t)\tfrac{x_{2i-1}(t)}{2} + l_{2i,2i-1}(t)\tfrac{u_{2i-1}(t)}{2} + k'_{2i}(t)\tfrac{e_{2i,2i-1}(t)}{2}) \\ & + \mathcal{M}_2(t)(k'_{2i,2i+1}(t)\tfrac{x_{2i+1}(t)}{2} \\ & + k'_{2i}(t)\tfrac{e_{2i,2i+1}(t)}{2}) \end{aligned}$$

where $\mathcal{M}_1(t)$ and $\mathcal{M}_2(t)$ are time-varying values that smoothly transit through 2-1-0 and 0-1-2 respectively during the different phases of the merging. The transition time is of around 5 s. In fact, it is possible to notice that eq. (4.22) embeds all possible control actions u_2 during all phases. In particular, in graph 1 we have $\mathcal{M}_1(t) = 2$ and $\mathcal{M}_2(t) = 0$, in graph 2 we have $\mathcal{M}_1(t) = 1$ and $\mathcal{M}_2(t) = 1$, and in graph 3 we have $\mathcal{M}_1(t) = 0$ and $\mathcal{M}_2(t) = 2$. Similarly, the adaptive gains for the same vehicle can be calculated according to the following smooth version of the adaptive laws

$$\begin{aligned} \dot{k}'_{2i,2i-1}(t) &= -\gamma_k b'_m P(\mathcal{M}_1(t)[e_{2i,2i-1}(t)] + \mathcal{M}_2(t)[e_{2i,2i+1}(t)])x'_{2i-1}(t) \\ \dot{k}'_{2i,2i+1}(t) &= -\gamma_k b'_m P(\mathcal{M}_1(t)[e_{2i,2i-1}(t)] + \mathcal{M}_2(t)[e_{2i,2i+1}(t)])x'_{2i+1}(t) \\ \dot{k}'_{2i}(t) &= -\gamma_k b'_m P(\mathcal{M}_1(t)[e_{2i,2i-1}(t)] + \mathcal{M}_2(t)[e_{2i,2i+1}(t)]) \\ &\quad (\mathcal{M}_1(t)[e_{2i,2i-1}(t)] + \mathcal{M}_2(t)[e_{2i,2i+1}(t)])' \\ \dot{l}_{2i,2i-1}(t) &= -\gamma_l b'_m P(\mathcal{M}_1(t)[e_{2i,2i-1}(t)] + \mathcal{M}_2(t)[e_{2i,2i+1}(t)])u_{2i-1}(t) \\ \dot{l}_{2i,2i+1}(t) &= -\gamma_l b'_m P(\mathcal{M}_1(t)[e_{2i,2i-1}(t)] + \mathcal{M}_2(t)[e_{2i,2i+1}(t)])u_{2i+1}(t). \end{aligned} \quad (4.23)$$

The same reasoning can be applied to all other vehicles.

4.3.4. Results

For the merging maneuver, Figs. 4.5, 4.7 and 4.8 show the response of p_i, v_i and a_i, respectively. Fig. 4.6 shows the relative distances of the vehicles from vehicle 1. In Fig. 4.5, we can observe, in the interval 0-50 seconds (graph 1), that vehicles 3 and 2 are maintaining a distance from vehicle 1 and align with each other; at the same time vehicle

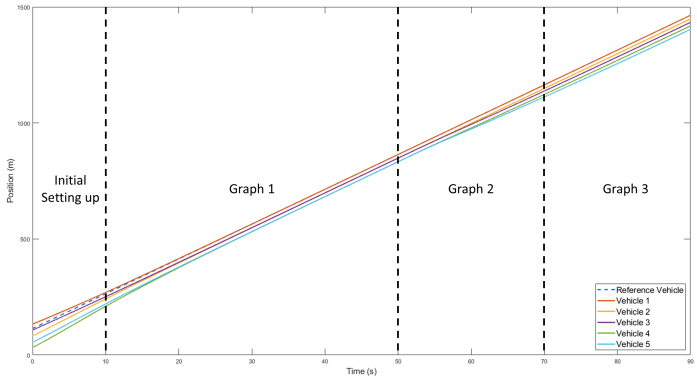

Figure 4.5: Merging: position response

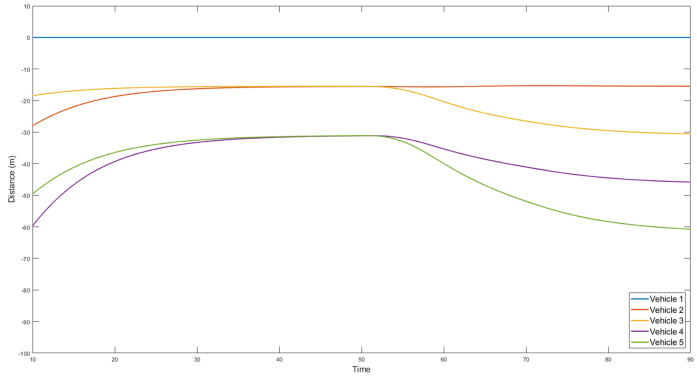

Figure 4.6: Merging: relative distances with respect to Vehicle 1

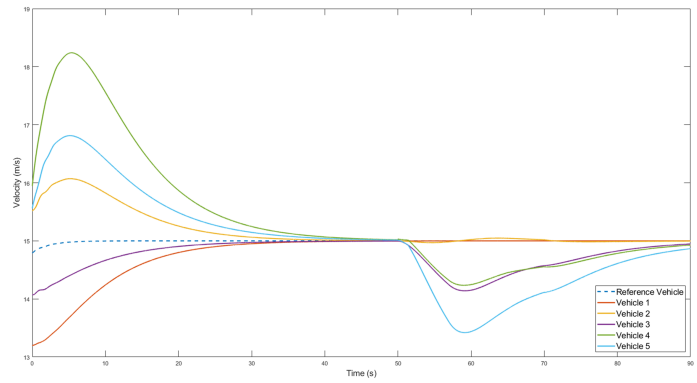

Figure 4.7: Merging: velocity response

1 synchronize to the virtual leading dynamics. During this time it can be seen that the velocity of vehicle 2 is greater than the velocity of vehicles 3 and 1 because it aligns with vehicle 3 which was initially ahead. Similarly, vehicles 4 and 5 are maintaining

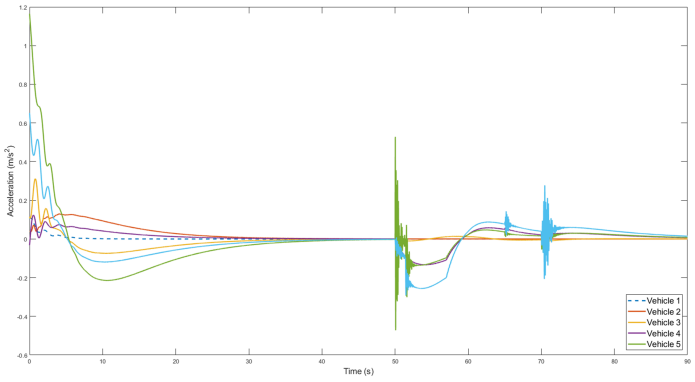

Figure 4.8: Merging: acceleration response

a distance from vehicle 2, hence the velocities of vehicle 5 remains close to velocity of vehicle 2 and vehicle 4 aligns itself to vehicle 5 and thus has the highest velocity at that time. Then, in the interval 50-70 seconds (graph 2), vehicle 3 creates a gap with vehicle 1 in order to allow vehicle 2 to merge and vehicle 5 creates a gap with vehicle 3 so that vehicle 4 can merge. Finally, in the interval 70-90 seconds (graph 3), the final formation is achieved.

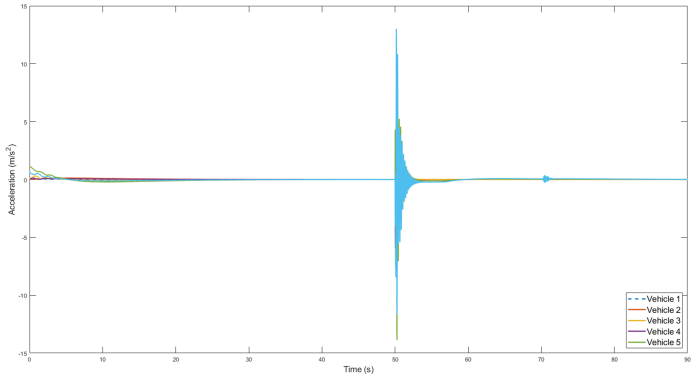

Figure 4.9: Merging: acceleration response without mixing

To show the effectiveness of mixing as compared to switching, Fig. 4.9 shows the acceleration response (for the same maneuver) when there is no mixing: as compared to Fig. 4.8 it can be clearly seen that the peak at 50 seconds is of almost an order of magnitude larger. Hence, it is clear from the figures that the input response is much smoother and with smaller peaks when the mixing architecture is implemented.

The proposed approach can be applied not only to merging, but also to splitting, which is the dual maneuver (the vehicles are in a unique platoon initially, and split in two platoons). The maneuver is organized as:

- **0-15 s:** vehicles 1, 2, 3, 4 and 5 aligns in a platoon formation.
- **15-50 s:** vehicle 3 aligns with vehicle 2 and vehicle 4 aligns with vehicle 5 while the vehicles 1, 3 and 5 maintains required distance with each other.
- **50-80 s:** vehicle 5 follows vehicle 3 which follows vehicle 1 maintaining the desired distance, whereas in a separate platoon vehicle 4 follows vehicle 2 maintaining desired distance.

Figs. 4.10, 4.12 and 4.13 show the response of p_i, v_i and u_i, respectively. Fig. 4.11 shows the relative distances of the vehicles from vehicle 1. The manuever is achieved smoothly in a synchronized way.

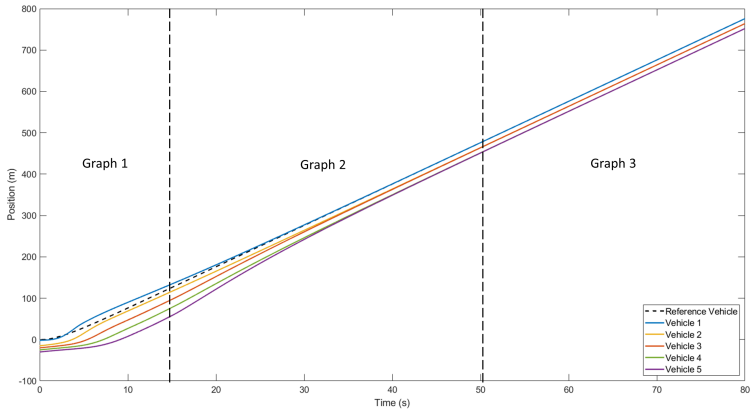

Figure 4.10: Splitting: Position response

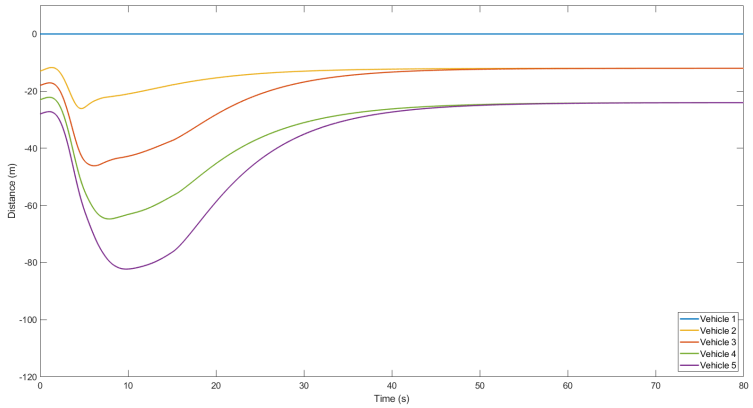

Figure 4.11: Splitting: relative distances with respect to vehicle 1

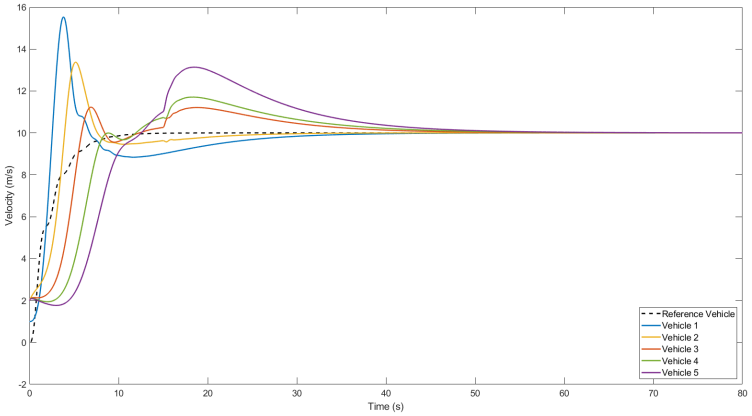

Figure 4.12: Splitting: velocity response

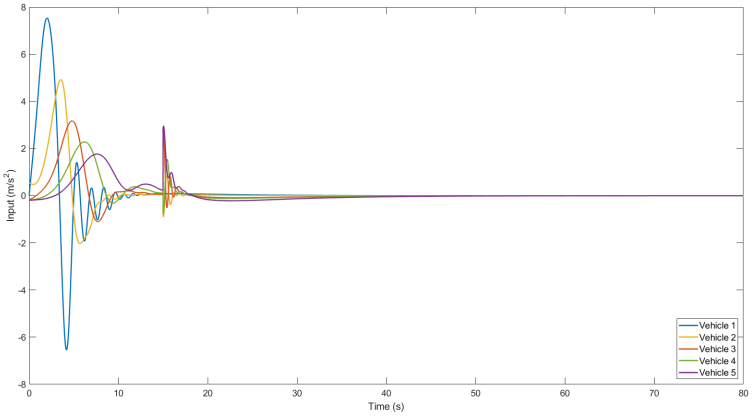

Figure 4.13: Splitting: input response

5

Platoon cohesiveness under heterogeneity (Vehicle Following)

In this chapter problems related to the vehicle following are looked upon. First the description of vehicle model is looked upon, on which analysis is done to find the saturation bounds for the leading vehicle. The saturation bounds are then implemented on the vehicle, and simulations are carried out in later part of this chapter.

5.1. CACC System Structure

Consider a heterogeneous platoon with M vehicles. Fig. 5.1 shows the platoon where v_i and d_i represent the velocity (m/s) of vehicle i, and the distance (m) between vehicle i and its preceding vehicle $i-1$, respectively. Furthermore, each vehicle in the platoon can only communicate with its preceding vehicle via wireless communication. The main goal of every vehicle in the platoon, except the leading vehicle, is to maintain a desired distance $d_{r,i}$ between itself and its preceding vehicle. Consistently with most CACC literature, we will consider a one-vehicle look-ahead topology [3]. Extension to multiple-vehicle look-ahead topologies is in principle possible using the tools of [29].

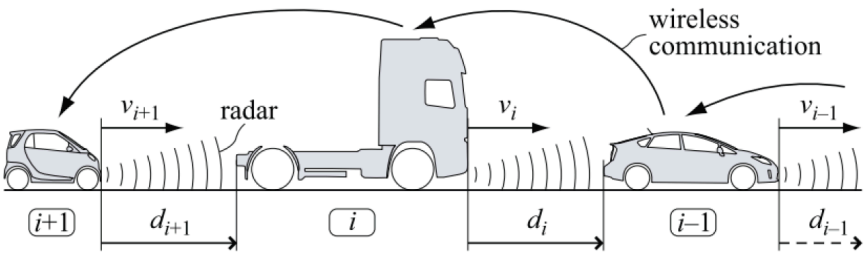

Figure 5.1: CACC-equipped heterogeneous vehicle platoon ([3])

A constant time headway (CTH) spacing policy is adopted to regulate the spacing be-

tween the vehicles, implemented by defining $d_{r,i}$ as:

$$d_{r,i}(t) = r_i + hv_i(t) \ , \ i \in S_M$$

where r_i is the standstill distance (m), h the time head-away (s), and $S_M = \{i \in \mathbb{N} | \ 1 \leq i \leq M\}$ with $i = 0$ reserved for the platoon's leader (leading vehicle). It is now possible to define the spacing error (m) of the i^{th} vehicle

$$e_i(t) = d_i(t) - d_{r,i}(t) \tag{5.1}$$
$$= (q_{i-1}(t) - q_i(t) - L_i) - (r_i + hv_i(t)) \tag{5.2}$$

with q_i and L_i representing vehicle i's rear-bumper position (m) and length (m), respectively.

The control objective is to regulate e_i to zero for all $i \in S_M$. The following model, derived by [3], is used to represent the vehicles in the platoon

$$\begin{pmatrix} \dot{d}_i \\ \dot{v}_i \\ \dot{a}_i \end{pmatrix} = \begin{pmatrix} v_{i-1} - v_i \\ a_i \\ -\frac{1}{\tau_i} a_i + \frac{1}{\tau_i} u_i \end{pmatrix}, \ i \in S_M \tag{5.3}$$

with a_i and u_i representing the acceleration (m/s^2) and external input (m/s^2) of the i^{th} vehicle, and τ_i (s) representing the vehicle's driveline time constant. For the time being, let us focus on the unsaturated case, while the saturated case will be covered in the next section.

Substituting (5.1) in (5.3) we obtain the state space system

$$\begin{pmatrix} \dot{e}_i \\ \dot{v}_i \\ \dot{a}_i \end{pmatrix} = \begin{pmatrix} 0 & -1 & -h \\ 0 & 0 & 1 \\ 0 & 0 & -\frac{1}{\tau_i} \end{pmatrix} \begin{pmatrix} e_i \\ v_i \\ a_i \end{pmatrix} + \begin{pmatrix} 1 \\ 0 \\ 0 \end{pmatrix} v_{i-1} + \begin{pmatrix} 0 \\ 0 \\ \frac{1}{\tau_i} \end{pmatrix} u_i. \tag{5.4}$$

At this point, we define the leading vehicle's model as

$$\begin{pmatrix} \dot{e}_0 \\ \dot{v}_0 \\ \dot{a}_0 \end{pmatrix} = \begin{pmatrix} 0 & 0 & 0 \\ 0 & 0 & 1 \\ 0 & 0 & -\frac{1}{\tau_0} \end{pmatrix} \begin{pmatrix} e_0 \\ v_0 \\ a_0 \end{pmatrix} + \begin{pmatrix} 0 \\ 0 \\ \frac{1}{\tau_0} \end{pmatrix} u_0. \tag{5.5}$$

The leading vehicle's model does not necessarily represent an actual vehicle, but rather it represents some desired dynamics to which all vehicles in the platoon should homogenize. Standard approaches to platooning had assumed all vehicles are already homogeneous, i.e. with the same dynamics τ_0 [3, 45]. Removing the homogeneous assumption implies considering that $\forall i \in S_M$, τ_i can be represented as

$$\tau_i = \tau_0 + \Delta\tau_i \tag{5.6}$$

where, $\Delta\tau_i$ is a perturbation of vehicle i's driveline dynamics from τ_0. Two approaches can be used to address $\Delta\tau_i$: the first one is that $\Delta\tau_i$ is perfectly known, leading to a

robust control approach; the second one is that $\Delta\tau_i$ is an unknown parameter, leading to an adaptive control approach. The main idea behind [21] is that all vehicles can homogenize to (5.5) in an adaptive way.

Consequently, the model of a vehicle in a heterogeneous platoon is obtained using (5.6) in the third equation of (5.4)

$$\dot{a}_i = -\frac{1}{\tau_0}a_i + \frac{1}{\tau_0}\left[u_i + \Omega_i^*\phi_i\right], \tag{5.7}$$

where $\Omega_i^* = -\frac{\Delta\tau_i}{\tau_i}$ is an unknown ideal constant scalar parameter, and $\phi_i = (u_i - a_i)$ is the known scalar regressor. Using (5.7) in (5.4), we can define the vehicle model as the uncertain LTI of the following form

$$\begin{aligned}\begin{pmatrix}\dot{e}_i\\ \dot{v}_i\\ \dot{a}_i\end{pmatrix} &= \begin{pmatrix}0 & -1 & -h\\ 0 & 0 & 1\\ 0 & 0 & -\frac{1}{\tau_0}\end{pmatrix}\begin{pmatrix}e_i\\ v_i\\ a_i\end{pmatrix} + \begin{pmatrix}1\\ 0\\ 0\end{pmatrix}v_{i-1}\\ &\quad + \begin{pmatrix}0\\ 0\\ \frac{1}{\tau_0}\end{pmatrix}\left[u_i + \Omega_i^*\phi_i\right],\ \forall i \in S_M.\end{aligned} \tag{5.8}$$

5.2. Engine-constrained Control

Under the baseline conditions of identical vehicles ($\Omega_i^* = \tau_0,\ \forall i \in S_M$), [3] derived the following CACC control

$$h\dot{u}_{i,bl} = -u_{i,bl} + \xi_{i,bl},\quad \forall i \in \{0\} \cup S_M \tag{5.9}$$

$$\xi_{i,bl} = \begin{cases} K_p e_i + K_d \dot{e}_i + u_{i-1,bl}, & \forall i \in S_M \\ u_r & i = 0, \end{cases} \tag{5.10}$$

where $\xi_{i,bl}$ is an auxiliary input u_r is the platoon input representing the desired acceleration of the leading vehicle, and $u_{i-1,bl}$ is received over the wireless communication between vehicle i and $i-1$.

Therefore, we can now design reference dynamics (to whose behaviour (5.4) and (5.5) should converge) as an "ideal" homogeneous platoon with $\Omega_i^* = 0$ and $u_i = u_{i,bl}$, $\forall i \in S_M$. Substituting (5.9) in (5.8) and extending the state vector with $u_{i,bl}$ we obtain the fol-

lowing reference model dynamics

$$\begin{pmatrix} \dot{e}_{i,m} \\ \dot{v}_{i,m} \\ \dot{a}_{i,m} \\ \dot{u}_{i,bl} \end{pmatrix} = \underbrace{\begin{pmatrix} 0 & -1 & -h & 0 \\ 0 & 0 & 1 & 0 \\ 0 & 0 & -\frac{1}{\tau_0} & \frac{1}{\tau_0} \\ \frac{K_p}{h} & -\frac{K_d}{h} & -K_d & -\frac{1}{h} \end{pmatrix}}_{A_m} \underbrace{\begin{pmatrix} e_{i,m} \\ v_{i,m} \\ a_{i,m} \\ u_{i,bl} \end{pmatrix}}_{x_{i,m}} + \underbrace{\begin{pmatrix} 1 & 0 \\ 0 & 0 \\ 0 & 0 \\ \frac{K_d}{h} & \frac{1}{h} \end{pmatrix}}_{B_w} \underbrace{\begin{pmatrix} v_{i-1} \\ u_{i-1,bl} \end{pmatrix}}_{w_i}, \ \forall i \in S_M \tag{5.11}$$

where $x_{i,m}$ and w_i are vehicle i's reference state vector and exogenous input vector, respectively. Consequently, (5.11) is of the following form

$$\dot{x}_{i,m} = A_m x_{i,m} + B_w w_i, \forall i \in S_M. \tag{5.12}$$

Furthermore, the leading vehicle model becomes

$$\begin{pmatrix} \dot{e}_0 \\ \dot{v}_0 \\ \dot{a}_0 \\ \dot{u}_0 \end{pmatrix} = \underbrace{\begin{pmatrix} 0 & 0 & 0 & 0 \\ 0 & 0 & 1 & 0 \\ 0 & 0 & -\frac{1}{\tau_0} & \frac{1}{\tau_0} \\ 0 & 0 & 0 & -\frac{1}{h} \end{pmatrix}}_{A_r} \underbrace{\begin{pmatrix} e_0 \\ v_0 \\ a_0 \\ u_0 \end{pmatrix}}_{x_0} + \underbrace{\begin{pmatrix} 0 \\ 0 \\ 0 \\ \frac{1}{h} \end{pmatrix}}_{B_r} u_r. \tag{5.13}$$

The first question is how to modify (5.9) in the presence of uncertain perturbations as in (5.6): this question will be answered in Sect. 5.2.1. The second question is how to modify (5.9) and the (5.13) in the presence of saturation constraints: this question will be answered in Sect. 5.2.2.

5.2.1. Model reference dynamics

The dynamics (5.12) can used as a reference model for the uncertain platoon's dynamics described by (5.5) and (5.8). With this scope in mind, we can augment the baseline controller (5.9) with an adaptive term

$$u_i = u_{i,bl} + u_{i,ad} \tag{5.14}$$

where $u_{i,bl}$ is the baseline controller defined in (5.9) and $u_{i,ad}$ the adaptive augmentation controller (to be constructed).

Replacing (5.14) into (5.5) and (5.8), and augmenting the state vector with $u_{i,bl}$ re-

sults in

$$\begin{pmatrix} \dot{e}_i \\ \dot{v}_i \\ \dot{a}_i \\ \dot{u}_{i,bl} \end{pmatrix} = \begin{pmatrix} 0 & -1 & -h & 0 \\ 0 & 0 & 1 & 0 \\ 0 & 0 & -\frac{1}{\tau_0} & \frac{1}{\tau_0} \\ \frac{K_p}{h} & -\frac{K_d}{h} & -K_d & -\frac{1}{h} \end{pmatrix} \underbrace{\begin{pmatrix} e_i \\ v_i \\ a_i \\ u_{i,bl} \end{pmatrix}}_{x_i} + \begin{pmatrix} 1 & 0 \\ 0 & 0 \\ 0 & 0 \\ \frac{K_d}{h} & \frac{1}{h} \end{pmatrix} \begin{pmatrix} v_{i-1} \\ u_{i-1} \end{pmatrix} + \underbrace{\begin{pmatrix} 0 \\ 0 \\ \frac{1}{\tau_0} \\ 0 \end{pmatrix}}_{B_u} \left[u_{i,ad} + \Omega_i^* \phi_i \right], \ \forall i \in S_M \tag{5.15}$$

which can be written in the following form:

$$\dot{x}_i = A_m x_i + B_w w_i + B_u [u_{i,ad} + \Omega_i^* \phi_i]. \tag{5.16}$$

With the leading vehicle's model as in (5.13), the adaptive augmentation controller can be designed to compensate for the unknown term $\Omega_i^* \phi_i$

$$u_{i,ad} = -\hat{\Omega}_i \phi_i \tag{5.17}$$

where $\hat{\Omega}_i$ is the estimate of Ω_i^*. Replacing (5.17) in (5.16) gives

$$\dot{x}_i = A_m x_i + B_w w_i - B_u \tilde{\Omega}_i^T \phi_i \tag{5.18}$$

where $\tilde{\Omega}_i = \hat{\Omega}_i - \Omega_i^*$ is the parameter estimation's error vector. Defining the state tracking error as

$$\tilde{x}_i = x_i - x_{i,m} \tag{5.19}$$

The following dynamics are obtained

$$\dot{\tilde{x}}_i = A_m \tilde{x}_i + B_u \tilde{\Omega}_i \phi_i \tag{5.20}$$

Remark 5.1. Using the model reference adaptive tools in [21], each vehicle can implement an adaptive law to drive $\tilde{x}_i$ to zero, thus converging to the behavior of the nominal vehicle (the dynamics of the nominal vehicle represent the reference model). It is important to notice that each vehicle can calculate $\tilde{x}_i$ by implementing a copy of the nominal vehicle.

In the following, we want to show how such reference model can be modified in order to handle saturation constraints.

5.2.2. Saturated case

Let us design a stable reference model as the model of a nominal vehicle with appropriately designed saturation: in other words, we assume that each vehicle implements a copy of the reference model according to the following lines.

First, let us define $\xi_{i,m} = K_p e_i + K_d \dot{e}_i + u_{i-1,m}$.
Then

$$h\dot{u}_{i,m} = \begin{cases} 0 & \text{if } u_{i,m} = u_{max,m} \text{ and } -u_{i,m} + \xi_{i,m} \geq 0 \\ -u_{i,m} + \xi_{i,m} & \text{if } u_{min,m} < u_{i,m} < u_{max,m} \\ & \text{or } u_{i,m} = u_{max,m} \text{ and } -u_{i,m} + \xi_{i,m} < 0 \\ & \text{or } u_{i,m} = u_{min,m} \text{ and } -u_{i,m} + \xi_{i,m} > 0 \\ 0 & \text{if } u_{i,m} = u_{min,m} \text{ and } -u_{i,m} + \xi_{i,m} \leq 0 \end{cases} \tag{5.21}$$

where $u_{min,m}$ and $u_{max,m}$ are the saturation levels to be designed. Such saturation levels guarantee that the reference model is not too demanding, in the sense that the vehicles will not hit their saturation bounds. It has to be noticed that (5.21) will provide an anti-windup action: in fact, $\dot{u}_{i,m} = 0$ whenever the saturation bounds are hit. That is, $u_{i,m}$ will stay at the saturation level, and will immediately exit the saturation whenever $u_{i,m} = u_{max,m}$ and $-u_{i,m} + \xi_{i,m} < 0$, or $u_{i,m} = u_{min,m}$ and $-u_{i,m} + \xi_{i,m} > 0$.

When saturation is hit, find γ such that $-\gamma u_{i,m} + K_p e_i + K_d \dot{e}_i + u_{i-1,m} = 0$. This leads to the saturated dynamics

$$\begin{pmatrix} \dot{e}_{i,m} \\ \dot{v}_{i,m} \\ \dot{a}_{i,m} \\ \dot{u}_{i,bl} \end{pmatrix} = \underbrace{\begin{pmatrix} 0 & -1 & -h & 0 \\ 0 & 0 & 1 & 0 \\ 0 & 0 & -\frac{1}{\tau_0} & \frac{1}{\tau_0} \\ \frac{K_p}{h} & -\frac{K_d}{h} & -K_d & -\frac{\gamma}{h} \end{pmatrix}}_{A_m^\gamma} \underbrace{\begin{pmatrix} e_{i,m} \\ v_{i,m} \\ a_{i,m} \\ u_{i,bl} \end{pmatrix}}_{x_{i,m}} + \underbrace{\begin{pmatrix} 1 & 0 \\ 0 & 0 \\ 0 & 0 \\ \frac{K_d}{h} & \frac{1}{h} \end{pmatrix}}_{B_w} \underbrace{\begin{pmatrix} v_{i-1} \\ u_{i-1,bl} \end{pmatrix}}_{w_i}, \ \forall i \in S_M \tag{5.22}$$

Let us now to design $u_{min,m}$ and $u_{max,m}$. We can prove that $u_{ad,i} \in [\bar{\Omega}(u_{i,min} - u_{i,max}), \bar{\Omega}(u_{i,max} - u_{i,min})]$, where $\bar{\Omega} = \max(|\Omega_{i,min}|, |\Omega_{i,max}|)$, with $\Omega_{i,min}$ and $\Omega_{i,max}$ the minimum and maximum bounds on $-\Delta\tau_i/\tau_i$, and $u_{i,min}$ and $u_{i,max}$ the actual saturation levels of vehicle i.

We used the fact that $\phi_i = sat(u_i) - a_i$ belongs to $[u_{i,min} - u_{i,max}, u_{i,max} - u_{i,min}]$ by exploiting the properties of a first order system with input sat(u_i) and output a_i. After establishing these bounds, we can say

$$u_{min,m} + \bar{\Omega}(u_{i,min} - u_{i,max}) < u_i < u_{max,m} + \bar{\Omega}(u_{i,min} - u_{i,max}) \tag{5.23}$$

where the result in [21] that $u_{i,bl}$ will converge to $u_{i,m}$ has been used. From (5.23), one can design $u_{min,m}$ and $u_{max,m}$

$$u_{min,m} \geq u_{i,min} - \bar{\Omega}(u_{i,min} - u_{i,max}) \tag{5.24}$$

$$u_{max,m} \leq u_{i,max} + \bar{\Omega}(u_{i,max} - u_{i,min}) \tag{5.25}$$

Remark 5.2. The bounds (5.24) and (5.25) are such that the saturation bounds of the vehicles will not be hit. This implies that the nominal vehicle cannot express its full potentialities, which is in line with the studies [57, 58], i.e. saturation can be systematically eliminated only at the price of losing performance. Note that, in order to find $\bar{\Omega}$ one must find bounds to the uncertainty $-\Delta\tau_i/\tau_i$: the more the heterogeneity of the vehicle, the more conservative the bounds. If the platoon would be completely homogeneous, (5.24) and (5.25) would become $u_{min,m} \geq u_{i,min}$ and $u_{max,m} \leq u_{i,max}$, i.e. the saturation bounds of the reference model could be selected to be the same as the saturation of the vehicles.

The dynamics of the vehicle with saturation now become

$$\dot{x}_i = A_m^{\gamma} x_i + B_w w_i + B_u[sat(u_{i,ad}) + \Omega^* \phi_i] \tag{5.26}$$

and

$$h\dot{u}_{i,bl} = \begin{cases} -\gamma u_{i,bl} + \xi_{i,bl} & \text{if } u_{i,m} = u_{min,m} \text{ and } -u_{i,m} + \xi_{i,m} \geq 0 \\ -u_{i,bl} + \xi_{i,bl} & \text{if } u_{min,m} < u_{i,m} < u_{max,m} \\ & \quad \text{or } u_{i,m} = u_{max,m} \text{ and } -u_{i,m} + \xi_{i,m} < 0 \\ & \quad \text{or } u_{i,m} = u_{min,m} \text{ and } -u_{i,m} + \xi_{i,m} > 0 \\ -\gamma u_{i,bl} + \xi_{i,bl} & \text{if } u_{i,m} = u_{min,m} \text{ and } -u_{i,m} + \xi_{i,m} \leq 0 \end{cases} \tag{5.27}$$

The last equation implies that $u_{i,bl}$ follows a similar law as $u_{i,m}$: furthermore, when $u_{i,bl} \to u_{i,m}$ the two inputs will saturate synchronously.

The following dynamics are obtained

$$\dot{\tilde{x}}_i = \begin{cases} A_m^{\gamma} \tilde{x}_i + B_u \tilde{\Omega}_i \phi_i & \text{if } u_{i,m} = u_{min,m} \text{ and } -u_{i,m} + \xi_{i,m} \geq 0 \\ A_m \tilde{x}_i + B_u \tilde{\Omega}_i \phi_i & \text{if } u_{min,m} < u_{i,m} < u_{max,m} \\ & \quad \text{or } u_{i,m} = u_{max,m} \text{ and } -u_{i,m} + \xi_{i,m} < 0 \\ & \quad \text{or } u_{i,m} = u_{min,m} \text{ and } -u_{i,m} + \xi_{i,m} > 0 \\ A_m^{\gamma} \tilde{x}_i + B_u \tilde{\Omega}_i \phi_i & \text{if } u_{i,m} = u_{min,m} \text{ and } -u_{i,m} + \xi_{i,m} \leq 0 \end{cases} \tag{5.28}$$

and the adaptive law (5.17) and

$$\dot{\tilde{\Omega}}_i = \Gamma_\Omega \phi_i \tilde{x}_i P_m B_u \tag{5.29}$$

with P_m a common symmetric positive-definite matrix satisfying

$$A_m^T P_m + P_m A_m < -Q_m \tag{5.30}$$

$$A_m^{\gamma\,T} P_m + P_m A_m^{\gamma} < -Q_m \tag{5.31}$$

with $Q_m = Q_m^T > 0$ a design matrix. Stability cannot be studied here due to space limitations (we aim to address this point in an extended version of the work). Let us

show the effectiveness of the approach via simulations.

Remark 5.3. From (5.30) and (5.31) it can be seen that stability relies on a common Lyapunov function between A_m and A_m^γ (i.e. between the unsaturated and saturated dynamics). A common Lyapunov function allows arbitrary switching among such dynamics, but also implies that A_m^γ (which can be eventually time-varying) should be close enough to A_m for P_m to exist. This implies that the unsaturated input in (5.27) should not be too far from the saturation bound. Using similar ideas as in [21], one might look for multiple Lyapunov functions for the different regimes, resulting in average dwell time constraints when switching from the saturated to the unsaturated dynamics.

Remark 5.4. The bounds in (5.23) are necessarily conservative for two reasons: they are based on the worst-case uncertainty for Ω_i; they are based in the worst-case excursion for $\phi_i = sat(u_i) - a_i$. To decrease conservativeness, an efficiency factor can be added to (5.23). In simulations, we verified that an efficiency factor of $2 \sim 3$ reduces conservativeness while still respecting all saturation bounds.

5.3. Simulation and Results for unidirectional case

In this section simulations are carried out for the proposed strategy, and the obtained results are then discussed.

5.3.1. Scenario 1

For testing the algorithm a platoon of 5+1 (5 followers and a leader) vehicles is considered, the leader vehicle would be denoted as vehicle 0. The leading vehicle is provided an input in such a manner that , it has a hard acceleration phase initially (with stop-and-go phase), followed by a deceleration phase which can be seen in figure 5.3.This is supposed to test, cohesiveness of the platoon during such acceleration and deceleration.

To test the algorithm three scenarios are considered:

- No saturation with standard control;
- Saturation with standard control;
- Saturation with proposed control.

5.3.2. parameters

Table 5.1 presents the platoon's characteristics.

Table 5.1: Platoon parameters, M=5, h=0.7s

i	0	1	2	3	4	5
$\tau_i(s)$	0.6	0.5	0.7	0.45	0.7	0.8
$u_{min,i}$	-0.83	-1.5	-2.5	-1.0	-2.0	-2.5
$u_{max,i}$	0.83	1.5	2.5	1.0	2.0	2.5
Ω_i^*		0.2	-0.143	0.333	-0.143	-0.25

Table 5.1 also shows the true values of the constant parametric uncertainties $\Omega_i^*,\ \forall i \in S_M$, which are unknown to the designer. However, it is assumed that the upper and lower bound of Ω_i^* are known, that can be used to design $u_{min,m}$ and $u_{max,m}$. Specifically, we have $\bar{\Omega} = 0.333$ and the worst case saturation bounds are $u_{min,m} = -1 + 0.333 * 2 = -0.333$ and $u_{max,m} = 1 - 0.333 * 2 = 0.333$. After including an efficiency factor of 2.5 as explained in Remark 5.4, we obtain the bounds -0.83 and 0.83.

The reference model (5.12) for the adaptive laws is characterized by $K_p = 0.2$ and $K_d = 0.7$. The adaptive input (5.29) is designed using (5.30) with $Q_m = 5I$ and $\Gamma_\Omega = 80$.

5.3.3. Results

The necessary results to prove the working of the developed control algorithms are presented in this section.

Fig. 5.2 shown the velocity response in case no saturation is present and the standard adaptive control of [21] is adopted. It can be seen that all vehicles properly follow

the velocity of the leader, which implies that platoon cohesiveness is attained.

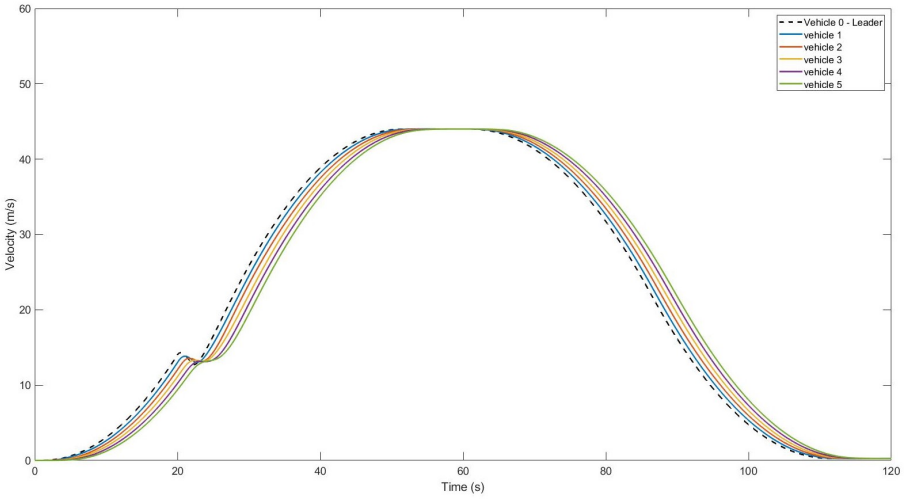

Figure 5.2: No saturation with standard control: velocity response.

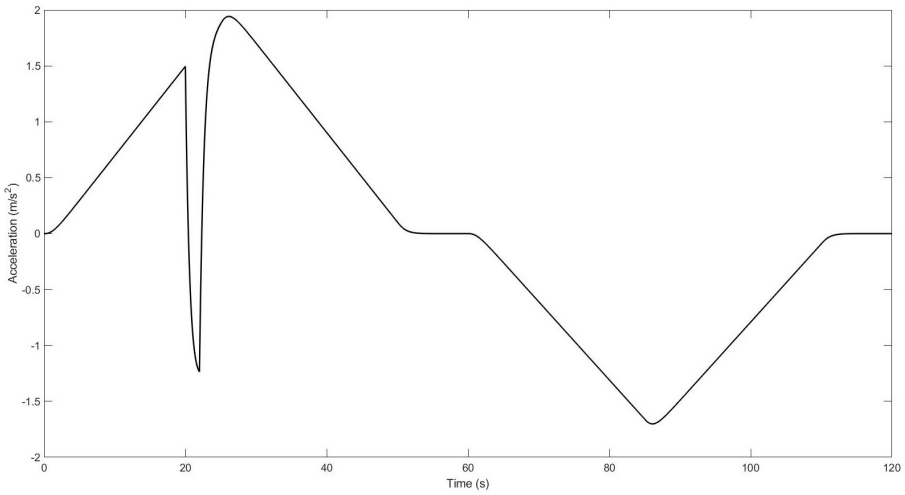

Figure 5.3: No saturation with standard control: unconstrained leader acceleration.

Fig. 5.3 shows the acceleration profile for the leader vehicle. It can be seen that at 20 secs. the acceleration value drops suddenly, brakes are applied at 20 secs to ensure that, even if brakes are applied abruptly the platoon still behaves in a proper manner; which is evident from figures 5.2 and 5.4

Fig. 5.4 shows that the distances between the vehicles increases with the increase in velocity of the vehicles, which is desired for safety reasons (the reason to use time headway in spacing policy). Through fig. 5.4 it can also be seen that at no point of time the vehicles cross each other i.e. there is no vehicle crashes into the other vehicle while performing vehicle following.

Now saturation for the respective vehicles are set, keeping the same control action.

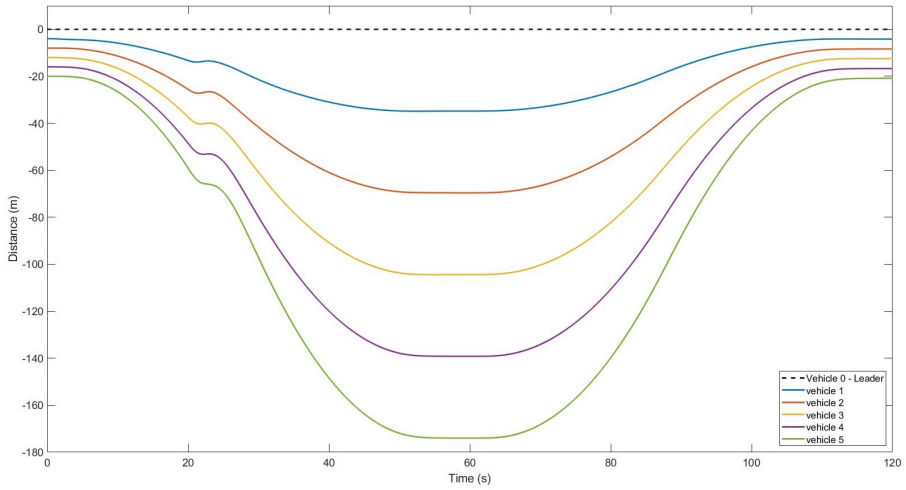

Figure 5.4: No saturation with standard control: relative distance with respect to vehicle 0

This is done to check how would the vehicles in the platoon behave if they have different acceleration potentials.

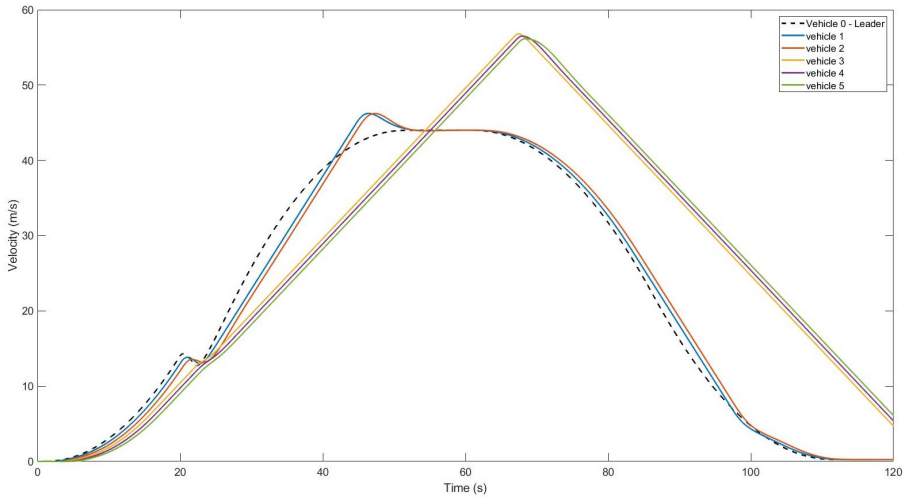

Figure 5.5: Saturation with standard control: velocity response.

From Fig. 5.5 It is evident that vehicle 3 (which has very harsh saturation bounds, cf. Table 5.2) is incapable of following the follower speed, which implies that the platoon is not cohesive anymore. Vehicles 4 and 5 will clearly follow vehicle 3 with lost cohesiveness.

The triangular shape of the velocity profile for vehicle 3 is the typical shape arising from the so-called wind-up phenomenon, highlighted in Fig. 5.7. Note that, even though vehicle 3 brakes at around time 68 seconds, its braking possibilities are also constrained: therefore, vehicle 3 will eventually collide at around 80 seconds with vehicle 2, as it can be seen from the distance plot in Fig. 5.7.

It is clear that standard control is insufficient for tackling the real case scenario (with

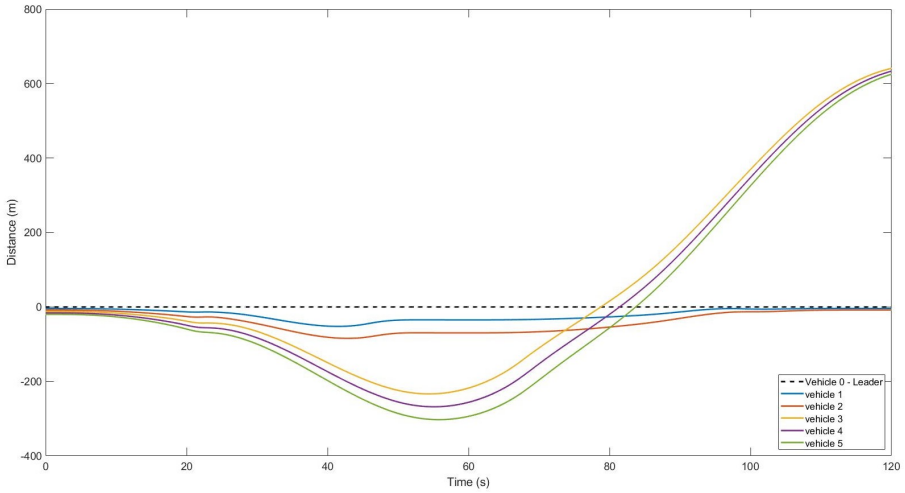

Figure 5.6: Saturation with standard control: relative distance with respect to vehicle 0

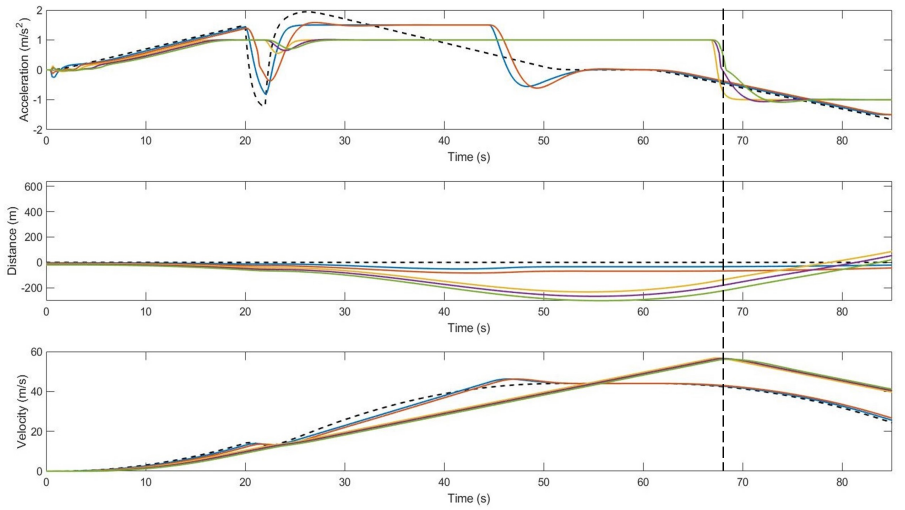

Figure 5.7: Saturation with standard control: wind up and loss of cohesiveness

vehicles having different acceleration potential bounds). Thus we now implement the proposed strategy to saturate the leader vehicle.

Finally, in the simulation of Fig. 5.8, the proposed control action is applied. It can be seen that this time all vehicles will maintain cohesiveness. Because of the saturation limits, cohesiveness is achieved at the price of reducing performance (the leading vehicle reaches a maximum speed of 30 m/s instead of 44 m/s): this is due to the fact that the reference model will apply saturation in order to result not too demanding for vehicles that might lose cohesiveness. This can be clearly seen from Fig. 5.9 where, as compared to Fig. 5.3 the high acceleration and deceleration peaks are chopped, thanks to the saturation applied to the leading vehicle.

Figure 5.10 shows that the vehicles do not collide with each other unlike the case seen in fig. 5.7. Hence, the spacing between the vehicles remain as desired.

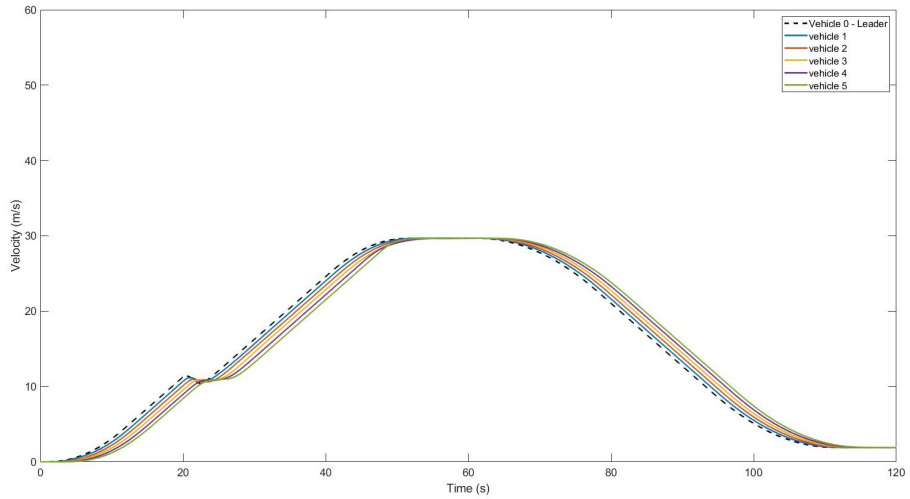

Figure 5.8: Saturation with proposed control: velocity response.

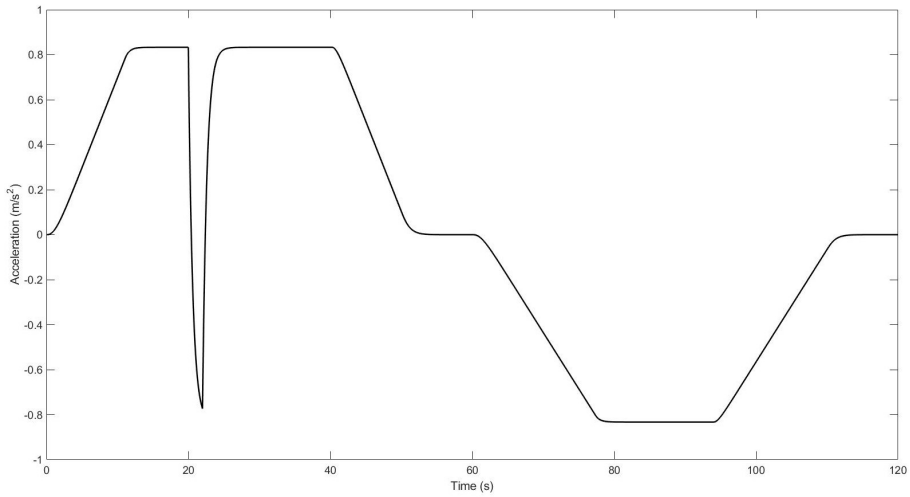

Figure 5.9: Saturation with proposed control: constrained leader acceleration.

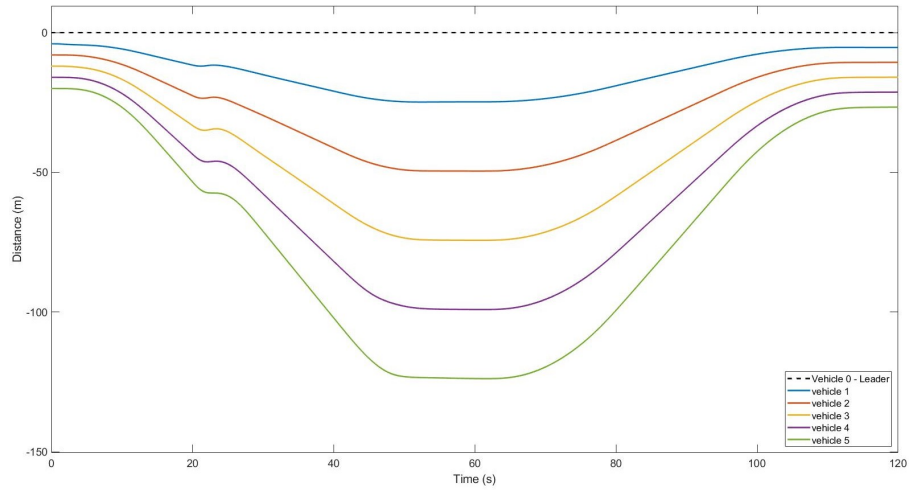

Figure 5.10: Saturation with proposed control: relative distance with respect to vehicle 0.

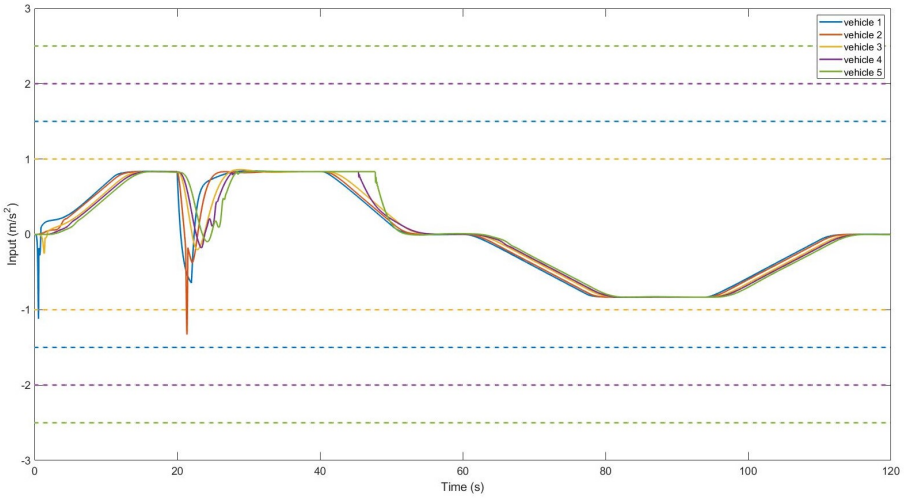

Figure 5.11: Saturation with standard control: input response

In fig. 5.11 the dotted lines represent the potential bounds of the vehicles and the solid lines represents the control input of the vehicles with time. It can be seen that the input calculated by the control algorithm always stays inside the potential limits (bounds) of the vehicles, hence the proposed strategy provides the desired results.

5.3.4. Scenario 2

In this scenario a homogeneous platoon is considered with again a 5+1 (5 followers and a leader) configuration. The leading vehicle is now provided with a ramp input. As the saturation for the vehicles are implemented, the input increases and then saturates at the potential limit of the vehicle. We now introduce a positive impulse in the distance between vehicle 2 and 3 (the position of vehicle 3 is pushed back). This is done to mimic the effect of a disturbance that can occur in the platoon (possible reasons being error in measurement of position, slippery road etc.).

5.3.5. parameters

Table 5.2 presents the platoon's characteristics.

Table 5.2: Platoon parameters, M=5, h=0.7s

i	0	1	2	3	4	5
$\tau_i(s)$	0.6	0.6	0.6	0.6	0.6	0.6
$u_{min,i}$	-1.0	-1.0	-1.0	-1.0	-1.0	-1.0
$u_{man,i}$	1.0	1.0	1.0	1.0	1.0	1.0
Ω_i^*	0	0	0	0	0	0

Table 5.2 also shows the true values of the constant parametric uncertainties $\Omega_i^*,\ \forall i \in S_M$, which are unknown to the designer. However, we assume to know the upper and lower bound of Ω_i^*, that can be used to design $u_{min,m}$ and $u_{max,m}$. Specifically, we have $\bar{\Omega} = 0$ and the worst case saturation bounds are $u_{min,m} = -1 + 0 * 2 = -1$ and $u_{max,m} = 1 - 0 * 2 = 1$. After including an efficiency factor of 2.5 as explained in Remark 5.4, we obtain the bounds -1 and 1.
K_p and K_d. Q_m and Γ_Ω remains the same as were in the previous scenario.

5.3.6. Results

As the platoon has a continuous acceleration, the position, velocity and acceleration plots do not give any insight for the scenario. Hence, in fig. 5.12 spacing error and Input are plotted.

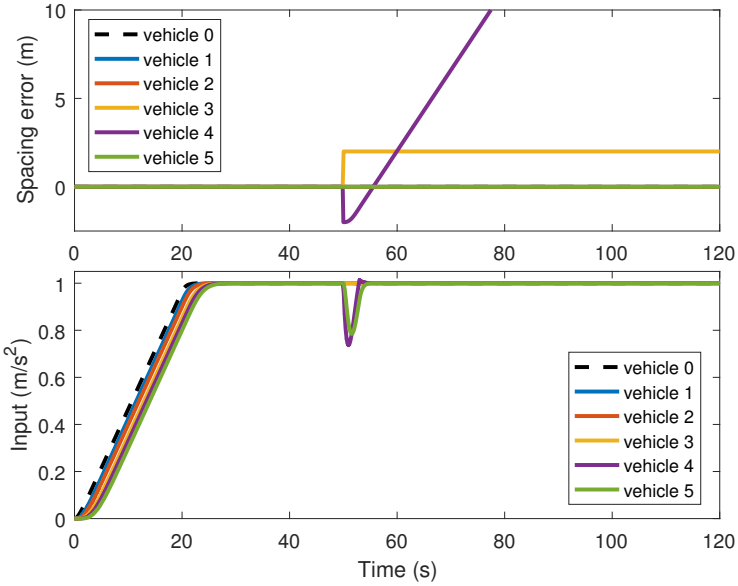

Figure 5.12: Extreme scenario with proposed unidirectional control: spacing errors and input response.

As all the vehicles have the same acceleration potential limits (homogeneous platoon) and the leader vehicle is moving forward with its maximum acceleration potential; vehicle 3 can never close the gap between it and vehicle 2. This is due to the fact that both vehicles are moving at their full potential, and hence, there is a constant gap created between them. In addition, the positive impulse causes vehicle 3 to approach vehicle 4, which slows down and then tries to catch up, but is unable to (initially negative spacing error in Fig. 5.12 which becomes positive and increases). In fact, vehicle 3 keeps maximum acceleration despite the gap being created, as it only cares about its spacing with vehicle 2 due to unidirectional interaction. Vehicle 3 is at maximum acceleration and at a higher velocity than vehicle 4, the spacing error between vehicles 3 and 4 thus keeps on increasing.

Hence, there is a need for the vehicles to act by not only looking at the vehicle in

front (predecessor vehicle), but also, at the vehicle behind (successor vehicle). In the next section a bi-directional communication vehicle model and control algorithm is proposed.

5.4. Model definition for bi-directional platooning

Consider the platoon in Fig. 5.1, where v_i and d_i represent the velocity (m/s) of vehicle i, and the spacing (m) between vehicle i and its preceding vehicle. Fig. 5.1 considers unidirectional look-ahead communication with preceding vehicle [3], whereas Fig. 5.13 considers bidirectional communication with preceding and succeeding vehicle. The goal of each vehicle in the platoon is to maintain a desired distance with the preceding vehicle (unidirectional case), or with the preceding and succeeding vehicles (bi-directional case).

A constant time headway policy regulates the spacing between vehicles, implemented by defining the look-ahead desired spacing $d_{des,f,i}$ and look-back desired spacing $d_{des,b,i}$:

$$\begin{aligned} d_{des,f,i}(t) &= r_i + hv_i(t) \\ d_{des,b,i}(t) &= r_i + hv_{i+1}(t) \ , \ i \in S_M \end{aligned}$$

where r_i is the standstill distance (m), h the time headway (s), and $S_M = \{i \in \mathbb{N} | \ 1 \leq i \leq M\}$, being M the number of vehicles and $i = 0$ reserved for the leading vehicle.

With bidirectionality, errors in both the look-ahead and look-back direction are considered, the look-ahead error being

$$\begin{aligned} e_{f,i}(t) &= d_{i-1,i}(t) - d_{des,f,i}(t) \\ &= (q_{i-1}(t) - q_i(t) - L_i) - (r_i + hv_i(t)) \end{aligned} \tag{5.32}$$

and the look-back error being

$$\begin{aligned} e_{b,i}(t) &= d_{i,i+1}(t) - d_{des,b,i}(t) \\ &= -((q_i(t) - q_{i+1}(t) - L_{i+1}) - (r_i + h_i v_{i+1}(t))) \end{aligned} \tag{5.33}$$

with, q_i and L_i representing vehicle i's rear-bumper position (m) and length (m), respectively. The quantities $d_{i-1,i}$ and $d_{i,i+1}$ represent the intervehicle distances. It is to be noted that the sign convention for the look-back error is chosen to be opposite to the look-ahead error. Finally, the total spacing error is taken as the convex combination of $e_{f,i}$ and $e_{b,i}$

$$e_i(t) = c_1 e_{f,i}(t) + c_2 e_{b,i}(t), \qquad 1 \leq i < M \tag{5.34}$$

with $c_1 \in (0, 1]$ and $c_2 = 1 - c_1$. Note that for $c_1 = 1$ and $c_2 = 0$ one would have the standard CACC unidirectional situation in which only the look-ahead spacing error is considered. For $c_1 = c_2 = 0.5$ one would have a bidirectional situation in which look-ahead and look-back errors are equally weighted. As the leading and the last vehicle can only measure look-back and look-ahead error respectively, their error is simply

$$\begin{aligned} e_0(t) &= e_{b,0}(t) = q_1(t) - q_0(t) + L_1 + r + hv_1(t) \\ e_M(t) &= e_{f,M}(t) = q_{M-1}(t) - q_M(t) - L_M - r - hv_M(t). \end{aligned}$$

The control objective is to regulate e_i to zero $\forall i \in S_M \cup \{0\}$, while ensuring string stability of the platoon. The following model is standard [3] to represent the vehicles in

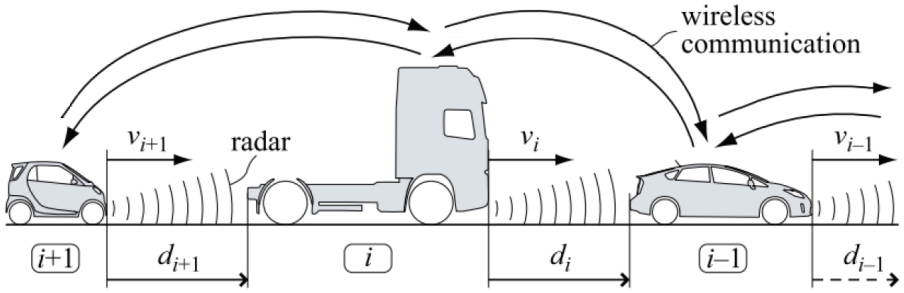

Figure 5.13: CACC-equipped heterogeneous vehicle platoon with bidirectional communication.

the platoon

$$\begin{pmatrix} \dot{d}_i \\ \dot{v}_i \\ \dot{a}_i \end{pmatrix} = \begin{pmatrix} v_{i-1} - v_i \\ a_i \\ -\frac{1}{\tau_i} a_i + \frac{1}{\tau_i} u_i \end{pmatrix}, \quad i \in S_M \cup \{0\} \tag{5.35}$$

with a_i and u_i being the acceleration (m/s^2) and input (m/s^2), and τ_i (s) being the engine time constant of the i^{th} vehicle.

The distance can be replaced by the spacing error (distance) term, the model thus can be represented by

$$\begin{aligned} \begin{pmatrix} \dot{e}_i \\ \dot{v}_i \\ \dot{a}_i \end{pmatrix} = & \begin{pmatrix} 0 & -(c_1 + c_2) & -c_1 h \\ 0 & 0 & 1 \\ 0 & 0 & -\frac{1}{\tau_i} \end{pmatrix} \begin{pmatrix} e_i \\ v_i \\ a_i \end{pmatrix} \\ & + \begin{pmatrix} c_1 & c_2 & hc_2 \\ 0 & 0 & 0 \\ 0 & 0 & 0 \end{pmatrix} \begin{pmatrix} v_{i-1} \\ v_{i+1} \\ a_{i+1} \end{pmatrix} + \begin{pmatrix} 0 \\ 0 \\ \frac{1}{\tau_i} \end{pmatrix} u_i. \end{aligned} \tag{5.36}$$

5.4.1. The CACC control structure

The control action can be designed by formulating the error dynamics. Define the error states as

$$\begin{pmatrix} e_{1,i} \\ e_{2,i} \\ e_{3,i} \end{pmatrix} = \begin{pmatrix} e_i \\ \dot{e}_i \\ \ddot{e}_i \end{pmatrix}, \quad 0 \le i \le M. \tag{5.37}$$

State-of-the-art CACC protocols design the control action assuming identical τ_i (baseline homogeneous condition) [3], so that the baseline control input (indicated with the subscript bl) can be derived from the dynamics of $e_{3,i}$, via (5.34) and (5.35).

For a detailed derivation of (5.38) Appendix C can be referred.

$$\dot{e}_{3,i} = -\frac{1}{\tau_i} e_{3,i} - \frac{1}{\tau_i} p_i + \frac{c_1}{\tau_i} u_{i-1,bl} + \frac{c_2}{\tau_i} u_{i+1,bl} + \frac{hc_2}{\tau_i} \dot{u}_{i+1,bl} \tag{5.38}$$

with $p_i = u_{i,bl} + hc_1\dot{u}_{i,bl}$.
From (5.38) it is clear that p_i should stabilize the error dynamics (5.37) while compensating for the terms $u_{i-1,bl}$, $u_{i+1,bl}$ and $\dot{u}_{i+1,bl}$. Hence, p_i is defined as

$$p_i = (k_p \; k_d \; k_{dd}) \begin{pmatrix} e_{1,i} \\ e_{2,i} \\ e_{3,i} \end{pmatrix} + c_1 u_{i-1,bl} + c_2 u_{i+1,bl} + hc_2 \dot{u}_{i+1,bl} \tag{5.39}$$

with k_p, k_d and k_{dd} being gains to be designed in order to have stability/string stability specifications. The feedforward terms $u_{i-1,bl}$, $u_{i+1,bl}$ and $\dot{u}_{i+1,bl}$ can be obtained via wireless communication with the preceding and succeeding vehicle [3].

From (5.39) the controller dynamics is given by

$$\dot{u}_{i,bl} = -\frac{1}{hc_1}u_{i,bl} + \frac{1}{hc_1}(k_p e_{1,i} + k_d e_{2,i} + k_{dd} e_{3,i}) + \frac{1}{h}u_{i-1,bl} + \frac{c_2}{hc_1}u_{i+1,bl} + \frac{c_2}{c_1}\dot{u}_{i+1,bl}. \tag{5.40}$$

It is well known in literature that k_{dd} can be set to be zero to avoid feedback from the relative acceleration, which is very difficult to get in practice [74]. This results in

$$\begin{aligned} \begin{pmatrix} \dot{e}_{1,i} \\ \dot{e}_{2,i} \\ \dot{e}_{3,i} \\ \dot{u}_{i,bl} \end{pmatrix} &= \begin{pmatrix} 0 & 1 & 0 & 0 \\ 0 & 0 & 1 & 0 \\ -\frac{k_p}{\tau_i} & -\frac{k_d}{\tau_i} & -\frac{1}{\tau_i} & 0 \\ \frac{k_p}{hc_1} & \frac{k_d}{hc_1} & 0 & -\frac{1}{hc_1} \end{pmatrix} \begin{pmatrix} e_{1,i} \\ e_{2,i} \\ e_{3,i} \\ u_{i,bl} \end{pmatrix} \\ &+ \begin{pmatrix} 0 & 0 & 0 \\ 0 & 0 & 0 \\ 0 & 0 & 0 \\ \frac{1}{h} & \frac{c_2}{hc_1} & \frac{c_2}{c_1} \end{pmatrix} \begin{pmatrix} u_{i-1,bl} \\ u_{i+1,bl} \\ \dot{u}_{i+1,bl} \end{pmatrix} \; \forall i \in S_M \setminus \{M\}. \end{aligned} \tag{5.41}$$

If the errors are written in terms of velocity and acceleration, (5.41) can be equivalently written, $\forall i \in S_M \setminus \{M\}$, as

$$\begin{aligned} \begin{pmatrix} \dot{e}_i \\ \dot{v}_i \\ \dot{a}_i \\ \dot{u}_{i,bl} \end{pmatrix} &= \begin{pmatrix} 0 & -1 & -hc_1 & 0 \\ 0 & 0 & 1 & 0 \\ 0 & 0 & -\frac{1}{\tau_i} & \frac{1}{\tau_i} \\ \frac{k_p}{hc_1} & -\frac{k_d}{hc_1} & -k_d & -\frac{1}{hc_1} \end{pmatrix} \begin{pmatrix} e_i \\ v_i \\ a_i \\ u_{i,bl} \end{pmatrix} \\ &+ \begin{pmatrix} c_1 & c_2 & hc_2 & 0 & 0 & 0 \\ 0 & 0 & 0 & 0 & 0 & 0 \\ 0 & 0 & 0 & 0 & 0 & 0 \\ \frac{k_d}{h} & \frac{k_d c_2}{hc_1} & \frac{k_d c_2}{c_1} & \frac{1}{h} & \frac{c_2}{hc_1} & \frac{c_2}{c_1} \end{pmatrix} \begin{pmatrix} v_{i-1} \\ v_{i+1} \\ a_{i+1} \\ u_{i-1,bl} \\ u_{i+1,bl} \\ \dot{u}_{i+1,bl} \end{pmatrix} \end{aligned} \tag{5.42}$$

which represents the dynamics of a vehicle equipped with baseline CACC protocol. Notice that (5.41) (or (5.42)) are valid for $i \in S_M \setminus \{M\}$, i.e. only for those vehicles with both a front and a rear vehicle. The leading vehicles and the last vehicle obey slightly different dynamics, as clarified hereafter.

5.4.2. String stability Analysis

Here we define criteria for the homogeneous platoon (comprising (5.42), the leading and the last vehicle) to be string stable (i.e. to attenuate disturbances as they propagate through the platoon). Available CACC string stability criteria are based on homogeneity of the vehicles: without loss of generality we consider homogeneity with respect to the leading vehicle, i.e., $\tau_i = \tau_0$, $\forall$ i. To write the interconnections among vehicles in a compact way, we define the state

$$\begin{aligned} t_i &= c_1 u_{i,bl} - c_2 u_{i+1,bl}, \quad 0 \le i < M-1 \\ t_M &= c_1 u_{M,bl}, \qquad\qquad\quad i = M. \end{aligned} \tag{5.43}$$

and we rearrange (5.42) as

$$\begin{aligned} \begin{pmatrix} \dot{e}_i \\ \dot{v}_i \\ \dot{a}_i \\ \dot{t}_i \end{pmatrix} &= \begin{pmatrix} 0 & -1 & -hc_1 & 0 \\ 0 & 0 & 1 & 0 \\ 0 & 0 & -\frac{1}{\tau_0} & 0 \\ \frac{k_p}{h} & -\frac{k_d}{h} & 0 & -\frac{1}{h} \end{pmatrix} \begin{pmatrix} e_i \\ v_i \\ a_i \\ t_i \end{pmatrix} + \begin{pmatrix} 0 & c_1 & 0 & 0 \\ 0 & 0 & 0 & 0 \\ 0 & 0 & 0 & 0 \\ 0 & \frac{k_d}{h} & 0 & \frac{1}{h} \end{pmatrix} \begin{pmatrix} e_{i-1} \\ v_{i-1} \\ a_{i-1} \\ t_{i-1} \end{pmatrix} \\ &+ \begin{pmatrix} 0 & c_2 & hc_2 & 0 \\ 0 & 0 & 0 & 0 \\ 0 & 0 & 0 & 0 \\ 0 & \frac{k_d c_2}{hc_1} & \frac{k_d c_2}{c_1} & 0 \end{pmatrix} \begin{pmatrix} e_{i+1} \\ v_{i+1} \\ a_{i+1} \\ t_{i+1} \end{pmatrix} + \begin{pmatrix} 0 \\ 0 \\ \frac{1}{\tau_0} \\ 0 \end{pmatrix} u_{i,bl}. \end{aligned} \tag{5.44}$$

It can be noticed that

$$c_1 u_{i,bl} = t_i + \frac{c_2}{c_1} t_{i+1} + \left(\frac{c_2}{c_1}\right)^2 t_{i+2} + \ldots + \left(\frac{c_2}{c_1}\right)^{M-i} t_M. \tag{5.45}$$

After manipulating (5.44) via (5.45) we obtain, $i \in S_M \setminus \{M\}$

$$\underbrace{\begin{pmatrix}\dot{e}_i\\ \dot{v}_i\\ \dot{a}_i\\ \dot{t}_i\end{pmatrix}}_{\dot{\chi}_i} = \underbrace{\begin{pmatrix}0 & -1 & -hc_1 & 0\\ 0 & 0 & 1 & 0\\ 0 & 0 & -\frac{1}{\tau_0} & \frac{1}{\tau_0 c_1}\\ \frac{k_p}{h} & -\frac{k_d}{h} & -k_d c_1 & -\frac{1}{h}\end{pmatrix}}_{A_0}\underbrace{\begin{pmatrix}e_i\\ v_i\\ a_i\\ t_i\end{pmatrix}}_{\chi_i} + \underbrace{\begin{pmatrix}0 & c_1 & 0 & 0\\ 0 & 0 & 0 & 0\\ 0 & 0 & 0 & 0\\ 0 & \frac{k_d c_1}{h} & 0 & \frac{1}{h}\end{pmatrix}}_{A_{-1}}\underbrace{\begin{pmatrix}e_{i-1}\\ v_{i-1}\\ a_{i-1}\\ t_{i-1}\end{pmatrix}}_{\chi_{i-1}}$$

$$+\underbrace{\begin{pmatrix}0 & c_2 & hc_2 & 0\\ 0 & 0 & 0 & 0\\ 0 & 0 & 0 & \frac{c_2}{\tau_0 {c_1}^2}\\ 0 & \frac{k_d c_2}{h} & k_d c_2 & 0\end{pmatrix}}_{A_1}\underbrace{\begin{pmatrix}e_{i+1}\\ v_{i+1}\\ a_{i+1}\\ t_{i+1}\end{pmatrix}}_{\chi_{i+1}} + \cdots + \underbrace{\begin{pmatrix}0 & 0 & 0 & 0\\ 0 & 0 & 0 & 0\\ 0 & 0 & 0 & \frac{{c_2}^{M-i}}{\tau_0 {c_1}^{M+1-i}}\\ 0 & 0 & 0 & 0\end{pmatrix}}_{A_{M-i}}\underbrace{\begin{pmatrix}e_M\\ v_M\\ a_M\\ t_M\end{pmatrix}}_{\chi_M}. \tag{5.46}$$

which holds for all vehicles in the platoon, excluding the leading and the last vehicle. In fact, as the last vehicle has no following vehicles, we define the unidirectional CACC control

$$h\dot{u}_{M,bl} = -u_{M,bl} + (k_p e_{1,M} + k_d e_{2,M}) + u_{M-1,bl} \tag{5.47}$$

which becomes, in terms of t_M,

$$h\dot{t}_M = \frac{c_2 - c_1}{c_1} t_M + c_1(k_p e_{1,M} + k_d e_{2,M}) + t_{M-1}. \tag{5.48}$$

Hence, the dynamics of the last vehicle can be described by

$$\dot{\chi}_M = \underbrace{\begin{pmatrix}0 & -1 & -h & 0\\ 0 & 0 & 1 & 0\\ 0 & 0 & -\frac{1}{\tau_0} & \frac{1}{\tau_0 c_1}\\ \frac{k_p c_1}{h} & -\frac{k_d c_1}{h} & -k_d c_1 & \frac{c_2 - c_1}{h c_1}\end{pmatrix}}_{E_0}\chi_M + \underbrace{\begin{pmatrix}0 & 1 & 0 & 0\\ 0 & 0 & 0 & 0\\ 0 & 0 & 0 & 0\\ 0 & \frac{k_d c_1}{h} & 0 & \frac{1}{h}\end{pmatrix}}_{E_{-1}}\chi_{M-1}. \tag{5.49}$$

On the other end, after using $t_0 = c_1 u_{0,bl} - c_2 u_{1,bl}$, the dynamics of the leading vehicle become

$$\dot{\chi}_0 = \begin{pmatrix}0 & -1 & 0 & 0\\ 0 & 0 & 1 & 0\\ 0 & 0 & -\frac{1}{\tau_0} & 0\\ \frac{k_p c_2}{h} & -\frac{k_d c_2}{h} & 0 & -\frac{1}{h} - \frac{c_2}{h c_1}\end{pmatrix}\chi_0$$

$$+\begin{pmatrix}0 & 1 & h & 0\\ 0 & 0 & 0 & 0\\ 0 & 0 & 0 & 0\\ 0 & \frac{k_d c_2}{h} & k_d c_2 & 0\end{pmatrix}\chi_1 + \begin{pmatrix}0\\ 0\\ \frac{1}{\tau_0}\\ -\frac{c_2}{h}\end{pmatrix}u_{0,bl} + \begin{pmatrix}0\\ 0\\ 0\\ \frac{c_1}{h}\end{pmatrix}u_r. \tag{5.50}$$

The leader vehicle is the only vehicle that can set the platoon acceleration u_r. That is, (5.50) has been derived by imposing the leader control action as

$$hc_1\dot{u}_{0,bl} = -u_{0,bl} + c_2(k_p e_{1,0} + k_d e_{2,0}) + u_r + c_2 u_{1,bl} + hc_2\dot{u}_{1,bl} \tag{5.51}$$

which, in terms of t becomes,

$$h\dot{t}_0 = \left(-1-\frac{c_2}{c_1}\right)t_0 + c_2(k_p e_{1,0} + k_d e_{2,0}) - \left(\frac{c2}{c1}\right)^2 t_1 - \left(\frac{c2}{c1}\right)^3 t_2 - \cdots - \left(\frac{c2}{c1}\right)^{M+1} + u_r. \tag{5.52}$$

The importance of (5.46), (5.49) and (5.50) is to allow writing all the vehicle interconnections and check how the effect of u_r propagates throughout the accelerations a_1, ..., a_M. This is a form of string stability as defined in [3] for unidirectional CACC. Bidirectional CACC string stability is open [53]. To address it, we write $u_{0,bl}$ in (5.50) as a function of the states of the vehicles via (5.45). Hence, (5.50) becomes

$$\begin{pmatrix} \dot{e}_0 \\ \dot{v}_0 \\ \dot{a}_0 \\ \dot{t}_0 \end{pmatrix} = \underbrace{\begin{pmatrix} 0 & -1 & 0 & 0 \\ 0 & 0 & 1 & 0 \\ 0 & 0 & -\frac{1}{\tau_0} & \frac{1}{\tau_0 c_1} \\ \frac{k_p c_2}{h} & -\frac{k_d c_2}{h} & 0 & -\frac{1}{h} - \frac{c_2}{hc_1} \end{pmatrix}}_{F_0} \begin{pmatrix} e_0 \\ v_0 \\ a_0 \\ t_0 \end{pmatrix} + \underbrace{\begin{pmatrix} 0 & 1 & h & 0 \\ 0 & 0 & 0 & 0 \\ 0 & 0 & 0 & \frac{1}{\tau_0 c_1}\frac{c_2}{c_1} \\ 0 & \frac{k_d c_2}{h} & k_d c_2 & -\frac{1}{h}(\frac{c_2}{c_1})^2 \end{pmatrix}}_{F_1} \begin{pmatrix} e_1 \\ v_1 \\ a_1 \\ t_1 \end{pmatrix}$$

$$+ \underbrace{\begin{pmatrix} 0 & 0 & 0 & 0 \\ 0 & 0 & 0 & 0 \\ 0 & 0 & 0 & \frac{1}{\tau_0 c_1}(\frac{c_2}{c_1})^2 \\ 0 & 0 & 0 & -\frac{1}{h}(\frac{c_2}{c_1})^3 \end{pmatrix}}_{F_2} \begin{pmatrix} e_2 \\ v_2 \\ a_2 \\ t_2 \end{pmatrix} + \ldots + \underbrace{\begin{pmatrix} 0 & 0 & 0 & 0 \\ 0 & 0 & 0 & 0 \\ 0 & 0 & 0 & \frac{1}{\tau_0 c_1}(\frac{c_2}{c_1})^M \\ 0 & 0 & 0 & -\frac{1}{h}(\frac{c_2}{c_1})^{M+1} \end{pmatrix}}_{F_M} \begin{pmatrix} e_M \\ v_M \\ a_M \\ t_M \end{pmatrix} + \underbrace{\begin{pmatrix} 0 \\ 0 \\ 0 \\ \frac{1}{h} \end{pmatrix}}_{B_0} u_r. \tag{5.53}$$

The coefficients $\frac{c_2}{c_1}$, $\left(\frac{c_2}{c_1}\right)^2$, ..., $\left(\frac{c_2}{c_1}\right)^M$ arise from the bidirectional interconnection (5.45). Now, let us define the platoon state $\chi_{pl} = (\chi_0^T\ \chi_1^T\ \ldots\ \chi_M^T)^T$, the platoon output $y_{pl} = (a_0\ a_1\ \ldots\ a_M)^T$ and write (5.43)-(5.53) in the form

$$\begin{aligned} \dot{\chi}_{pl} &= A_{pl}\chi_{pl} + B_{pl}u_r \\ y_{pl} &= C_{pl}\chi_{pl} \end{aligned} \tag{5.54}$$

with

$$A_{pl} = \begin{pmatrix} F_0 & F_1 & F_2 & \ldots & F_{M-1} & F_M \\ A_{-1} & A_0 & A_1 & \ldots & A_{M-2} & A_{M-1} \\ 0 & A_{-1} & A_0 & \ldots & A_{M-3} & A_{M-2} \\ \vdots & \vdots & \vdots & \ddots & \vdots & \\ 0 & 0 & 0 & \ldots & E_{-1} & E_0 \end{pmatrix}$$

$$B_{pl} = \begin{pmatrix} B_0 \\ 0 \\ \vdots \\ 0 \end{pmatrix},\ C_{pl} = \begin{pmatrix} C & 0 & \ldots & 0 \\ 0 & C & \ldots & 0 \\ \vdots & \vdots & \ddots & \vdots \\ 0 & 0 & \ldots & C \end{pmatrix}$$

where $C = (0\ 0\ 1\ 0)$. Let us denote with $G_{i,r}(s)$, $i \in S_M \cup \{0\}$, the transfer functions from u_r to a_i, calculated from (5.54). The following notion of string stability is proposed here, valid for both the unidirectional and bidirectional cases: The platoon represented by (5.43)-(5.53) is said to be string stable if $G_{i,r}(s)$ is stable and

$$\left|G_{i+1,r}(j\omega)\right| \leq \left|G_{i,r}(j\omega)\right|, \quad \forall\omega, 0 \leq i \leq M \tag{5.55}$$

where $|\cdot|$ indicates the magnitude of the transfer function.

Remark 5.5. The definition (5.55) implies that at each frequency the effect of a disturbance entering in u_r will be attenuated throughout the platoon. Note that such definition is consistent with the one in [3], which requires $\left\|G_{i+1,i}(j\omega)\right\|_\infty \leq 1$, being $G_{i+1,i}(s)$ the transfer function between from a_i to a_{i+1}.

Additionally, the propagation of velocity or acceleration error down the string of the platoon can be checked, the magnitude of which should be less than 1. To check this we would now consider the velocity or acceleration as the input.
Hence, for acceleration to acceleration transfer function

$$B = A(:,\ 3) \text{ and } C = (0\ 0\ 1\ 0)$$

For the velocity to velocity transfer function

$$B = A(:,\ 2) \text{ and } C = (0\ 1\ 0\ 0)$$

Augmenting Saturations in bi-directional control architecture

Now that we are able to define a string stability for a homogeneous platoon with bidirectional communication, let us see how to handle heterogeneity in τ_i.

5.5. Engine-constrained Control

Under the baseline conditions of identical vehicles ($\Omega_i^* = 0$), the following CACC control was derived in Sect. 5.2

$$hc_1\dot{u}_{i,bl} = -u_{i,bl} + \xi_{i,bl}, \quad \forall i \in S_M \cup \{0\} \tag{5.56}$$

$$\xi_{i,bl} = \begin{cases} c_1 u_r + k_p e_0 + k_d \dot{e}_0 \\ \quad +c_2 u_{1,bl} + hc_2 \dot{u}_{1,bl} & i = 0. \\ k_p e_i + k_d \dot{e}_i + c_1 u_{i-1,bl} \\ \quad +c_2 u_{i+1,bl} + hc_2 \dot{u}_{i+1,bl} & i \in S_M \setminus \{M\} \\ k_p e_M + k_d \dot{e}_M + u_{M-1,bl} & i = M. \end{cases}$$

We want to use the homogeneous baseline platoon as "ideal" reference dynamics to which the heterogeneous platoon should converge. To this purpose, we define, $\forall i \in S_M \setminus \{M\}$ (index $i = M$ follows similarly and is omitted for brevity)

$$\begin{pmatrix} \dot{e}_{i,m} \\ \dot{v}_{i,m} \\ \dot{a}_{i,m} \\ \dot{u}_{i,m} \end{pmatrix} = \underbrace{\begin{pmatrix} 0 & -1 & -hc_1 & 0 \\ 0 & 0 & 1 & 0 \\ 0 & 0 & -\frac{1}{\tau_0} & \frac{1}{\tau_0} \\ \frac{k_p}{hc_1} & -\frac{k_d}{hc_1} & -k_d & -\frac{1}{hc_1} \end{pmatrix}}_{A_m} \underbrace{\begin{pmatrix} e_{i,m} \\ v_{i,m} \\ a_{i,m} \\ u_{i,m} \end{pmatrix}}_{x_{i,m}} + \underbrace{\begin{pmatrix} c_1 & c_2 & hc_2 & 0 & 0 & 0 \\ 0 & 0 & 0 & 0 & 0 & 0 \\ 0 & 0 & 0 & 0 & 0 & 0 \\ \frac{k_d}{h} & \frac{k_d c_2}{hc_1} & \frac{k_d c_2}{c_1} & \frac{1}{h} & \frac{c_2}{hc_1} & \frac{c_2}{c_1} \end{pmatrix}}_{B_w} \underbrace{\begin{pmatrix} v_{i-1} \\ v_{i+1} \\ a_{i+1} \\ u_{i-1,bl} \\ u_{i+1,bl} \\ \dot{u}_{i+1,bl} \end{pmatrix}}_{w_i} \tag{5.57}$$

where the subscript m stands for model-reference, $x_{i,m}$ and w_i are vehicle i's reference state vector and exogenous input vector. Note that the input to (5.57) are variables v_{i-1}, v_{i+1}, a_{i+1}, $u_{i-1,bl}$, $u_{i+1,bl}$ and $\dot{u}_{i+1,bl}$ coming from the actual vehicles in (5.42).

Furthermore, the leading vehicle model becomes

$$\begin{pmatrix} \dot{e}_0 \\ \dot{v}_0 \\ \dot{a}_0 \\ \dot{u}_{0,bl} \end{pmatrix} = \underbrace{\begin{pmatrix} 0 & 0 & 0 & 0 \\ 0 & 0 & 1 & 0 \\ 0 & 0 & -\frac{1}{\tau_0} & \frac{1}{\tau_0} \\ \frac{k_p}{hc_1} & -\frac{k_d}{hc_1} & -k_d & -\frac{1}{hc_1} \end{pmatrix}}_{A_r} \underbrace{\begin{pmatrix} e_0 \\ v_0 \\ a_0 \\ u_{0,bl} \end{pmatrix}}_{x_0} + \begin{pmatrix} c_2 & hc_2 & 0 & 0 \\ 0 & 0 & 0 & 0 \\ 0 & 0 & 0 & 0 \\ \frac{k_d c_2}{hc_1} & \frac{k_d c_2}{c_1} & \frac{c_2}{hc_1} & \frac{c_2}{c_1} \end{pmatrix} \begin{pmatrix} v_1 \\ a_1 \\ u_{1,bl} \\ \dot{u}_{1,bl} \end{pmatrix} + \underbrace{\begin{pmatrix} 0 \\ 0 \\ 0 \\ \frac{1}{h} \end{pmatrix}}_{B_r} u_r. \tag{5.58}$$

Having defined the reference dynamics (5.57), two questions are now addressed: introduce adaptation in (5.56) to handle heterogeneities (5.6) (Sect. 5.5.1).

5.5.1. Adaptive CACC augmentation

The dynamics (5.58) can used as a reference model for the uncertain platoon's dynamics. With this scope in mind, we augment the baseline controller (5.56) with an adaptive term

$$u_i = u_{i,bl} + u_{i,ad} \tag{5.59}$$

where $u_{i,ad}$ is the adaptive augmentation controller (to be constructed). Using (5.59) we obtain results in

$$\begin{pmatrix} \dot{e}_i \\ \dot{v}_i \\ \dot{a}_i \\ \dot{u}_{i,bl} \end{pmatrix} = \underbrace{\begin{pmatrix} 0 & -1 & -hc_1 & 0 \\ 0 & 0 & 1 & 0 \\ 0 & 0 & -\frac{1}{\tau_0} & \frac{1}{\tau_0} \\ \frac{k_p}{hc_1} & -\frac{k_d}{hc_1} & -k_d & -\frac{1}{hc_1} \end{pmatrix}}_{x_i} \underbrace{\begin{pmatrix} e_i \\ v_i \\ a_i \\ u_{i,bl} \end{pmatrix}}_{x_i} + \begin{pmatrix} c_1 & c_2 & hc_2 & 0 & 0 & 0 \\ 0 & 0 & 0 & 0 & 0 & 0 \\ 0 & 0 & 0 & 0 & 0 & 0 \\ \frac{k_d}{h} & \frac{k_d c_2}{hc_1} & \frac{k_d c_2}{c_1} & \frac{1}{h} & \frac{c_2}{hc_1} & \frac{c_2}{c_1} \end{pmatrix} \begin{pmatrix} v_{i-1} \\ v_{i+1} \\ a_{i+1} \\ u_{i-1,bl} \\ u_{i+1,bl} \\ \dot{u}_{i+1,bl} \end{pmatrix} + \underbrace{\begin{pmatrix} 0 \\ 0 \\ \frac{1}{\tau_0} \\ 0 \end{pmatrix}}_{B_u} \left[u_{i,ad} + \Omega_i^* \phi_i \right], \quad \forall i \in S_M \tag{5.60}$$

It can be seen that the model takes similar form as was seen in Section 5.2 for the unidirectional case. The bounds for the saturation are thus calculated in the same way as were calculated for unidirectional case.

5.6. Simulation and Results for bidirectional case

5.6.1. String Stability

Before we test the algorithm for its effectiveness, it is important to check whether the model is string stable or not, as the algorithm would only be implementable and useful if it is string stable. Results for string stability analysis are given here.

C1 = 1, C2 = 0

This case is nothing but the unidirectional model (state of the art - Ploeg's model).

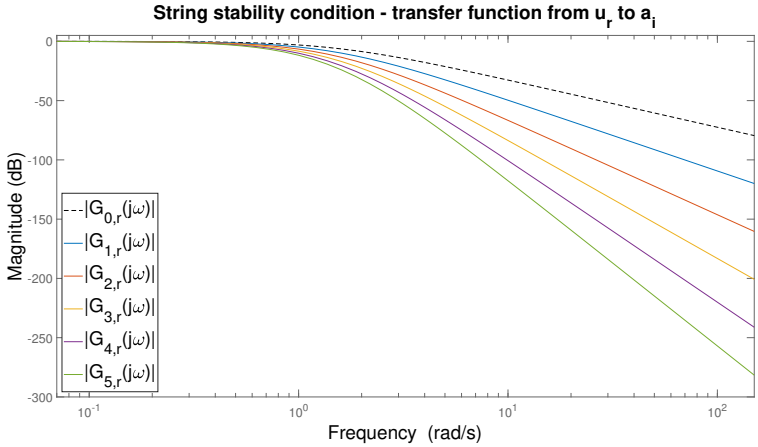

Figure 5.14: Magnitude(Bode) plot for the transfer function between reference input and acceleration states of vehicles; c1 = 1, c2 = 0

In fig. 5.14 it can be seen that any perturbation that enters through the reference input gets attenuated throughout the platoon, at any frequency. Hence the platoon is stable for and disturbances that mey enter through the input.

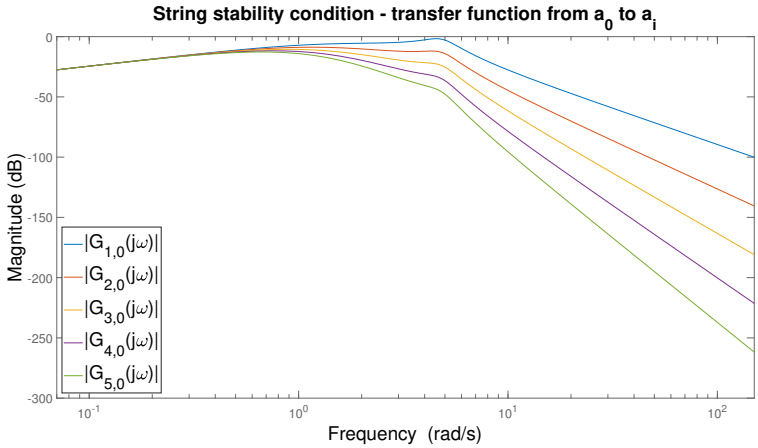

Figure 5.15: Magnitude(Bode) plot for the transfer function between acceleration of leader vehicle and acceleration states of other vehicles; c1 = 1, c2 = 0

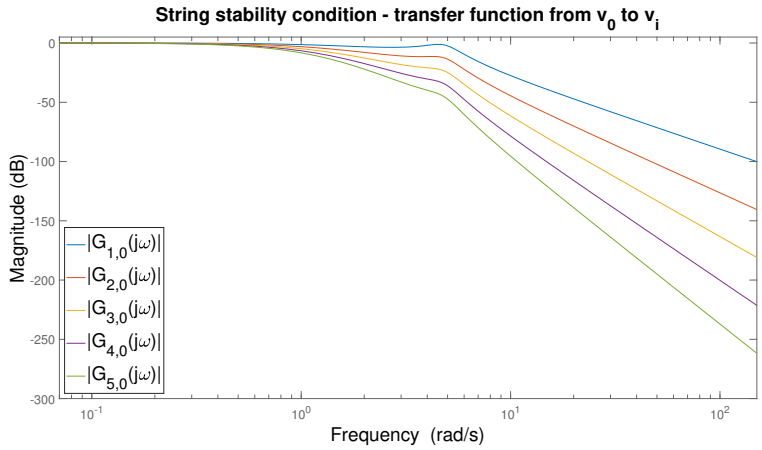

Figure 5.16: Magnitude(Bode) plot for the transfer function between velocity of leader vehicle and velocity states of other vehicles; c1 = 1, c2 = 0

Fig. 5.16 and 5.15 shows that if any disturbance in acceleration or velocity enters the platoon it would be attenuated as it propagates through the string. Hence, the model is string stable, which is coherent with the study done in [3].

C1 = 0.5, C2 = 0.5

Fig. 5.17, 5.18 and 5.19 shows the magnitude plots for transfer functions from reference input to acceleration states, velocity of leader vehicle to velocity of other vehicles and acceleration of leader vehicle to acceleration of other vehicles respectively.

The plots for this case ($c1 = 0.5$, $c2 = 0.5$) seem identical to the plots for the uni-

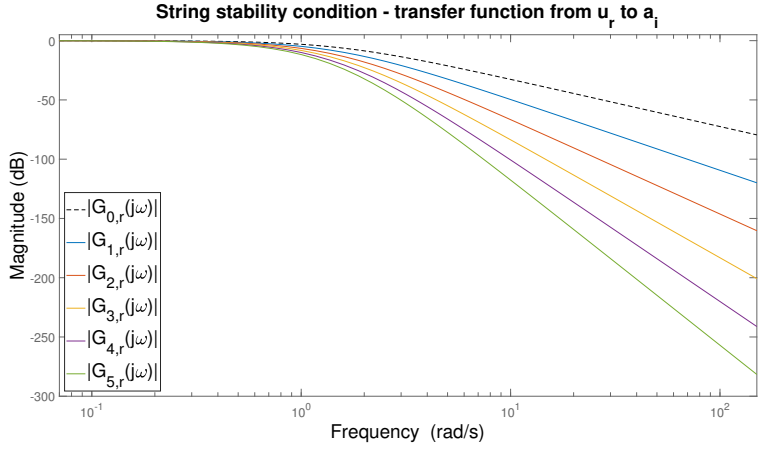

Figure 5.17: Magnitude(Bode) plot for the transfer function between reference input and acceleration states of vehicles; c1 = 0.5, c2 = 0.5

directional case and the magnitude in all the plots remain below 0. Hence, it can be confirmed that the proposed algorithm provides string stability.

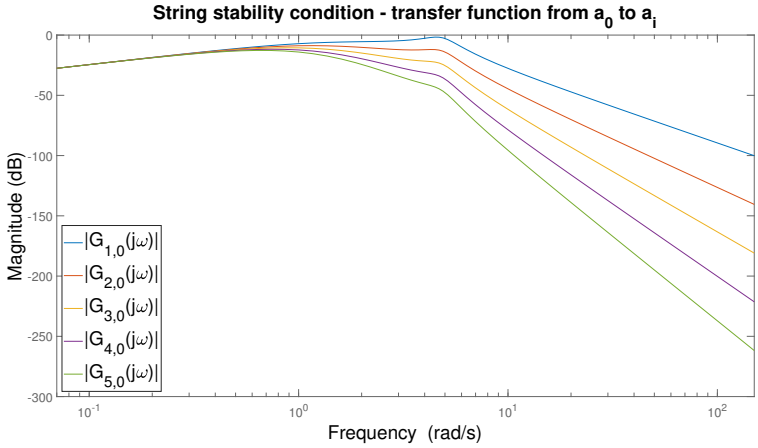

Figure 5.18: Magnitude(Bode) plot for the transfer function between acceleration of leader vehicle and acceleration states of other vehicles; c1 = 0.5, c2 = 0.5

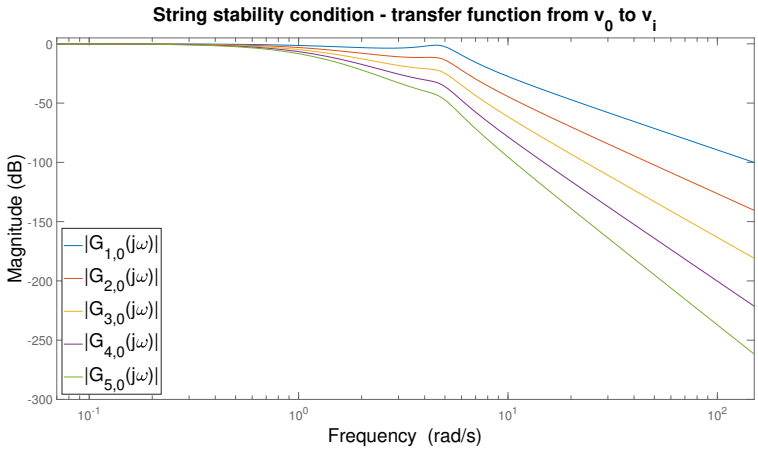

Figure 5.19: Magnitude(Bode) plot for the transfer function between velocity of leader vehicle and velocity states of other vehicles; c1 = 0.5, c2 = 0.5

Note : The plots for other values of $c1$ and $c2$, such that $c1$ and $c2 \in [0, 1]$ and $c1 + c2 = 1$ produce identical plots to the above given plots and hence, the algorithm is string stable for all the combinations of $c1$ and $c2$.

5.6.2. Scenario

Now that it is established that the proposed algorithm is string stable, we need to check the effectiveness of the algorithm. For this, we consider the case where the unidirectional communication algorithm fails.

Thus, again a homogeneous platoon is considered with a 5+1 (5 followers and a leader) configuration. The leading vehicle is now provided with a ramp input. As the saturation for the vehicles are implemented, the input increases and then saturates at the potential limit of the vehicle. We now introduce a positive impulse in the distance between vehicle 2 and 3 (the position of vehicle 3 is pushed back). This is done to mimic the effect of a disturbance that can occur in the platoon (possible reasons being error in measurement of position, slippery road etc.).

5.6.3. Results

It is to be noted, that the k_p and k_d values are needed to be tuned in order to ensure string stability, one of the examples of the values for string stability is $k_p = 0.2$ and $k_d = 1.4$. For the purpose of simulations here the same values are used.

Fig. 5.20 shows the spacing error and the input response during the course of platooning. As opposed to unidirectional case (fig 5.12) in the bi-directional case the spacing error is reduced to zero for all the vehicles. Thanks to the bidirectional interaction, vehicle 3 modulates its acceleration input in order to reduce its spacing error with both vehicle 2 and 4 (the spacing error now includes both the look-ahead and look-back error). At the same time, vehicle 2 and vehicle 1 slow down a bit, in order for vehicle 3 to close the gap and reaching maximum acceleration again. This highlights the benefits of considering bidirectional interaction together with adaptation to uncertain vehicle dynamics.

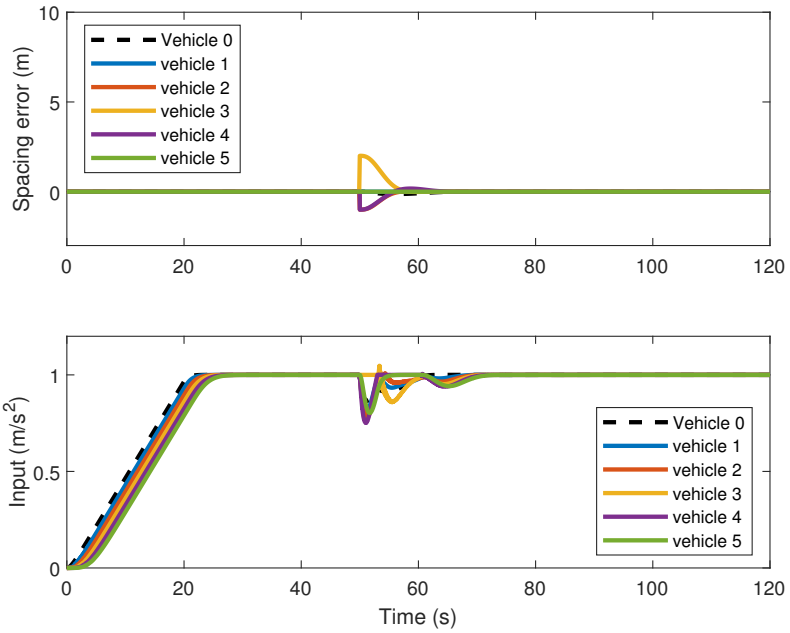

Figure 5.20: Extreme scenario with proposed bidirectional control: spacing error and input response. Case - $c1 = 0.5; c2 = 0.5$

Fig. 5.20 shows the results for the case when $c1 = 0.5; c2 = 0.5$, but as it was established before, that the algorithm is string stable for all values of $c1$ and $c2$. Also, it has already been established that unidirectional case ($c1 = 1; c2 = 0$) fails in this scenario, and if we consider $c1 = 0; c2 = 1$ (another unidirectional case), the vehicle only looks at the vehicle behind and thus the vehicles following would be lost, hence it is fruitless to simulate these cases.

Now, the case with $c1 = 0.3; c2 = 0.7$ is considered

Fig. 5.21 shows the results for the case when $c1 = 0.3; c2 = 0.7$, similar to the previous case, even this setting can push the spacing error to zero for all the vehicles. It is worth

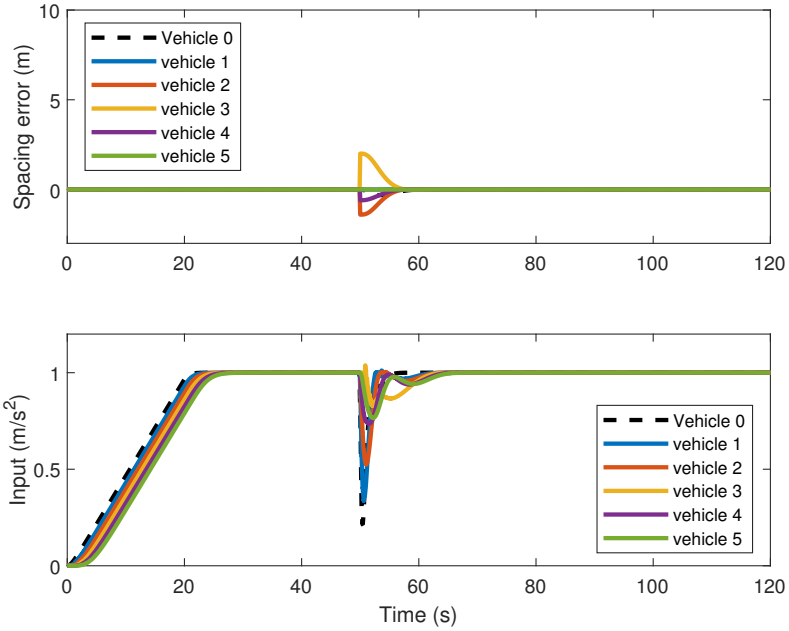

Figure 5.21: Extreme scenario with proposed bidirectional control: spacing error and input response. Case - $c1 = 0.3; c2 = 0.7$

noting though, that, the error goes to zero quicker than in case of $c1 = 0.5; c2 = 0.5$ also there is a greater impact of the error on the reducing of velocity, for the leader vehicle. This is probably due to the fact that, more weightage is given to the backward error, and hence, the same amount of error would provide a greater braking input to the vehicles.

Now, the case with $c1 = 0.7; c2 = 0.3$ is considered

Fig. 5.22 shows the results for the case when $c1 = 0.7; c2 = 0.3$, similar to the previous cases, even this setting can push the spacing error to zero for all the vehicles. Although, the error takes a longer time to attenuate in this setting, it can be noticed that the velocity is not reduced by much. As the weightage to the backward error is less there is a smaller impact of the backward error on the input, hence, the same error provides a smaller braking action.

As all the settings of $c1$ and $c2$ pushes the errors to zero, it depend on the designer to pick these weighting factors, although if the value of $c1$ is kept very high, the error does not attenuate quickly which is the main purpose of bi-directional approach. On the other hand if the value is too low, the platoon is highly sensitive to any backward error and the front vehicle would slow down quickly to get rid of the error. As the vehicle brakes quickly there might also be a problem of comfort for the passengers. I would recommend the value of $c1$ ranging in between 0.4 to 0.6 as, from the results above 0.5 seems to provide the attenuation in a decently small amount of time and the change in input value was not very abrupt. Hence, weighting both the errors equally is a good option, but the selection of the weighting may vary according to the application.

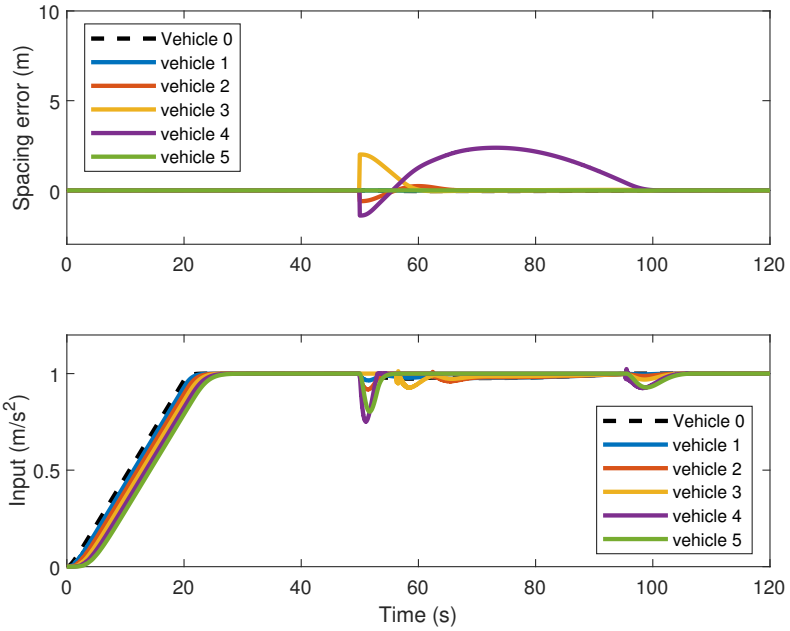

Figure 5.22: Extreme scenario with proposed bidirectional control: spacing error and input response. Case - $c1 = 0.7; c2 = 0.3$

6

Conclusion and Future work

The conclusion can be split into two parts again, the first part draws out the conclusion for the merging maneuver method proposed, then in the second part conclusions relating to Vehicle following are drawn out. Later in the section the possible future work relevant to the topic of research is proposed.

6.1. Conclusion

Vehicles have become an essential part in our lives and their demand is increasing continuously. Due to the increase in the number of vehicles on the road, there are problems relating to traffic congestion and vehicle emission. If the vehicles are grouped one behind the other in a platoon, the space taken by the vehicles is less when compared to the same number of vehicles not in a platoon. Also, because of the presence of a vehicle in front of another, the aerodynamic drag reduces because of which, the vehicle uses less fuel resulting in less emission. The algorithms (CACC) used in platooning also ensures the ride is more comfortable as well.

6.1.1. Merging

Adaptive strategies for formation keeping in platoons of automated vehicles have been recently proposed, that are able to cope with uncertain vehicle parameters. However, all proposed strategies suffer from the drawback of handling only acyclic graphs for look-ahead topology. This prevents from considering more complex platooning maneuvers such as merging and splitting.

This thesis has proposed an adaptive strategy for establishing merging maneuvers in the presence uncertain vehicle parameters. The strategy has been framed as a synchronization protocol with an adaptive control law. The main contribution of this work is that, despite the cyclic communication graph instantiated during the merging maneuver, it is possible to exploit the graph structure to implement appropriate parameter projection and guarantee well posedness of the actual inputs at all time instants. A benchmark scenario in which two platoons formed in different lanes are required to merge (e.g. due to a lane closure because of roadworks), was presented to show the effectiveness of the

proposed strategy. It was shown that merging is achieved, while the cyclic communication is handled in a suitable way. The cyclic communication enables the platoon to complete the maneuver closer to the human driving behaviour during merging. In addition, scalability to platoons with arbitrary number of vehicles has been successfully proven, both in terms of control/adaptive laws and in terms of parameter projection strategies guaranteeing well posedness.

6.1.2. Vehicle following

In this work adaptive CACC strategies were augmented with a mechanism to cope with saturation constraints. The mechanism is based on making the reference dynamics 'not too demanding', by applying a properly designed saturation. Such saturation will allow all vehicles in the platoon not to hit their engine bounds, at the price of losing some performance. The results of this strategy are in line with the studies [57, 58], i.e. saturation can be systematically eliminated only at the price of losing performance.

It was also proven that, bidirectional interaction (with front and rear vehicle) can be handled in such a way, that it is string stable (which the literature fails to establish [54, 55]). The saturation mechanism can also retain cohesiveness while handling bidirectional interaction in a string stable way.

6.2. Future work

Platooning and vehicle following is a relatively old concept and it has gone through a lot of development since it was proposed. Still there a lot of scope for development as it is still in the preliminary stages of implementation. Some of the work predicted to be studied soon and would have an impact on the area of platooning are as follows :

- Experimental studies are needed to check how effective and comfortable the merging maneuver is and how can the comfort be improved.

- In this work we have assumed the saturation bounds to be known. It would be relevant to study the case in which the saturation bounds can be learned online, and thus $u_{min,m}$ and $u_{max,m}$ can be selected in an adaptive way. Furthermore, τ_0 is also assumed to be known. It would be relevant to learn in an adaptive way the best τ_0 that might lead to the best performance of the platoon.

- Unmatched uncertainties such as communication delays can be included. Furthermore, a formal proof for switching topologies (e.g. using dwell-time concepts [75, 76]) or for mixing topologies (e.g. using adaptive mixing concepts) is still open. Finally, the behavior of the proposed strategy in situations of mixed traffic (human/automated) is a topic of extreme interest that will be studied in the future.

- In this thesis different models were considered for merging maneuver and for vehicle following, it was also seen that switching causes a huge variation in control action which in turn gives rise to oscillations. If the merging maneuver is implemented with the bidirectional model we would have the cyclic graph proposed in the thesis and possibly no oscillations in the input, during the merging maneuver.

- Current studies focus mainly on vehicle following, merging and splitting maneuvers. If these maneuvers are combined together, they can replicate overtaking. Overtaking might be useful in many cases. if a vehicle breaks down or runs into an error overtaking maneuver would ensure that the platoon can still carry on without being disrupted, leaving the broken vehicle behind. Also, if a platoon is highly heterogeneous (the difference in the potentials of the vehicles is too much), vehicles may split themselves into multiple platoons in order to not reduce the performance of certain vehicles very much.

- If the environment is cluttered, then according to the surroundings, the velocity of the platoon as a whole (leader vehicle) can be reduced to maintain safety. The limit of safe velocity depending on the environment can be studied.

Bibliography

[1] J. Ploeg, E. Semsar-Kazerooni, G. Lijster, N. van de Wouw, and H. Nijmeijer. Graceful degradation of cacc performance subject to unreliable wireless communication. In *16th International IEEE Conference on Intelligent Transportation Systems (ITSC 2013)*, pages 1210–1216, Oct 2013.

[2] J. Ploeg, E. Semsar-Kazerooni, A. I. Morales Medina, J. F. C. M. de Jongh, J. van de Sluis, A. Voronov, C. Englund, R. J. Bril, H. Salunkhe, Á. Arrúe, A. Ruano, L. García-Sol, E. van Nunen, and N. van de Wouw. Cooperative automated maneuvering at the 2016 Grand Cooperative Driving Challenge. *IEEE Transactions on Intelligent Transportation Systems*, 19(4):1213–1226, April 2018.

[3] J. Ploeg, N. van de Wouw, and H. Nijmeijer. l_p string stability of cascaded systems: Application to vehicle platooning. *IEEE Transactions on Control Systems Technology*, 22:786–793, 2014.

[4] Simone Baldi, Iakovos Michailidis, Vasiliki Ntampasi, Elias Kosmatopoulos, Ioannis Papamichail, and Markos Papageorgiou. A simulation-based traffic signal control for congested urban traffic networks. *Transportation Science*, 53(1):6–20, 2019.

[5] M. Papageorgiou and A. Kotsialos. Freeway ramp metering: an overview. *IEEE Transactions on Intelligent Transportation Systems*, 3(4):271–281, Dec 2002.

[6] P. Varaiya. Smart cars on smart roads: problems of control. *IEEE Transactions on Automatic Control*, 38(2):195–207, Feb 1993.

[7] S E Shladover. Automated vehicles for highway operations (automated highway systems). *Proceedings of the Institution of Mechanical Engineers, Part I: Journal of Systems and Control Engineering*, 219(1):53–75, 2005.

[8] Marc Green. "how long does it take to stop?" methodological analysis of driver perception-brake times. *Transportation Human Factors*, 2(3):195–216, 2000.

[9] M. E. Khatir and E. J. Davison. Decentralized control of a large platoon of vehicles using non-identical controllers. In *Proceedings of the 2004 American Control Conference*, volume 3, pages 2769–2776 vol.3, June 2004.

[10] D. Swaroop and J. K. Hedrick. String stability of interconnected systems. In *Proceedings of 1995 American Control Conference - ACC'95*, volume 3, pages 1806–1810 vol.3, June 1995.

[11] S. Sheikholeslam and C. A. Desoer. Control of interconnected nonlinear dynamical systems: the platoon problem. *IEEE Transactions on Automatic Control*, 37(6):806–810, June 1992.

[12] S. K. Yadlapalli, S. Darbha, and K. R. Rajagopal. Information flow and its relation to stability of the motion of vehicles in a rigid formation. *IEEE Transactions on Automatic Control*, 51(8):1315–1319, Aug 2006.

[13] A. Chakravarthy, K. Song, and E. Feron. Preventing automotive pileup crashes in mixed-communication environments. *IEEE Transactions on Intelligent Transportation Systems*, 10(2):211–225, June 2009.

[14] Arnab Bose and Petros Ioannou. Mixed manual/semi-automated traffic: a macroscopic analysis. *Transportation Research Part C: Emerging Technologies*, 11(6):439 – 462, 2003.

[15] Qi Wang, Zhiheng Li, Danya Yao, Yi Zhang, Li Li, and Jianmin Hu. *Analysis on Road Capacity for Mixed Manual/Automated Traffic*, pages 351–358.

[16] P. A. Ioannou and C. C. Chien. Autonomous intelligent cruise control. *IEEE Transactions on Vehicular Technology*, 42(4):657–672, Nov 1993.

[17] Greg Marsden, Mike McDonald, and Mark Brackstone. Towards an understanding of adaptive cruise control. *Transportation Research Part C: Emerging Technologies*, 9(1):33 – 51, 2001.

[18] R. Rajamani and. Semi-autonomous adaptive cruise control systems. In *Proceedings of the 1999 American Control Conference (Cat. No. 99CH36251)*, volume 2, pages 1491–1495 vol.2, June 1999.

[19] S. Öncü, J. Ploeg, N. van de Wouw, and H. Nijmeijer. Cooperative adaptive cruise control: Network-aware analysis of string stability. *IEEE Transactions on Intelligent Transportation Systems*, 15(4):1527–1537, 2014.

[20] Y. A. Harfouch, S. Yuan, and S. Baldi. Adaptive control of interconnected networked systems with application to heterogeneous platooning. In *2017 13th IEEE International Conference on Control Automation (ICCA)*, pages 212–217, 2017.

[21] Youssef Abou Harfouch, Shuai Yuan, and Simone Baldi. An adaptive approach to cooperative longitudinal platooning of heterogeneous vehicles with communication losses. *IFAC-PapersOnLine*, 50(1):1352–1357, 2017.

[22] G. J. L. Naus, R. P. A. Vugts, J. Ploeg, M. J. G. van de Molengraft, and M. Steinbuch. String-stable cacc design and experimental validation: A frequency-domain approach. *IEEE Transactions on Vehicular Technology*, 59(9):4268–4279, Nov 2010.

[23] K. C. Dey, L. Yan, X. Wang, Y. Wang, H. Shen, M.Chowdhury, L. Yu, C. Qiu, and V. Soundararaj. A review of communication, driver characteristics, and controls aspects of cooperative adaptive cruise control (CACC). *IEEE Transactions on Intelligent Transportation Systems*, 17:491–509, 2016.

[24] E. Larsson, G. Sennton, and J. Larson. The vehicle platooning problem: Computational complexity and heuristics. *Transportation Research Part C: Emerging Technologies*, 60:258 – 277, 2015.

[25] Ö. Ş. Taş, N. O. Salscheider, F. Poggenhans, S. Wirges, C. Bandera, M. R. Zofka, T. Strauss, J. M. Zöllner, and C. Stiller. Making Bertha cooperate–team annieWAY's entry to the 2016 Grand Cooperative Driving Challenge. *IEEE Transactions on Intelligent Transportation Systems*, 19(4):1262–1276, April 2018.

[26] W. Yu, G. Chen, and M. Cao. Consensus in directed networks of agents with nonlinear dynamics. *IEEE Transactions on Automatic Control*, 56(6):1436–1441, June 2011.

[27] W. Yu, P. DeLellis, G. Chen, M. di Bernardo, and J. Kurths. Distributed adaptive control of synchronization in complex networks. *IEEE Transactions on Automatic Control*, 57(8):2153–2158, Aug 2012.

[28] Y. Cao, W. Yu, W. Ren, and G. Chen. An overview of recent progress in the study of distributed multi-agent coordination. *IEEE Transactions on Industrial Informatics*, 9(1):427–438, Feb 2013.

[29] S. Baldi and P. Frasca. Adaptive synchronization of unknown heterogeneous agents: an adaptive virtual model reference approach. *Journal of The Franklin Institute*, 2018.

[30] W. Wang, C. Wen, J. Huang, and Z. Li. Hierarchical decomposition based consensus tracking for uncertain interconnected systems via distributed adaptive output feedback control. *IEEE Transactions on Automatic Control*, 61(7):1938–1945, 2016.

[31] L. Zheng, C. Zhu, Z. He, and T. He. Safety rule-based cellular automaton modeling and simulation under V2V environment. *Transportmetrica A: Transport Science*, 0(0):1–26, 2018.

[32] C. Englund, L. Chen, J. Ploeg, E. Semsar-Kazerooni, A. Voronov, H. H. Bengtsson, and J. Didoff. The Grand Cooperative Driving Challenge 2016: boosting the introduction of cooperative automated vehicles. *IEEE Wireless Communications*, 23(4):146–152, August 2016.

[33] M. Aramrattana, J. Detournay, C. Englund, V. Frimodig, O. U. Jansson, T. Larsson, W. Mostowski, V. D. Rodríguez, T. Rosenstatter, and G. Shahanoor. Team Halmstad approach to cooperative driving in the Grand Cooperative Driving Challenge 2016. *IEEE Transactions on Intelligent Transportation Systems*, 19(4):1248–1261, 2018.

[34] I. Parra Alonso, R. Izquierdo Gonzalo, J. Alonso, Á. García-Morcillo, D. Fernández-Llorca, and M. Á. Sotelo. The experience of DRIVERTIVE-DRIVERless cooperaTIve VEhicle-Team in the 2016 GCDC. *IEEE Transactions on Intelligent Transportation Systems*, 19(4):1322–1334, 2018.

[35] V. Dolk, J. d. Ouden, S. Steeghs, J. G. Devanesan, I. Badshah, A. Sudhakaran, K. Elferink, and D. Chakraborty. Cooperative automated driving for various traffic scenarios: Experimental validation in the GCDC 2016. *IEEE Transactions on Intelligent Transportation Systems*, 19(4):1308–1321, April 2018.

[36] M. Amoozadeh, H. Deng, C. Chuah, H. Michael Zhang, and D. Ghosal. Platoon management with cooperative adaptive cruise control enabled by VANET. *Vehicular Communications*, 2(2):110 – 123, 2015.

[37] S. Maiti, S. Winter, and L. Kulik. A conceptualization of vehicle platoons and platoon operations. *Transportation Research Part C: Emerging Technologies*, 80:1 – 19, 2017.

[38] R. Scarinci, A. Hegyi, and B. Heydecker. Definition of a merging assistant strategy using intelligent vehicles. *Transportation Research Part C: Emerging Technologies*, 82:161 – 179, 2017.

[39] C.C. Chien, Y. Zhang, M. Lai, A. Hammad, and C.K. Chu. Regulation layer controller design for automated highway system: Platoon merge and split controller design. In D.B. Schaechter and K.R. Lorell, editors, *Automatic Control in Aerospace 1994 (Aerospace Control '94)*, pages 357 – 362. Pergamon, Oxford, 1995.

[40] R. Rai, B. Sharma, and J. Vanualailai. Real and virtual leader-follower strategies in lane changing, merging and overtaking maneuvers. In *2015 2nd Asia-Pacific World Congress on Computer Science and Engineering (APWC on CSE)*, pages 1–12, 2015.

[41] H. H. Bengtsson, L. Chen, A. Voronov, and C. Englund. Interaction protocol for highway platoon merge. In *2015 IEEE 18th International Conference on Intelligent Transportation Systems*, pages 1971–1976, 2015.

[42] M. Goli and A. Eskandarian. Evaluation of lateral trajectories with different controllers for multi-vehicle merging in platoon. In *2014 International Conference on Connected Vehicles and Expo (ICCVE)*, pages 673–678, 2014.

[43] H. J. Günther, S. Kleinau, O. Trauer, and L. Wolf. Platooning at traffic lights. *IEEE Intelligent Vehicles Symposium (IV)*, pages 1047–1053, 2016.

[44] Carlos Flores and Vicente Milanés. Fractional-order-based acc/cacc algorithm for improving string stability. *Transportation Research Part C: Emerging Technologies*, 95:381 – 393, 2018.

[45] M. Hafez, M. Ariffin, M.A. Abdul Rahman, and H. Zamzuri. Effect of leader information broadcasted throughout vehicle platoon in a constant spacing policy. *IEEE International Symposium on Robotics and Intelligent Sensors*, pages 132–137, 2015.

[46] J. Ploeg, E. Semsar-Kazerooni, G. Lijster, N. van de Wouw, and H. Nijmeijer. Graceful degradation of cooperative adaptive cruise control. *IEEE Transactions on Intelligent Transportation Systems*, 16(1):488–497, 2015.

[47] A. Firooznia, J. Ploeg, N. van de Wouw, and H. Zwart. Co-design of controller and communication topology for vehicular platooning. *IEEE Transactions on Intelligent Transportation Systems*, 18(10):2728–2739, 2017.

[48] U. Montanaro, G. Fiengo M. Tufo, M. di Bernardo, A. Salvi, and S. Santini. Extended cooperative adaptive cruise control. *IEEE Intelligent Vehicles Symposium (IV)*, pages 605–610, 2014.

[49] F. Acciani, P. Frasca, A. Stoorvogel, E. Semsar-Kazerooni, and G. Heijenk. Cooperative adaptive cruise control over unreliable networks: an observer-based approach to increase robustness to packet loss. In *2018 European Control Conference (ECC)*, pages 1399–1404, 2018.

[50] Y. A. Harfouch, S. Yuan, and S. Baldi. An adaptive switched control approach to heterogeneous platooning with intervehicle communication losses. *IEEE Transactions on Control of Network Systems*, 5(3):1434–1444, 2018.

[51] V. S. Dolk, J. Ploeg, and W. P. M. H. Heemels. Event-triggered control for string-stable vehicle platooning. *IEEE Transactions on Intelligent Transportation Systems*, 18(12):3486–3500, 2017.

[52] M. Di Vaio, G. Fiengo, A. Petrillo, A. Salvi, S. Santini, and M. Tufo. Cooperative shock waves mitigation in mixed traffic flow environment. *IEEE Transactions on Intelligent Transportation Systems*, pages 1–15, 2019.

[53] J. C. Zegers, E. Semsar-Kazerooni, J. Ploeg, N. van de Wouw, and H. Nijmeijer. Consensus-based bi-directional CACC for vehicular platooning. In *2016 American Control Conference (ACC)*, pages 2578–2584, 2016.

[54] M.R.I. Nieuwenhuijze. String stability analysis of bidirectional adaptive cruise control. Master's thesis, Eindhoven University of Technology, The Netherlands, 2010.

[55] M. Pirani, E. Hashemi, J. W. Simpson-Porco, B. Fidan, and A. Khajepour. Graph theoretic approach to the robustness of k -nearest neighbor vehicle platoons. *IEEE Transactions on Intelligent Transportation Systems*, 18(11):3218–3224, 2017.

[56] G. Rodonyi. An adaptive spacing policy guaranteeing string stability in multi-brand ad-hoc platoons. *IEEE Transactions on Intelligent Transportation Systems*, 19(6):1902–1912, 2018.

[57] S. C. Warnick and A. A. Rodriguez. Longitudinal control of a platoon of vehicles with multiple saturating nonlinearities. In *Proceedings of 1994 American Control Conference - ACC '94*, volume 1, pages 403–407 vol.1, 1994.

[58] M. R. Jovanovic, J. M. Fowler, B. Bamieh, and R. D'Andrea. On avoiding saturation in the control of vehicular platoons. In *Proceedings of the 2004 American Control Conference*, volume 3, pages 2257–2262 vol.3, 2004.

[59] E. Semsar-Kazerooni and K. Khorasani. Team consensus for a network of unmanned vehicles in presence of actuator faults. *IEEE Transactions on Control Systems Technology*, 18(5):1155–1161, 2010.

[60] J. C. Zegers, E. Semsar-Kazerooni, J. Ploeg, N. van de Wouw, and H. Nijmeijer. Consensus control for vehicular platooning with velocity constraints. *IEEE Transactions on Control Systems Technology*, 26(5):1592–1605, 2018.

[61] W. Gao, F. Rios-Gutierrez, W. Tong, and L. Chen. Cooperative adaptive cruise control of connected and autonomous vehicles subject to input saturation. In *2017 IEEE 8th Annual Ubiquitous Computing, Electronics and Mobile Communication Conference (UEMCON)*, pages 418–423, 2017.

[62] S. C. Warnick and A. A. Rodriguez. A systematic antiwindup strategy and the longitudinal control of a platoon of vehicles with control saturations. *IEEE Transactions on Vehicular Technology*, 49(3):1006–1016, 2000.

[63] X. Guo, J. Wang, F. Liao, W. Xiao, and H. Li. A low-complexity control for nonlinear vehicular platoon with asymmetric actuator saturation. In *2018 IEEE 14th International Conference on Control and Automation (ICCA)*, pages 387–392, 2018.

[64] X. Guo, J. Wang, F. Liao, and R. S. H. Teo. Cnn-based distributed adaptive control for vehicle-following platoon with input saturation. *IEEE Transactions on Intelligent Transportation Systems*, 19(10):3121–3132, 2018.

[65] S. Baldi, S. Yuan, and P. Frasca. Output synchronization of unknown heterogeneous agents via distributed model reference adaptation. *IEEE Transactions on Control of Network Systems*, 2018.

[66] L. Guvenc, I. M. C. Uygan, K. Kahraman, R. Karaahmetoglu, I. Altay, M. Senturk, M. T. Emirler, A. E. Hartavi Karci, B. Aksun Guvenc, E. Altug, M. C. Turan, Ö. S. Tas, E. Bozkurt, Ü. Ozguner, K. Redmill, A. Kurt, and B. Efendioglu. Cooperative adaptive cruise control implementation of Team Mekar at the Grand Cooperative Driving Challenge. *IEEE Transactions on Intelligent Transportation Systems*, 13(3):1062–1074, 2012.

[67] R. Kianfar, B. Augusto, A. Ebadighajari, U. Hakeem, J. Nilsson, A. Raza, R. S. Tabar, N. V. Irukulapati, C. Englund, P. Falcone, S. Papanastasiou, L. Svensson, and H. Wymeersch. Design and experimental validation of a cooperative driving system in the Grand Cooperative Driving Challenge. *IEEE Transactions on Intelligent Transportation Systems*, 13(3):994–1007, 2012.

[68] X. Guo, J. Wang, F. Liao, and R. S. H. Teo. String stability of heterogeneous leader-following vehicle platoons based on constant spacing policy. *IEEE Intelligent Vehicles Symposium (IV)*, pages 761–766, 2016.

[69] G. Tao. *Adaptive Control Design and Analysis*. Wiley, 2003.

[70] P. Ioannou and J. Sun. *Robust Adaptive Control*. Dover Publications, 2012.

[71] D. Liberzon. *Switching in Systems and Control*. Systems & Control: Foundations & Applications. Birkhäuser Boston, 2003.

[72] S. Baldi, P. Ioannou, and E. Mosca. Multiple model adaptive mixing control: The discrete-time case. *IEEE Transactions on Automatic Control*, 57(4):1040–1045, April 2012.

[73] S. Baldi and P. A. Ioannou. Stability margins in adaptive mixing control via a Lyapunov-based switching criterion. *IEEE Transactions on Automatic Control*, 61(5):1194–1207, 2016.

[74] J. Ploeg, D. P. Shukla, N. van de Wouw, and H. Nijmeijer. Controller synthesis for string stability of vehicle platoons. *IEEE Transactions on Intelligent Transportation Systems*, 15(2):854–865, 2014.

[75] S. Yuan, B. De Schutter, and S. Baldi. Robust adaptive tracking control of uncertain slowly switched linear systems. *Nonlinear Analysis: Hybrid Systems*, 27:1 – 12, 2018.

[76] S. Yuan, B. De Schutter, and S. Baldi. Adaptive asymptotic tracking control of uncertain time-driven switched linear systems. *IEEE Transactions on Automatic Control*, 62(11):5802–5807, 2017.

A

Proof of synchronization

The proof is shown explicitly for 5 vehicles in order to make the idea clear: this implies that we want to prove that vehicle 3 synchronizes to vehicles 1 and 2 ($e_{3,1}, e_{3,2} \to 0$), while vehicle 2 synchronizes to vehicles 1 and 3 ($e_{2,1}, e_{2,3} \to 0$); also, vehicle 5 synchronizes with vehicle 3 and vehicle 4 ($e_{5,3}, e_{5,4} \to 0$), while vehicle 4 synchronizes with vehicle 5 and vehicle 3 ($e_{4,5}, e_{4,3} \to 0$). The extension to an arbitrarily number of vehicles follows accordingly.

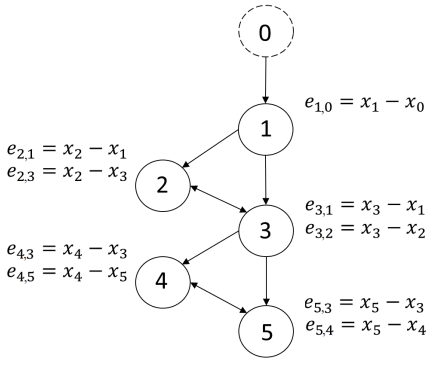

Figure A.1: The synchronization errors

Proving synchronization exploits the Lyapunov function $V_1 + V_{3,2,1} + V_{2,3,1} + V_{5,4,3} + V_{4,5,3}$,

where,

$$
\begin{aligned}
V_1 &= e'_{1,0}Pe_{1,0} + \left(\frac{\tilde{k}'_{1,0}\tilde{k}_{1,0}}{\gamma_k \left|l_1^*\right|}\right) + \left(\frac{\tilde{k}'_1\tilde{k}_1}{\gamma_k \left|l_1^*\right|}\right) + \frac{\tilde{l}_1^2}{\gamma_l \left|l_1^*\right|} \qquad \text{(A.1)}\\
V_{3,2,1} &= e'_{3,2,1}Pe_{3,2,1} + \left(\frac{\tilde{k}'_{3,1}\tilde{k}_{3,1}}{\gamma_k \left|l_3^*\right|}\right) + \left(\frac{\tilde{k}'_{3,2}\tilde{k}_{3,2}}{\gamma_k \left|l_3^*\right|}\right) + \left(\frac{\tilde{k}'_3\tilde{k}_3}{\gamma_k \left|l_3^*\right|}\right) + \frac{\tilde{l}_{3,1}^2}{\gamma_l \left|l_3^*\right|} + \frac{\tilde{l}_{3,2}^2}{\gamma_l \left|l_3^*\right|}\\
V_{2,3,1} &= e'_{2,3,1}Pe_{2,3,1} + \left(\frac{\tilde{k}'_{2,1}\tilde{k}_{2,1}}{\gamma_k \left|l_2^*\right|}\right) + \left(\frac{\tilde{k}'_{2,3}\tilde{k}_{2,3}}{\gamma_k \left|l_2^*\right|}\right) + \left(\frac{\tilde{k}'_2\tilde{k}_2}{\gamma_k \left|l_2^*\right|}\right) + \frac{\tilde{l}_{2,1}^2}{\gamma_l \left|l_2^*\right|} + \frac{\tilde{l}_{2,3}^2}{\gamma_l \left|l_3^*\right|}\\
V_{5,4,3} &= e'_{5,4,3}Pe_{5,4,3} + \left(\frac{\tilde{k}'_{5,3}\tilde{k}_{5,3}}{\gamma_k \left|l_5^*\right|}\right) + \left(\frac{\tilde{k}'_{5,4}\tilde{k}_{5,4}}{\gamma_k \left|l_5^*\right|}\right) + \left(\frac{\tilde{k}'_5\tilde{k}_5}{\gamma_k \left|l_5^*\right|}\right) + \frac{\tilde{l}_{5,3}^2}{\gamma_l \left|l_5^*\right|} + \frac{\tilde{l}_{5,4}^2}{\gamma_l \left|l_5^*\right|}\\
V_{4,5,3} &= e'_{4,5,3}Pe_{4,5,3} + \left(\frac{\tilde{k}'_{4,3}\tilde{k}_{4,3}}{\gamma_k \left|l_4^*\right|}\right) + \left(\frac{\tilde{k}'_{4,5}\tilde{k}_{4,5}}{\gamma_k \left|l_4^*\right|}\right) + \left(\frac{\tilde{k}'_4\tilde{k}_4}{\gamma_k \left|l_4^*\right|}\right) + \frac{\tilde{l}_{4,3}^2}{\gamma_l \left|l_4^*\right|} + \frac{\tilde{l}_{4,5}^2}{\gamma_l \left|l_4^*\right|}
\end{aligned}
$$

and the error dynamics, as depicted in Fig. A.1 are

$$
\begin{aligned}
\dot{e}_{1,0} &= A_m e_{1,0} + b_1(\tilde{k}'_{1,0}x_m + \tilde{k}'_1 e_{1,0} + \tilde{l}_{1,0}u_0) \qquad \text{(A.2)}\\
\dot{e}_{3,2,1} &= A_m e_{3,2,1} + b_3(\tilde{k}'_{3,1}x_1 + \tilde{k}'_3 e_{3,1} + \tilde{l}_{3,1}u_1) + b_3(\tilde{k}'_{3,2}x_2 + \tilde{k}'_3 e_{3,2} + \tilde{l}_{3,2}u_2)\\
\dot{e}_{2,3,1} &= A_m e_{2,3,1} + b_2(\tilde{k}'_{2,1}x_1 + \tilde{k}'_2 e_{2,1} + \tilde{l}_{2,1}u_1) + b_2(\tilde{k}'_{2,3}x_3 + \tilde{k}'_2 e_{2,3} + \tilde{l}_{2,3}u_3)\\
\dot{e}_{5,4,3} &= A_m e_{5,4,3} + b_5(\tilde{k}'_{5,3}x_3 + \tilde{k}'_5 e_{5,3} + \tilde{l}_{5,3}u_3) + b_5(\tilde{k}'_{5,4}x_4 + \tilde{k}'_5 e_{5,4} + \tilde{l}_{5,4}u_4)\\
\dot{e}_{4,5,3} &= A_m e_{4,5,3} + b_4(\tilde{k}'_{4,3}x_3 + \tilde{k}'_4 e_{4,3} + \tilde{l}_{4,3}u_3) + b_4(\tilde{k}'_{4,5}x_5 + \tilde{k}'_4 e_{4,5} + \tilde{l}_{4,5}u_5)
\end{aligned}
$$

where $\tilde{k} = k - k^*$, $\tilde{l} = l - l^*$ are the parameter estimation errors (taken with the appropriate subscript), and $e_{3,2,1} = e_{3,1} + e_{3,2}$, $e_{2,3,1} = e_{2,1} + e_{2,3}$, $e_{5,4,3} = e_{5,3} + e_{4,3}$ and $e_{4,5,3} = e_{4,3} + e_{5,3}$. Using standard Lyapunov arguments and the Barbalat's lemma we can show $\dot{V}_1 + \dot{V}_{3,2,1} + \dot{V}_{2,3,1} + \dot{V}_{5,4,3} + \dot{V}_{4,5,3} \to 0$ as $t \to \infty$ and hence all errors go to zero. Theorem B.1 (Appendix B) assumes that the inputs are well defined at very time instant. Therefore, the presence of a cycle in graph 2 requires us to find some well-posedness conditions on the input, as discussed in next section.

B

Well Posedness of the input

Well-posedness of the input is studied explicitly for 5 vehicles in order to make the idea clear. The need to study well-posedness of the input arises from the fact that the inputs appear both at the right-hand and left-hand side of the control laws. In particular, by considering graph 2 in Fig. 4.2, the inputs to the five vehicles can be written as

$$
\begin{aligned}
u_1(t) &= k'_{1,0}(t)x_m(t) + k'_1(t)e_{1,0}(t) + l_{1,0}(t)u_0(t) \\
2u_i(t) &= k'_{i,i-1}(t)x_{i-1}(t) + k'_i(t)(x_i(t) - x_i - 1(t)) + l_{i,i-1}(t)u_i - 1(t) \\
&\quad + k'_{i,i+1}(t)x_i + 1(t) + k'_i(t)(x_i(t) - x_i + 1(t)) + l_{i,i+1}(t)u_i + 1(t) \\
2u_3(t) &= k'_{3,1}(t)x_1(t) + k'_3(t)(x_3(t) - x_1(t)) + l_{3,1}(t)u_1(t) \\
&\quad + k'_{3,2}(t)x_2(t) + k'_3(t)(x_3(t) - x_2(t)) + l_{3,2}(t)u_2(t) \\
2u_4(t) &= k'_{4,3}(t)x_3(t) + k'_4(t)(x_4(t) - x_3(t)) + l_{4,3}(t)u_3(t) \\
&\quad + k'_{4,5}(t)x_5(t) + k'_4(t)(x_4(t) - x_5(t)) + l_{4,5}(t)u_5(t) \\
2u_5(t) &= k'_{5,3}(t)x_3(t) + k'_5(t)(x_5(t) - x_3(t)) + l_{5,3}(t)u_3(t) \\
&\quad + k'_{5,4}(t)x_4(t) + k'_5(t)(x_5(t) - x_4(t)) + l_{5,4}(t)u_4(t)
\end{aligned}
\tag{B.1}
$$

or, in a more compact matrix form

$$
\underbrace{\begin{bmatrix} 1 & 0 & 0 & 0 & 0 \\ -l_{2,1} & 2 & -l_{2,3} & 0 & 0 \\ -l_{3,1} & -l_{3,2} & 2 & 0 & 0 \\ 0 & 0 & -l_{4,3} & 2 & -l_{4,5} \\ 0 & 0 & -l_{5,3} & -l_{5,4} & 2 \end{bmatrix}}_{U} \begin{bmatrix} u_1 \\ u_2 \\ u_3 \\ u_4 \\ u_5 \end{bmatrix} = \begin{bmatrix} (k_{1,0} - k_1)'x_0 + k'_1x_1 + l_{1,0}u_0 \\ (k_{2,1} - k_2)'x_1 + 2k'_2x_2 + (k_{2,3} - k_2)'x_3 \\ (k_{3,1} - k_3)'x_1 + (k_{3,2} - k_3)'x_2 + 2k'_3x_3 \\ (k_{4,2} - k_4)'x_2 + 2k'_4x_4 + (k_{4,5} - k_4)'x_5 \\ (k_{5,2} - k_5)'x_2 + (k_{5,4} - k_5)'x_4 + 2k'_5x_5 \end{bmatrix}
$$

where it has to be noticed that the leading input u_0 is not affected by other inputs and thus can be left on the right-hand side. Even though the vehicles do not need to invert U to obtain their inputs, if we want to guarantee that u_i are well posed at all time steps, we need the matrix U to be invertible. To this purpose, let us calculate the determinant of U, so to obtain

$$\det\begin{bmatrix} 1 & 0 & 0 & 0 & 0 \\ -l_{2,1} & 2 & -l_{2,3} & 0 & 0 \\ -l_{3,1} & -l_{3,2} & 2 & 0 & 0 \\ 0 & 0 & -l_{4,3} & 2 & -l_{4,5} \\ 0 & 0 & -l_{5,3} & -l_{5,4} & 2 \end{bmatrix} = l_{2,3}l_{3,2}l_{4,5}l_{5,4} - 4l_{4,5}l_{5,4} - 4l_{2,3}l_{3,2} + 16 \quad \text{(B.2)}$$
$$= (4 - l_{2,3}l_{3,2})(4 - l_{4,5}l_{5,4}).$$

In the ideal case (with the actual parameters from Proposition 3.1), the determinant could be calculated from $(4 - l^*_{2,3}l^*_{3,2})(4 - l^*_{4,5}l^*_{5,4})$, giving a determinant equal to 9 (because $l^*_{2,3}l^*_{3,2} = 1$ and $l^*_{4,5}l^*_{5,4} = 1$ from the matching conditions). However, in the presence of uncertainties we have to replace the actual parameters with the estimated ones. Therefore, the determinant of U would be possibly different than 9 and could result in the degenerate case equal to 0. This would make the inputs u_i not well defined at all time steps. A simple approach to guarantee well posedness of the inputs at all time steps is to allow vehicles 2 and 3 to exchange their estimates $l_{2,3}(t)$ and $l_{3,2}(t)$, and vehicles 4 and 5 to exchange their estimates $l_{4,5}(t)$ and $l_{5,4}(t)$ in a distributed way (i.e. across the already existing communication links).
For example, let us assume that we can constrain $l_{2,3}l_{3,2}$ and $l_{4,5}l_{5,4}$ to be positive and not greater than 4: because we also know that all estimates l_{ji} should be positive, it is now possible to guarantee that $(4 - l_{2,3}l_{3,2})(4 - l_{4,5}l_{5,4}) > 0$, so that the matrix U would be always invertible. To this purpose, the following assumption is made.

Assumption 1. The actual parameters $l^*_{2,3}$, $l^*_{3,2}$, $l^*_{4,5}$ and $l^*_{5,4}$ are known to reside in some convex compact sets (call them Ω_l) that does not contain the set $(4 - l_{2,3}l_{3,2})(4 - l_{4,5}l_{5,4}) = 0$.

An example of Ω_l (among infinite other choices) is $l_{2,3} \geq 0$, $l_{3,2} \geq 0$, $l_{4,5} \geq 0$, $l_{5,4} \geq 0$, $l_{2,3} \leq -l_{3,2} + 3.99$, $l_{4,5} \leq -l_{5,4} + 3.99$ as represented in Fig. B.1. Note that, thanks to the factorization in (B.2), Ω_l can be decoupled in two regions defined in the planes $(l_{2,3}, l_{3,2})$ and $(l_{4,5}, l_{5,4})$, respectively. Note that Ω_l should be constructed in such a way to avoid any intersection with the singular sets $l_{2,3}l_{3,2} = 4$ and $l_{4,5}l_{5,4} = 4$. In general, the set Ω_l can be written as

$$\Omega_l = \{l_{2,3}, l_{3,2}, l_{4,5}, l_{5,4} \mid g(l_{2,3}, l_{3,2}, l_{4,5}, l_{5,4}) \leq 0\} \quad \text{(B.3)}$$

for some appropriate vector function $g(l_{2,3}, l_{3,2}, l_{4,5}, l_{5,4})$. The following main result follows.

It is important to notice that Assumption 1 limits to some extent the level of heterogeneity that can be handled by the approach: this is clearer from Fig. B.1, showing that the uncertainty on some $l_{j,i}$ cannot be arbitrarily large (specifically, the uncertainty has to reside inside the triangle in Fig. B.1). Note that the region in Fig. B.1 can include an uncertainty of the order of 100% as compared to some nominal (homogeneous) value of the driveline time constant (such region is highlighted in Fig. B.2). Therefore, from a practical point of view a quite large uncertainty can be addressed by the proposed method.

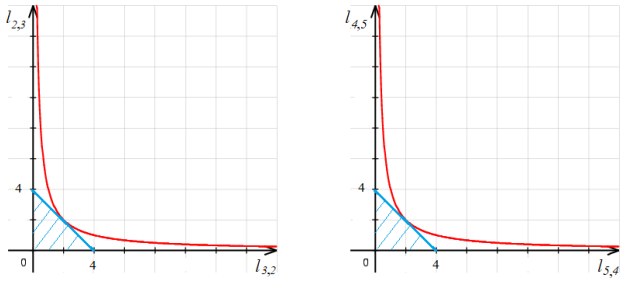

Figure B.1: Singular set (red curve) and projection set (shaded blue area) for the case of 5 vehicles. Both sets are not unique, and infinitely many projection sets can be chosen.

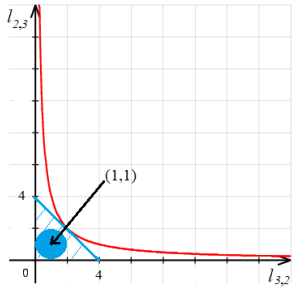

Figure B.2: The blue circle is the ball around the nominal point $(1, 1)$ (nominal homogeneous driveline constant) and with radius 1, representing a 100% uncertainty around such nominal value.

An interesting observation concerns how the uncertainty region is affected by the number of vehicles. To this purpose, let us consider the case of the first three vehicles merging: it is not difficult to show that for this case one would obtain

$$\det \begin{bmatrix} 1 & 0 & 0 \\ -l_{2,1} & 2 & -l_{2,3} \\ -l_{3,1} & -l_{3,2} & 2 \end{bmatrix} = 4 - l_{2,3} l_{3,2}. \tag{B.4}$$

By comparing (B.4) with (B.2), one can see that (B.2) is the product of two determinants calculated for groups of three vehicles. In fact, the merging maneuver can be thought as a maneuver involving groups of three vehicles (vehicles 1-2-3 and vehicles 2-4-5, as highlighted in Fig. 5.1). The corresponding projection set for three vehicles is exactly the same as the first region in Fig. B.1 must be considered if well posedness is to be guaranteed. In other words, full scalability of the approach is guaranteed and the bounds on the uncertainties do not become smaller for larger platoons.

Theorem B.1 *Consider the merging phase described by graph 2 in Fig. 4.2. Under Assumption 1, consider the five vehicles described by* (4.5) *and the leading vehicle described by* (4.6)*, the controllers* (4.10), (4.18), (4.20) *and the adaptive laws* (4.11), (4.19), (4.21) *with the following modifications*

$$\dot{l}_{2i+1,2i}(t) = \mathbb{P}_{\Omega_l}[\underbrace{-\gamma_l b'_m P(e_{2i+1,2i}(t) + e_{2i+1,2i-1}(t))u_{2i}(t)}_{\delta_{l_{2i+1,2i}}(t)}] \tag{B.5}$$

$$= \begin{cases} \delta_{l_{2i+1,2i}}(t) & \text{if } l_{2i+1,2i}(t) \in \Omega_l, \text{or} \\ & l_{2i+1,2i}(t) \in \partial\Omega_l \text{ with } \delta_{l_{2i+1,2i}} \nabla g \leq 0 \\ 0 & \text{otherwise} \end{cases}$$

$$\begin{aligned}\dot{l}_{2i,2i+1}(t) &= \mathbb{P}_{\Omega_l}[\underbrace{-\gamma_l b'_m P(e_{2i,2i+1}(t)+e_{2i,2i-1}(t))u_{2i+1}(t)}_{\delta_{l_{2i,2i+1}}(t)}] \\ &= \begin{cases} \delta_{l_{2i,2i+1}}(t) & \text{if } l_{2i,2i+1}(t)\in\Omega_l, \text{or} \\ & l_{2i,2i+1}(t)\in\partial\Omega_l \text{ with } \delta_{l_{2i,2i+1}}\nabla g\le 0 \\ 0 & \text{otherwise} \end{cases}\end{aligned}$$

where $i=1,2,...$, and $\mathbb{P}_{\Omega_l}$ has been defined as a projection operator in the set Ω_l. In particular, $\partial\Omega_l$ is the border of Ω_l and ∇g is the derivative of g with respect to $l_{2i,2i+1}$ or $l_{2i+1,2i}$. Then, merging is achieved in graph 2.

Proof The proof exploits again the Lyapunov function (A.1), and it follows the same lines as adaptive control designs with parameter projection [70, Sects. 6.6 and 8.5]. In fact, we have

$$\begin{aligned}&\dot{V}_1+\dot{V}_{3,2,1}+\dot{V}_{2,3,1}+\dot{V}_{5,4,3}+\dot{V}_{4,5,3} \\ &\le -e'_1Qe_1-e'_{3,2,1}Qe_{3,2,1}-e'_{2,3,1}Qe_{2,3,1}-e'_{5,4,3}Qe_{5,4,3}-e'_{4,5,3}Qe_{4,5,3}+V_p\end{aligned}$$

where

$$V_p(t) \quad \begin{cases} =0 & \text{if } l_{2,3}(t), l_{3,2}(t)\in\Omega_l, \text{or} \\ & l_{2,3}(t)\in\partial\Omega_l \text{ with } \delta_{l_{2,3}}\nabla g\le 0, \text{or} \\ & l_{3,2}(t)\in\partial\Omega_l \text{ with } \delta_{l_{3,2}}\nabla g\le 0, \text{or} \\ & l_{4,5}(t)\in\partial\Omega_l \text{ with } \delta_{l_{4,5}}\nabla g\le 0, \text{or} \\ & l_{5,4}(t)\in\partial\Omega_l \text{ with } \delta_{l_{5,4}}\nabla g\le 0 \\ \le 0 & \text{otherwise} \end{cases}$$

i.e. V_p is a term that due to the convexity of the projection set Ω_l verifies $V_p\le 0$. Therefore, V_p can only make the derivative of the Lyapunov function more negative [70, Sects. 6.6 and 8.5]. Hence,

$$\begin{aligned}&\dot{V}_1+\dot{V}_{3,2,1}+\dot{V}_{2,3,1}+\dot{V}_{5,4,3}+\dot{V}_{4,5,3} \\ &\le -e'_1Qe_1-e'_{3,2,1}Qe_{3,2,1}-e'_{2,3,1}Qe_{2,3,1}-e'_{5,4,3}Qe_{5,4,3}-e'_{4,5,3}Qe_{4,5,3}\end{aligned}$$

and stability follows from Barbalat's Lemma as in Theorem 4.1.

Remark B.1 The importance of Theorem B.1 lies in stating that the structure of the network can be exploited to implement appropriate projection laws (cf. (B.5)) that make the input well posed at every time instant, even in the presence of cycles. Some additional communication is necessary (vehicles 2 and 3 must exchange their estimates $l_{2,3}(t)$ and $l_{3,2}(t)$, and vehicles 4 and 5 must exchange their estimates $l_{4,5}(t)$ and $l_{5,4}(t)$), but this can be done in a distributed way along the existing communication links. The benefits of such extra communication is to guarantee well posedness of the input in a rigorous way (an issue overlooked in state-of-the-art CACC methods). Finally, it has to be remarked that full scalability is guaranteed since the adaptive/control laws can be extended to arbitrarily N vehicles without the need to modify the approach.

C

3^{rd} Error derivative

In this appendix the steps involved in obtaining the derivative of the 3^{rd} error state can be found.

$$\begin{aligned} e_i =& c_1 q_{i-1} + c_2 q_{i+1} - d_i - c_1 L_i + c_2 L_{i+1} - (c_1 + c_2) r \\ &+ h(c_2 v_{i+1} - C_i v_i) \end{aligned}$$

$$\dot{e}_i = c_1 v_{i-1} + c_2 v_{i+1} - v_i + h c_2 a_{i+1} - h c_1 a_i$$

We also know that,

$$\tau \dot{a}_i = -a_i + u_i$$

$$\begin{aligned} \ddot{e}_i =& c_1 a_{i-1} + c_2 a_{i+1} - a_i + h c_2 [-\frac{1}{\tau} a_{i+1} + \frac{1}{\tau} u_{i+1}] \\ &- h c_1 [-\frac{1}{\tau} a_i + \frac{1}{\tau} u_i] \end{aligned}$$

$$\begin{aligned} \dddot{e}_i =& c_1 [-\frac{1}{\tau} a_{i-1} + \frac{1}{\tau} u_{i-1}] + c_2 [-\frac{1}{\tau} a_{i+1} + \frac{1}{\tau} u_{i+1}] \\ &- [-\frac{1}{\tau} a_i + \frac{1}{\tau} u_i] + h c_2 [-\frac{1}{\tau} [-\frac{1}{\tau} a_{i+1} + \frac{1}{\tau} u_i + 1] \\ &+ \frac{1}{\tau} \dot{u}_{i+1}] - h c_1 [-\frac{1}{\tau} [-\frac{1}{\tau} a_i + \frac{1}{\tau} u_i] + \frac{1}{\tau} \dot{u}_i] \end{aligned}$$

$$\begin{aligned} \dddot{e}_i =& -\frac{1}{\tau} c_1 a_{i-1} + c_2 a_{i+1} - a_i + h c_2 [-\frac{1}{\tau} a_{i+1} + \frac{1}{\tau} u_{i+1}] \\ &- h c_1 [-\frac{1}{\tau} a_i + \frac{1}{\tau} u_i] \\ &- \frac{1}{\tau} u_i + h \frac{c_1}{\tau} \dot{u}_i + \frac{c_1}{\tau} u_{i-1} + \frac{c_2}{\tau} u_{i+1} + h \frac{c_2}{\tau} \dot{u}_{i+1} \end{aligned}$$

$$\dot{e}_{3,i} = -\frac{1}{\tau} e_{3,i} - \frac{1}{\tau} q_i + \frac{c_1}{\tau} u_{i-1} + \frac{c_2}{\tau} u_{i+1} + h \frac{c_2}{\tau} \dot{u}_{i+1}$$

where,

$$e_{3,i} = -\frac{1}{\tau}c_1 a_{i-1} + c_2 a_{i+1} - a_i + hc_2[-\frac{1}{\tau}a_{i+1} + \frac{1}{\tau}u_{i+1}] - hc_1[-\frac{1}{\tau}a_i + \frac{1}{\tau}u_i]$$

and,

$$p_i = -\frac{1}{\tau}u_i + h\frac{c_1}{\tau}\dot{u}_i$$